This file is the last version that was already reviewed by editor Huw Horgan on 20 May 2025. The minor technical changes requested by Huw, and corrected versions of the final reference list following TC guidelines, have been implemented in the text file “egusphere-2024-2593-text-version1”

# Review Article

# AntArchitecture:

# Building an age–depth model from Antarctica's radiostratigraphy to explore ice-sheet evolution

Robert G. Bingham[1]*, Julien A. Bodart[2,3]*, Marie G. P. Cavitte[4]*, Ailsa Chung[5]*, Rebecca J. Sanderson[6]*, Johannes C. R. Sutter[2,3]*, Olaf Eisen[7,8], Nanna B. Karlsson[9], Joseph A. MacGregor[10], Neil Ross[6], Duncan A. Young[11], David W. Ashmore[12], Andreas Born[13,14], Winnie Chu[15], Xiangbin Cui[16], Reinhard Drews[17], Steven Franke[7,17], Vikram Goel[18], John W. Goodge[19,20], A. Clara J. Henry[21], Antoine Hermant[2,3], Benjamin H. Hills[22], Nicholas Holschuh[23], Michelle R. Koutnik[24], Gwendolyn J.-M. C. Leysinger Vieli[25], Emma J. MacKie[26], Elisa Mantelli[7,27], Carlos Martín[28], Felix S. L. Ng[29], Falk M. Oraschewski[9], Felipe Napoleoni[1], Frédéric Parrenin[5], Sergey V. Popov[30,31], Therese Rieckh[13,14], Rebecca Schlegel[17], Dustin M. Schroeder[32,33], Martin J. Siegert[34], Xueyuan Tang[16,,35], Thomas O. Teisberg[33], Kate Winter[36], Shuai Yan[11], Harry Davis[1], Christine F. Dow[37,38], Tyler J. Fudge[24], Tom A. Jordan[28], Bernd Kulessa[39], Kenichi Matsuoka[40], Clara J. Nyqvist[1], Maryam Rahnemoonfar[41,42], Matthew R. Siegfried[22], Shivangini Singh[11,43], Vjeran Višnjević[2,3], Rodrigo Zamora[44], Alexandra Zuhr[17]

* These authors contributed equally to this work.

*Correspondence to:* Robert G. Bingham (r.bingham@ed.ac.uk)

**Affiliations**

[1] School of GeoSciences, University of Edinburgh, UK

[2] Climate and Environmental Physics, Physics Institute, University of Bern, Switzerland

[3] Oeschger Centre for Climate Change Research, University of Bern, Switzerland

[4] Department of Water and Climate, Vrije Universiteit Brussel, Belgium

[5] Univ. Grenoble Alpes, CNRS, INRAE, IRD, Grenoble INP, IGE, 38000 Grenoble, France

[6] School of Geography, Politics and Sociology, Newcastle University, UK

[7] Alfred Wegener Institute Helmholtz Centre for Polar and Marine Research, Bremerhaven, Germany

[8] Department of Geosciences, University of Bremen, Germany

[9] Geological Survey of Denmark and Greenland (GEUS), Copenhagen, Denmark

[10] Cryospheric Sciences Laboratory, NASA Goddard Space Flight Centre, Greenbelt, Maryland, USA

[11] University of Texas Institute for Geophysics, Jackson School of Geosciences, University of Texas at Austin, Texas, USA

[12] Met Office, FitzRoy Road, Exeter, UK

[13] Department of Earth Science, University of Bergen, Norway

[14] Bjerknes Centre for Climate Research, University of Bergen, Norway

[15] School of Earth and Atmospheric Science, Georgia Institute of Technology, Atlanta, Georgia, USA

[16] Polar Research Institute of China, Shanghai, China

[17] Department of Geosciences, University of Tübingen, Germany

[18] National Centre for Polar and Ocean Research (NCPOR), Ministry of Earth Sciences, Vasco da Gama, Goa, India

[19] Department of Earth and Environmental Sciences, University of Minnesota Duluth, Duluth, Minnesota, USA

[20] Planetary Science Institute, Tucson, Arizona, USA

[21] Department of Mathematics, Stockholm University, Sweden

[22] Department of Geophysics, Colorado School of Mines, Golden, Colorado, USA

[23] Department of Geology, Amherst College, Massachusetts, USA

[24] Department of Earth and Space Sciences, University of Washington, Seattle, Washington, USA

[25] Department of Geography, University of Zurich, Switzerland

[26] Department of Geological Sciences, University of Florida, Gainesville, Florida, USA

[27] Department of Earth and Environmental Sciences, Ludwig-Maximillians-Universität, Munich, Germany

[28] British Antarctic Survey, Cambridge, UK

[29] Department of Geography, University of Sheffield, Sheffield, UK

[30] St Petersburg State University, Russia

[31] Polar Marine Geosurvey Expedition, St. Petersburg, Russia

[32] Department of Geophysics, Stanford University, California, USA

[33] Department of Electrical Engineering, Stanford University, California, USA

[34] Tremough House, Penryn Campus, University of Exeter, Cornwall, UK

[35] School of Oceanography, Shanghai Jiao Tong University, China

[36] Department of Geography and Environmental Sciences, Northumbria University, Newcastle, UK

[37] Department of Geography and Environmental Management, University of Waterloo, Ontario, Canada

[38] Department of Applied Mathematics, University of Waterloo, Ontario, Canada

[39] School of Biosciences, Geography and Physics, Swansea University, UK

[40] Norwegian Polar Institute, Tromsø, Norway

[41] Department of Computer Science and Engineering, Lehigh University, Pennsylvania, USA

[42] Department of Civil and Environmental Engineering, Lehigh University, Pennsylvania, USA

[43] Department of Earth and Planetary Sciences, University of Texas at Austin, Austin, Texas, USA

[44] Centro de Estudios Científicos, Valdivia, Chile

**Abstract.** Radio-echo sounding (RES) has revealed an internal architecture within both the West and East Antarctic ice sheets that records their depositional, deformational and melting histories. Crucially, RES-imaged internal-reflecting horizons, tied to ice-core age-depth profiles, can be treated as isochrones that record the age-depth structure across the Antarctic ice sheets. These enable the reconstruction of past climate and ice-dynamical processes on large scales, which are complementary to but more spatially extensive than commonly used proxy records (e.g., former ice limits constrained by cosmogenic dating, or offshore sediment sequences) around Antarctica. We review progress towards building a pan-Antarctic age-depth model from these data by first introducing the relevant RES datasets that have been acquired across Antarctica over the last six decades (focussing specifically on those that detected internal-reflecting horizons), and outlining the processing steps typically undertaken to visualise, trace and date (by intersection with ice cores, or modelling) the RES-imaged isochrones. We summarise the scientific applications to which Antarctica's internal architecture has been applied to date and present a pathway to expanding Antarctic radiostratigraphy across the continent to provide a benchmark for a wider range of investigations: (1) Identification of optimal sites for retrieving new ice-core palaeoclimate records targeting different periods; (2) Reconstruction of surface mass balance on millennial or historical timescales; (3) Estimates of basal melting and geothermal heat flux from radiostratigraphy and comprehensively mapping basal-ice units, to complement inferences from other geophysical and geological methods; (4) Advancing knowledge of volcanic activity and fallout across Antarctica; (5) The refinement of numerical models that leverage radiostratigraphy to tune time-varying accumulation, basal melting and ice flow, firstly to reconstruct past behaviour, and then to reduce uncertainties in projecting future ice-sheet behaviour.

## 1 Introduction

Throughout the Quaternary (2.58 Ma to present), Antarctica's ice cover has waxed and waned, inducing concomitant rises and falls in global sea level on the order of several tens of metres (e.g., Drewry, 1983; Pollard and DeConto, 2009; Dutton et al., 2015). It is critical to understand the rates and drivers of these past oscillations in order to contextualise current observations of persistent and accelerating losses from the contemporary Antarctic ice sheets (e.g., Fox-Kemper et al., 2021; Otosaka et al., 2023) and thereby project as accurately as possible the rates at which future global sea-level rise fuelled by ice melt will occur (e.g., Scambos et al., 2017; Oppenheimer et al., 2019). The evidence for past Antarctic ice-sheet fluctuations has been derived predominantly from sampling sediments deposited offshore around the continent (Escutia et al., 2009; Naish et al., 2009; Cook et al., 2013; Bentley et al., 2014; Gulick et al., 2017; Hillenbrand et al., 2017), dating the exposure history of onshore bedrock and moraine boulders (Brook and Kurz, 1993; Stone et al., 2003; Johnson et al., 2008; Mackintosh et al., 2014; Hein et al., 2016; Hillebrand et al., 2021), and by analysing the ice itself recovered from ice-core sites (e.g., EPICA Community Members, 2004; Jouzel et al., 2007; Higgins et al., 2015; WAIS Divide Project Members, 2015; Dome Fuji Ice Core Project Members, 2017; Yan et al., 2021) (see Brook and Buizert, 2018 for an overview). Together, these form the palaeoclimate records that underpin numerical-modelling reconstructions of past and present ice-sheet extents and inform projections of how these may evolve into the future and affect sea-level change (e.g., Gasson et al., 2016; Golledge et al., 2019; DeConto et al., 2021; Pittard et al., 2022). Recovery of further sediment and ice cores around Antarctica to refine these records and projections remains a scientific imperative – and yet these records are intrinsically spatially limited, are often restricted on the timescales of observation, and for the most part are indirect with respect to ice conditions. Radio-echo sounding across Antarctica complements these records by providing *spatially continuous* data that record past and present ice conditions and, by extension, past and present climate conditions, across the ice sheets.

Radio-echo sounding (RES) describes the investigation of the subsurface of ice sheets using electromagnetic waves, and has been conducted from both airborne and ground-based platforms across the Antarctic ice sheets for over 60 years (see reviews by Dowdeswell and Evans, 2004; Bingham and Siegert, 2007; Allen, 2008; Schroeder et al., 2020). Primarily deployed for mapping the ice-sheet bed and thereby measuring ice thickness and thus ice volume, the majority of RES surveys have also imaged numerous englacial features, predominantly internal-reflection horizons (a.k.a. internal or englacial layers), crevasses and rheologically-distinct "basal units" of ice that occur between the more obvious reflections of the ice surface and bed (Fig. 1). For this review, we collectively term all of the Antarctic ice sheets' RES-imaged englacial features its *internal architecture*. We will demonstrate that although great progress has already been made in using some of this resource to elucidate ice and climate history, Antarctica's internal architecture has yet to be exploited to its full potential in refining our understanding of past, present and future ice-sheet behaviour.

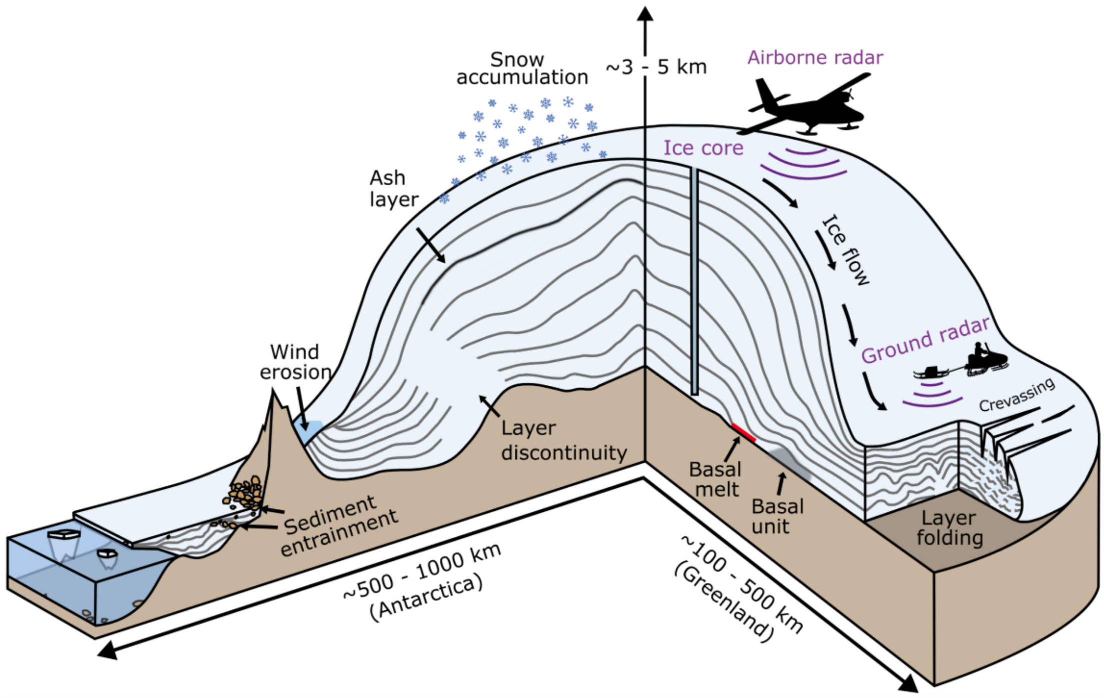


**Figure 1.** Schematic illustration of Antarctica's internal architecture and the key processes governing its structure. Internal-reflection horizons - the ice sheet's "radiostratigraphy" - are represented by grey lines between the surface and bed.

In Greenland, a comprehensive archive of internal architecture has already been assembled (see MacGregor et al., 2015a; 2025), facilitating the ice-sheet-wide reconstruction of past accumulation and dynamics, to improve past and future sea-level estimates (MacGregor et al., 2016; Born and Robinson, 2021). However, several major issues have confounded progress in capturing and applying internal architecture across Antarctica, including:

1) The Antarctic ice sheets together cover eight times the area of the Greenland Ice Sheet.

2) RES data have been collected, processed and archived by multiple international groups across the Antarctic ice sheets, and hence are not available in a standardised form across Antarctica.

3) A comprehensive suite of strategies for using internal architecture in numerical ice-sheet models has not been developed.

4) Much internal architecture in RES data is highly challenging to identify and map with automated methods.

To address these challenges and work collectively towards consistently capturing and utilising Antarctica's internal architecture, an international community called *AntArchitecture* was formed in 2018. This community, coordinated via the *Scientific Committee for Antarctic Research* (SCAR), aspires to the ultimate scientific aim of using Antarctica's internal architecture to deconvolve its ice sheets' histories and thereby facilitate improved projections of their future behaviour in the face of global climate warming. A first step in this process, and one of the aims of this review, collectively written by the *AntArchitecture* community, is to compile the international community's understanding of the present state of the field in terms of available RES data across the Antarctic ice sheets and their potential applications. Additionally, we seek here to relay community aspirations to address the aforementioned challenges and position Antarctica's internal architecture as a valuable resource for improving our understanding of its ice/climate interactions.

We begin with a brief overview of what gives rise to internal architecture in ice, especially the internal-reflection horizons (hereafter IRHs) that are measured by RES (Sect. 2). We then describe how RES data have been, and can be, processed to optimise the extraction of internal architecture and its visualisation, and discuss the common methods currently used to characterise and date IRHs (Section 3). In Sect. 4, we summarise the key RES datasets acquired across Antarctica that image internal architecture, to contextualise in a single place the type and quality of information recorded by each institute and survey in the past six decades, and present an inventory of which existing RES data have so far had several IRHs traced through them. In Sect. 5, we review how internal architecture has been used to reconcile ice-core records, calculate changes to past surface mass balance, explore basal melting in association with subglacial lakes and areas of enhanced geothermal heat flux, and investigate ice-sheet dynamics and other glaciological questions; and outline how the internal architecture has begun to be used in in numerical-modelling applications to date. In Sect. 6, we outline a recommended pathway to building a pan-Antarctic database of Antarctica's internal architecture, and discuss key science activities that can be facilitated by its delivery.

## 2 Internal architecture in ice sheets

The most common way in which internal architecture is viewed and assessed is as radargrams, which are two-dimensional profiles of echo power arrayed in the along-track direction (e.g., Fig. 2). Antarctic radargrams commonly display clear *radiostratigraphy*, the collective term for the multiple sub-parallel and closely-spaced IRHs that are seen in radargrams and often, although do not always, broadly follow the shape of the ice-bed interface (e.g., Fig. 2). IRHs occur as radio-waves propagate down through the ice column and reflect off any boundary where there is a contrast in the dielectric properties within the ice. The propagation of radio-waves through snow, firn and ice is controlled by the relative permittivities of these materials, which are functions of density, electrical conductivity, and/or the development of ice-fabric anisotropy where ice crystals align into a preferential orientation as a result of large englacial stress. Where contrasts in any of these properties are sufficiently strong and sharp, the incident energy will partition and a small fraction of it will be reflected back to the RES receiver at or above the ice surface.

In the upper and middle part of the ice column, radiostratigraphy typically arises from (a) density variations, as snow compacts into ice (as explained in pioneering work by Robin et al. (1969) and Clough (1977)) and (b) variations in electrical conductivity, as volcanic aerosols present in the air during snow deposition are

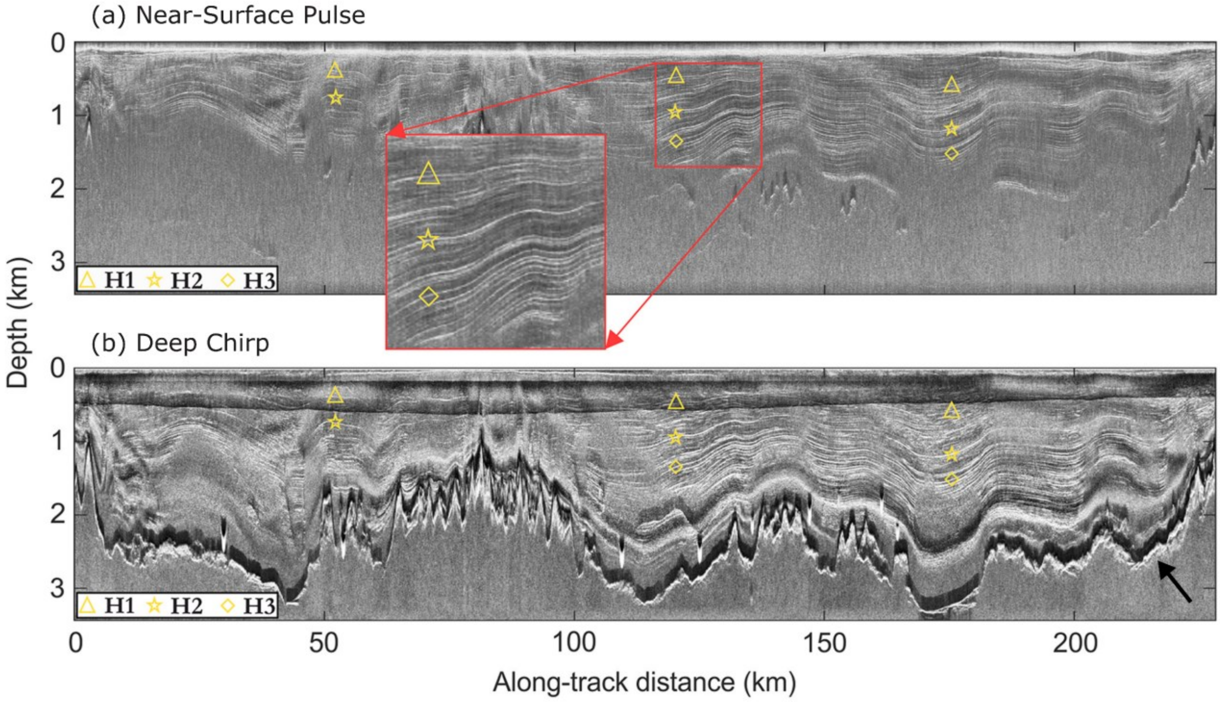


**Figure 2.** Radargrams from Institute Ice Stream, West Antarctica, obtained by the British Antarctic Survey PASIN RES system in (a) pulse (shallow-sounding) and (b) chirp (deep-sounding) radar modes (Frémand et al., 2022), vertically differentiated to accentuate fine detail. Symbols highlight three IRHs found widely across West Antarctica in airborne radar data. The bed reflection (black-white interface) is partially visible in (a) and clearly visible in (b), marked by the black arrow. Figure modified from Ashmore et al. (2020).

incorporated into the firn (Hammer, 1980; Millar, 1981; Millar, 1982). These density- and electrical-conductivity-derived IRHs are related to snow and ice layers of a specific age buried under subsequent snow accumulation, and thus may be considered isochronous (Hempel et al., 2000; Eisen et al., 2006). Such RES-imaged isochrones may often represent composites of multiple real horizons in the ice, and their thickness is dependent on RES-system resolution (Harrison, 1973; Winter et al., 2017). They are often traceable for considerable distances on RES profiles: some IRHs in the Antarctic and Greenland ice sheets are continuous for hundreds or even thousands of kilometres (e.g., MacGregor et al., 2015a; Winter et al., 2019a; Ashmore et al., 2020). For the focus of this review, isochronous reflections arising from density and electrical conductivity are of significant interest, and IRHs that can be dated at ice cores and traced continuously over long distances to form a "*dated radiostratigraphy*" are particularly valuable (as explored in-depth in Sect. 4 and 5). There are, however, some cases, especially in the lower part of the ice column, where diachronous IRHs (i.e. IRHs that cannot be treated as single time markers) may be visualised in radargrams. The most common such examples are IRHs that are thought to manifest sudden changes in ice-crystal-orientation fabric that cause anisotropic radio-wave propagation, or cold-warm ice transitions where the pore space on the warm side is filled with meltwater instead of air (Harrison, 1973; Fujita et al., 1999; Eisen et al., 2007). Over ice shelves, pervasive IRHs can mark the boundary between atmospherically-derived (meteoric) and subglacially/submarine-accreted (marine) ice (Holland et al., 2009; Das et al., 2020).

The specular behaviour of IRHs also positions them as ideal targets for repeated observations of vertical velocity over time, directly tracking the deformation of the ice sheet, via static phase-sensitive repeat measurements at a point (autonomous phase-sensitive radio-echo sounder, or ApRES; Nicholls et al., 2015) or from airborne re-flights of transects with coherent RES systems (Castelletti et al., 2021). Although these methods have been practised in recent field campaigns (e.g., Hills et al., 2022; Chung et al., 2023; Fudge et al., 2023), we do not discuss this aspect of radiostratigraphy further in this review, beyond noting that establishing the distribution of appropriate IRHs could be a valuable component in expedition planning. A review of static techniques is found in Kingslake et al. (2014), while repeat-pass airborne interferometry of IRH is an active field of research (Castelletti et al., 2021).

While the imaging and analysis of radiostratigraphy and its application to assessing ice-sheet evolution form the main focus of this paper, other significant features of internal architecture also convey information that can be used to help understand current and past ice-sheet processes (as depicted in Fig. 1). These include basal units which exhibit different dielectric properties to the surrounding ice and may result from ice-folding due to contrasts in material properties, to accretion, melting due to high rates of geothermal heat flux or overburden pressure from the ice above, or freeze-on processes taking place at the base of the ice sheet (Bell et al., 2011; Bell et al., 2014; Bons et al., 2016; Leysinger Vieli et al., 2018; Wrona et al., 2018; Ross et al., 2020; Franke et al., 2023). Additionally, buried near-surface and basal crevassing imaged by RES systems may be indicative of past grounding-line evolution or ice-stream stagnation events (Retzlaff et al., 1993; Matsuoka et al., 2009; Catania et al., 2010; Kingslake et al., 2018; Wearing and Kingslake, 2019). We elaborate further on these other significant features of internal architecture in Sect. 5.5.

## 3 Extracting and dating internal architecture from RES data

The information available from radargrams (e.g. Fig. 2), and the degree to which the internal architecture can be used for different applications, depend firstly on the settings of the RES system acquiring the data and secondly on choices made in processing the data. Below we summarise the typical processing workflow for radargram generation and highlight key decisions that influence interpretation of the resulting radiostratigraphy. Figure 3 presents a conceptual support to this discussion. We then discuss the different methods used to trace radiostratigraphy through radargrams, and to assign dates to key IRHs.

### 3.1 Data processing for optimising IRH tracing

RES data acquisition (Fig. 3a) can be categorised broadly based on two criteria: (a) Phase control of the transmitter or phase sampling by the receiver (i.e., coherent vs. incoherent); and (b) the nature of the transmitted wave (pulsed versus chirped; Gogineni et al. (1998); Peters et al. (2005)). Processing (depicted in Fig. 3b) is similar for all systems, so here we highlight differences that affect radargram quality. Direct

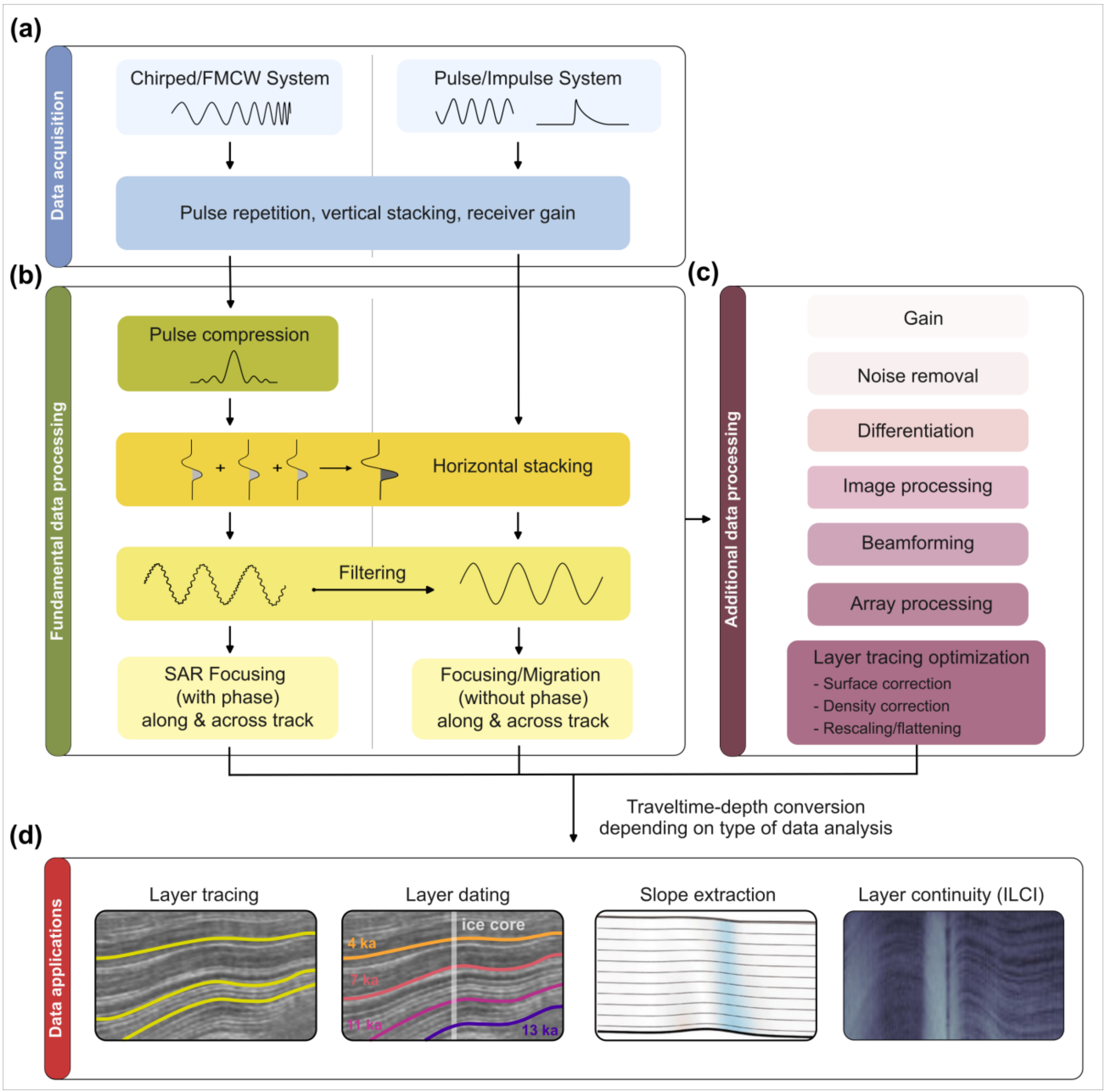


**Figure 3.** Flowchart illustrating key steps for the processing of RES data from chirp and pulse systems for subsequent radiostratigraphic analysis. (a) Basic configurations and parameters defined on data acquisition. (b) Fundamental and (c) additional steps commonly taken when processing data to visualise IRHs. (d) Depiction of some common ways of tracing or otherwise quantifying IRH geometry.

measurements of the dielectric properties of ice cores show that ice conductivity varies on much smaller length scales than can be imaged by RES (Harrison, 1973; Eisen et al., 2003). Therefore, each RES system represents subsurface reflectors differently, and data acquired from the same area but by different RES systems may show different IRHs on intersecting radargrams due to the differences in RES imaging capabilities (see Fig. 4, after Winter et al. (2017), for an example of a comparison between different RES systems). For pulsed systems, processing cannot improve the vertical resolution, which is controlled by the bandwidth and the rate of sampling of the received waveform. For chirped systems, the waveform must be

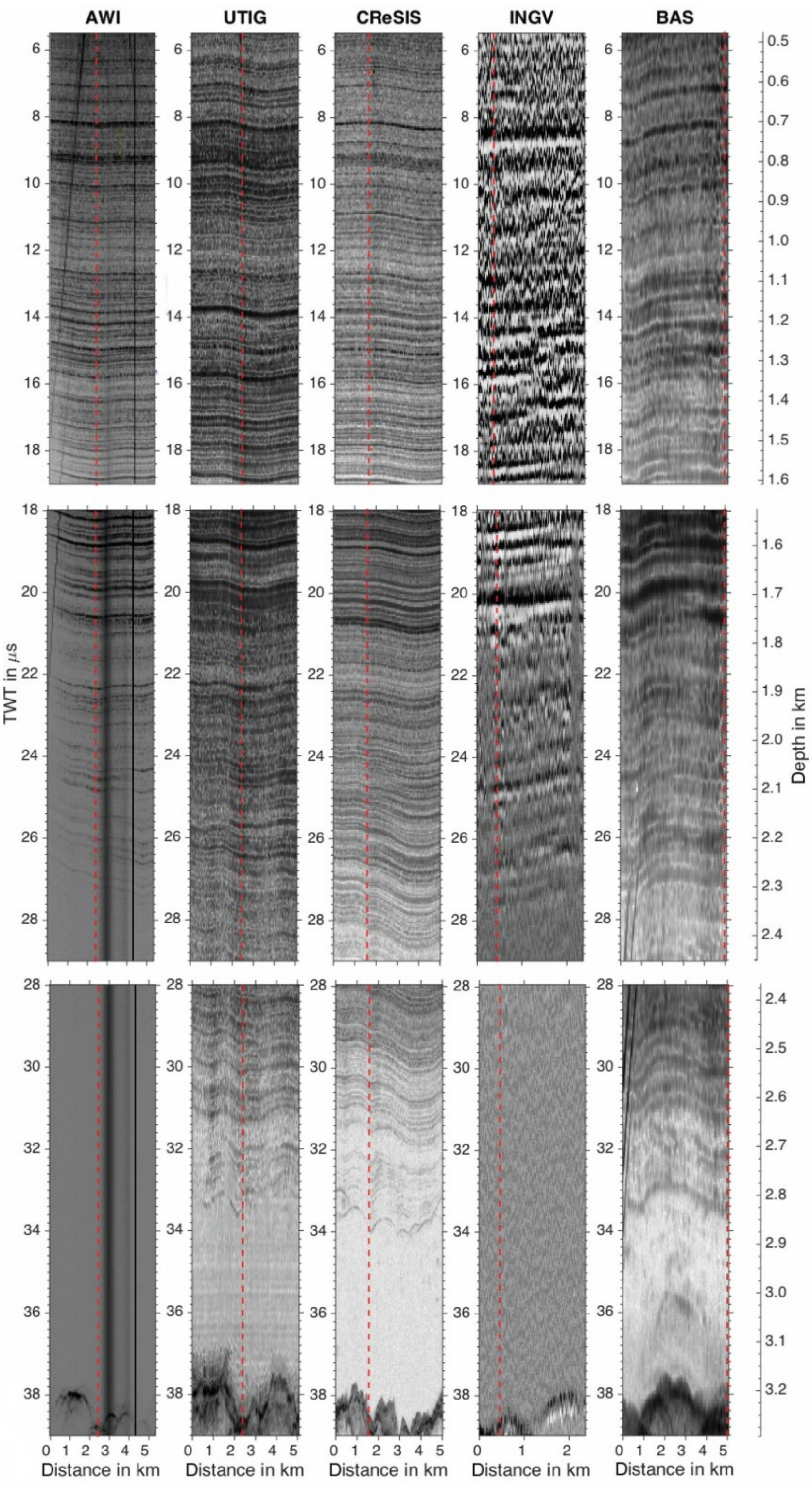


**Figure 4**. RES profiles of a few km length for five RES systems, that have profiled across or near Dome C (location in Fig. 6d). The vertical red line in each profile marks the position of the trace closest to Dome C. The surface reflections are shifted to time zero and the length of the RES profiles is indicated on the horizontal axes. For the bottom UTIG and CReSIS panels a 2-D-focused processing is applied. The RES data were acquired with: 1. AWI 150 MHz Aero-EMR; 2. UTIG 60 MHz HiCARS; 3. CReSIS 194 MHz MCoRDS; 4. Italian National Institute of Geophysics and Volcanology (INGV) 150 MHz RES system; and 5. BAS 150 MHz PASIN; for full details and original figure from which this is modified, see Winter et al. (2017).

fully sampled first and then match-filtered, integrating the received power while also finely resolving radiostratigraphy targets based on the chirp's bandwidth (Hélière et al., 2007; Peters et al., 2007). This "pulse compression" is the first step in producing a radargram from a chirped system.

Following initial data acquisition, RES data are typically processed using geophysical techniques of varying sophistication (Fig. 3b). For example, incoherent noise is typically reduced by various forms of horizontal averaging, and bandpass-filtering can remove irrelevant components of the measured signal. Finally, if possible the data should be focused or migrated to reposition the received signal energy as precisely as possible to their true subsurface locations. This can be done via several methods: (a) Incoherent echo summation, often termed *migration* as in reflection seismology (Yilmaz, 2001); (b) SAR-focusing for point scatterers, common in satellite applications (Ulaby and Lang, 2015); or (c) applying algorithms designed specifically for RES of specular reflections (Heister and Scheiber, 2018; Castelletti et al., 2019; Xu et al., 2022). SAR-focusing has a proven ability to reduce image artefacts and improve along-track resolution, especially in areas with steeply-sloping radiostratigraphy (Holschuh et al., 2014; Castelletti et al., 2019). Multiple SAR-processing techniques currently exist for coherent RES systems, including: (a) unfocused SAR (short apertures without phase correction and equivalent in name to Doppler filtering or coherent echo summation; Hélière et al. (2007)); or (b) more advanced focused SAR, using either 1-D correlations resulting in intermediate apertures, or 2-D correlations resulting in longer apertures (Peters et al., 2005; Peters et al., 2007). The latter is the processing of choice for modern coherent systems for the detection of IRHs in areas with steeply dipping reflections. Unfocused and 1-D SAR approaches will emphasise flat specular reflectors and reduce clutter, at a cost of dipping specular horizons. Large SAR apertures are critical for tracking steeply dipping IRHs, but present greater computational costs and an overall reduction of signal to noise ratio. Cross-track antenna arrays can allow for determination of cross-track IRH slopes.

A series of additional corrections and image-processing steps can also be taken to optimise RES data for tracing radiostratigraphy (Fig. 3c). For radar data acquired by airborne platforms, the aircraft-to-ice surface space on the radargram must be removed to obtain true depths below the ice surface; this is often conducted by shifting the vertical axis of the radargram to time zero for each RES trace and flattening the surface based on the location of the surface reflection on the radargram. This can be done using data from the altimeter and/or LIDAR onboard the aircraft, high-resolution surface DEMs, or using the picked surface reflection from the radargram itself (e.g., MacGregor et al., 2015a). Localised density corrections, based on ground-truthing measurements in the upper section of ice cores or other geophysical measurements (e.g., radar data acquired by airborne platforms; Eisen et al., 2002), may also be applied to convert the two-way-travel time from the RES data to ice-equivalent depths. Alternatively, for depth-correcting RES below the pore close-off depth, a spatially uniform firn-depth correction that is typically of the order of several metres may be used to obtain ice-equivalent depths (e.g., Ashmore et al., 2020), although this assumption may only be valid in dry and stable parts of the ice sheet and not in highly dynamic regions (Dowdeswell and Evans, 2004). Others have also vertically rescaled (or flattened) RES data to facilitate the tracing of continuous reflections by semi-automatic pickers (e.g., Fahnestock et al., 2001a; Sect. 3.2; MacGregor et al., 2015a; 2025). Finally, specific image-processing filters can also be applied to enhance the gain and reduce incoherent noise, which can facilitate IRH tracing on RES data (Ashmore et al., 2020; Bodart et al., 2021; Wang et al., 2023; Franke et al., 2025).

Importantly for users interested in tracing IRHs, and especially the deepest IRHs, most RES data over Antarctica, including those available from open-access repositories, are not optimised for detecting radiostratigraphy. Typically the data have been acquired and processed to optimise retrieval of the bed echo, and some datasets require considerable reprocessing from the raw data to improve the clarity of the radiostratigraphy between the ice surface and the bed (Castelletti et al., 2019). In particular, for thick or unusually heterogenous ice, the best strategy is often to experiment with filtering data differently at different depths until the IRHs at selected depths are most clearly visualised.

### 3.2 Tracing radiostratigraphy

The primary method for extracting internal architecture from radargrams (e.g. Fig. 3d) has been to trace or "pick" IRHs, typically using semi-automated techniques (e.g., Cavitte et al., 2016; Koch et al., 2023). Where radargram quality is high, IRHs are easily traced and continuous, and fully automated methods may also perform well (e.g., Panton, 2014; Xiong et al., 2018; Delf et al., 2020). Machine-learning methods are in their infancy but show promise for more rapidly tracing radiostratigraphy , as demonstrated recently by Moqadam et al. (2025) on deep IRHs. However, so far most successful applications have been limited to near-surface IRHs in the upper few tens of metres of the ice column (e.g., Dong et al., 2021; Rahnemoonfar et al., 2021; Yari et al., 2021), primarily due to the lack of vertical disturbances and low noise in surface-conformable IRHs. Thus, for most radargrams and deep-ice applications, semi-automated tracing of IRHs is still required. This relies on algorithms that typically follow the local maxima in return power between adjacent traces within a predetermined vertical window, using either open-source or commercial and bespoke software from the seismic industry (e.g., Winter et al., 2019a; Ashmore et al., 2020; Chung et al., 2023; Sanderson et al., 2024). A comprehensive overview of IRH-tracing methods is provided by Moqadam et al. (2025).

The process of tracing IRHs can be categorised into two approaches: (a) tracing as many IRHs as possible regardless of their amplitudes or continuity (MacGregor et al., 2015a; 2025); or (b; more commonly) by identifying IRHs that have a high echo-power, appear distinguishably brighter than adjacent IRHs on radargrams and are continuous for long distances (>100 km), using crossovers between intersecting RES profiles to ensure reliability in the tracing process (e.g., Cavitte et al., 2016; Winter et al., 2019a; Ashmore et al., 2020; Bodart et al., 2021; Wang et al., 2023).

Importantly, the thickness of a given IRH in a radargram is dependent on the range resolution of the RES system used to image it, such that RES systems with high pulse-width, and thus finer vertical resolution, may detect several thinner IRHs that would otherwise appear as a single, broader reflection in coarser-resolution systems (see Fig. 4 and Harrison, 1973; Millar, 1982; Karlsson et al., 2014; Winter et al., 2017; Bodart et al., 2021; Cavitte et al., 2021; Franke et al., 2025). This must be accounted for when comparing the position and aspect of IRHs traced in data from RES systems operating with different frequencies and system characteristics (Winter et al., 2017, Franke et al., 2025).

### 3.3 Complementary approaches to tracing IRHs for characterising radiostratigraphy

Even having applied all possible data processing strategies described above, radiostratigraphy may remain challenging or impossible to trace over some regions due to the innate physical properties of ice in such areas. For example, IRHs may become warped/buckled or disrupted by differential ice flow or flow over steep topography (e.g., Siegert et al., 2003b; Ross et al., 2011; Bingham et al., 2015; Franke et al., 2023; Jansen et al., 2024), while unconformities can be introduced by significant wind scouring of the ice surface (e.g., Welch and Jacobel, 2005; Luo et al., 2022). This variability in itself provides important information about past and present ice behaviour (as we explore further in Sect. 5), and hence warrants alternate methods to characterise the radiostratigraphy where IRHs cannot readily be traced.

One method for assessing the general variability of radiostratigraphy across large regions of ice sheets is the Internal Layering Continuity Index (ILCI) developed by Karlsson et al. (2012). This tool maps the variability in vertical signal strength for individual RES traces, acting as a relative measure of the number of dielectric contrasts compared to signal-to-noise ratio. High ILCI values typically indicate regions of an ice sheet characterised by multiple, traceable IRHs, while low ILCI values tend to indicate regions of ice sheet with disrupted or discontinuous IRHs or regions with very few or no IRHs detected by the RES system. Although the method is not easily transferable between different RES systems due to acquisition and processing differences, ILCI has been extensively applied to several regions both in Antarctica (Fig. 5) and Greenland as a mechanism for identifying rapidly the specific sub-regions in which IRHs are likely to be traceable (e.g., Sime et al., 2014; Bingham et al., 2015; Karlsson et al., 2018; Frémand et al., 2022; Tang et al., 2022; Sanderson et al., 2023).

Alternative methods have focussed on the extraction of IRH slopes. This avenue acknowledges the challenges of tracing and dating radiostratigraphy in areas of fast or complex ice flow, or where the acquisition or processing methods that have been used were not tailored to the recovery of radiostratigraphy. For discontinuous radiostratigraphy, local slope information is valuable, because radiostratigraphic slope is closely related to particle trajectories within the ice sheet (Hindmarsh et al., 2006; Parrenin and Hindmarsh, 2007; Ng and King, 2011; Holschuh et al., 2017). Several methods have therefore been developed to extract slope information, such as incoherent averaging methods (Sime et al., 2011; Holschuh et al., 2017; Delf et al.,

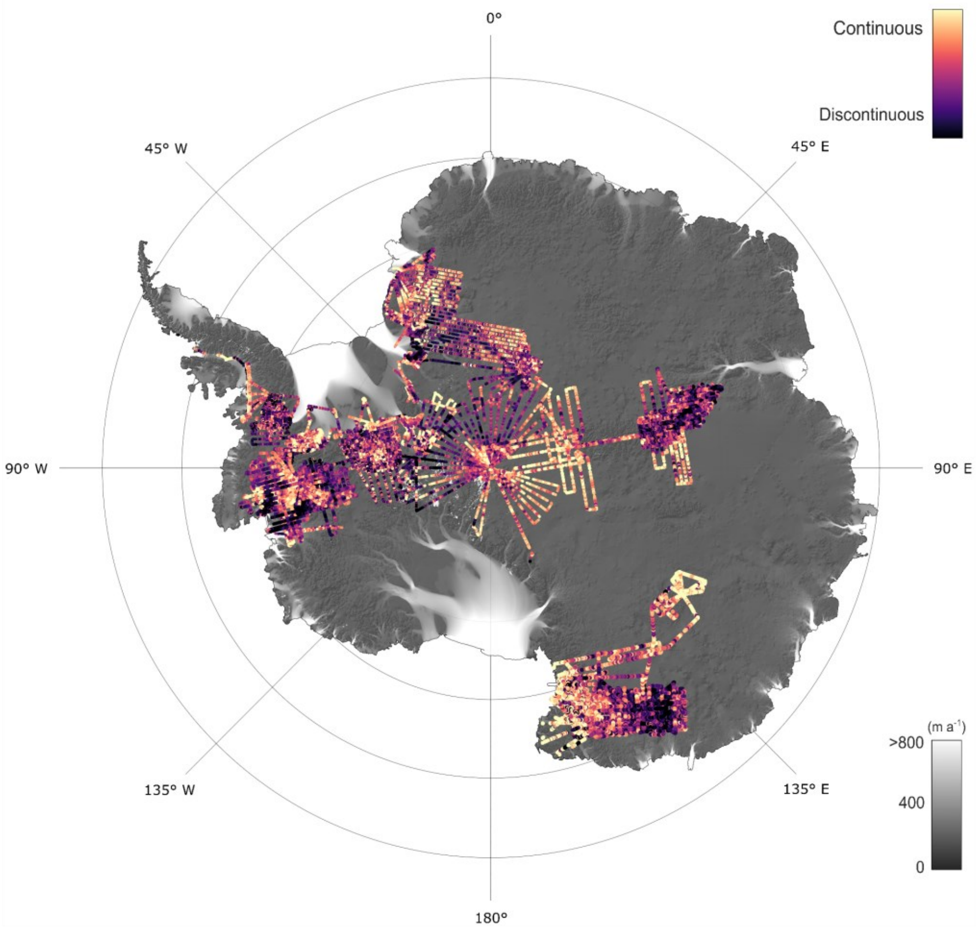


**Figure 5.** Radiostratigraphic continuity (ILCI) calculated over 10 airborne RES datasets acquired by BAS. Continuous and readily traceable IRHs are indicated in the slow-flowing regions of the ice sheet (high ILCI; bright yellow) whereas disrupted or absent IRHs are likely in the faster-flowing sections of ice streams or where subglacial topography is highly variable (low ILCI; dark purple). The background maps show ice-flow velocities from MEaSUREs (Rignot et al., 2017) and a hillshade of the bedrock from BedMachine (Morlighem, 2020). Figure modified from Frémand et al. (2022).

2020) and methods that use along-track phase information during SAR processing to estimate IRH slope (MacGregor et al., 2015a; Castelletti et al., 2019; Oraschewski et al., 2024).

### 3.4 Dating internal-reflection horizons (isochrones)

As introduced in Sect. 2, most RES-imaged IRHs have been shown to be isochronous, and the majority of those we treat in this review (i.e. that are imaged in between approximately the first and last few hundreds of metres of the ice column) arise due to the RES systems imaging variations in the electrical conductivity (i.e. acidic content) of the ice with depth. Hereafter in this paper, reiterating that most IRHs are isochrones, we will use the term isochrones to refer to IRHs, and will only re-use the term IRH where it may be ambiguous concerning whether IRHs are isochronous.

Ages can be assigned to isochrones at intersections with deep ice cores where age-depth models have already been derived from chemistry analyses (e.g., McConnell et al., 2017; Cole-Dai et al., 2021; Bouchet et al., 2023), but also using modelling techniques where this is not possible. Before any age can be assigned, the age uncertainty that arises from the RES system itself must first be assessed. Uncertainty in reflector depth arises from several sources: (a) proximity of the RES profile to the ice-core site, otherwise a specific reflector geometry (typically flat) must be assumed between the point of closest approach and the ice-core site (MacGregor et al., 2015a); (b) the radio-wave speed, which varies based on permittivity variations as a function of englacial density and anisotropy (e.g., Kovacs et al., 1995; Fujita et al., 2000); (c) the range resolution of the RES system and the signal-to-noise ratio of each traced reflection at (or near) the ice-core site, which enable an estimate of the depth precision to which each traced reflection can be known (e.g., Cavitte et al., 2016); and (d) the picking accuracy of both the ice surface and the isochrones themselves, which can add several metres of uncertainty. This latter point may include the uncertainty arising from the source of the surface product (i.e. either from cm-resolution onboard altimeter/LIDAR), or directly from the RES data which have much lower resolution of the order of several metres); and whether the picking algorithm is tailored to extract the onset of the reflection, the half-amplitude, or the peak value.

The ideal scenario for assigning ages to isochrones is that a RES profile intersects or passes sufficiently close (~500 m vicinity) to the location of an ice-core site for the ice core's depth-age scale (from chemical profiling or layer counting) to be useable for directly assigning ages to the RES-imaged isochrones. In such cases, direct dating at the ice core can be done in two ways: (1) direct age-matching by comparing the isochrone depth from the RES to the age-depth scale of the ice core (e.g. MacGregor et al., 2015a; Cavitte et al., 2016; Bodart et al., 2021), or (2) by matching observed RES isochrones to simulated RES isochrones based on the measured dielectric profiling at the ice core (e.g. Eisen et al., 2003; Winter et al., 2017; Franke et al., 2025). The former can be applied to any isochrones but results in larger uncertainties due to the conversion of the two-way-travel time from the RES data to ice-equivalent depths, whereas the latter is more accurate as the conductivity peaks represent the true physical origin of the isochrones. However, the condition that a reflection must rise above the background noise of the RES system limits its application to specific isochrones (Franke et al., 2025). For either case, the isochrone-depth uncertainty can then be combined with the ice-core age uncertainty to assign a total age uncertainty to the mapped reflections; in these cases, uncertainty is generally dominated by the ice-core-derived age uncertainty in the upper third of the ice column, while the RES-derived depth uncertainty increasingly dominates at larger depth (e.g., MacGregor et al., 2015a; Cavitte et al., 2016; Muldoon et al., 2018; Winter et al., 2019a; Wang et al., 2023). More recently, some isochrones have been dated not by their direct intersection with an ice core, but rather by intersecting other RES datasets that in turn have already been dated by their intersection with a distant ice core. As a result, the age-depth profile is transferred to the new dataset at the crossover(s) between the intersecting RES datasets (e.g., Ashmore et al., 2020; Bodart et al., 2021). In these cases, the relative uncertainties of the different RES systems at the intersections between RES datasets additionally need be factored into the final age estimation, and the final age estimates are commonly checked using the modelling techniques introduced next (e.g., Bodart et al., 2021; Sanderson et al., 2024).

Where isochrones cannot be directly correlated to an ice-core age-depth relationship due to a lack of nearby ice cores, any intersections with previously dated isochrones, or missing sections in the record (e.g., due to disrupted englacial stratigraphy), age-depth modelling is required to assign ages to isochrones. This is typically done using 1-D models in stable parts of the ice sheet such as at ice divides (e.g., Nye, 1957; Dansgaard and Johnsen, 1969; Ashmore et al., 2020; Bodart et al., 2021; Sanderson et al., 2024); or using more complex multidimensional (2D/3D) models in areas with challenging ice-flow or bed conditions (e.g., Waddington et al., 2007; MacGregor et al., 2015a; Parrenin et al., 2017; Lilien et al., 2021).

## 4 RES data availability and quality for characterising Antarctica's internal architecture

RES data have been acquired across Antarctica spanning six decades. An impression of the history can be gained from the periodic release of maps of subglacial topography, the first by Drewry (1975) and Drewry (1983; Antarctica Glaciological and Geophysical Folio Sheet 9), and then through the Bedmap series, now in its third iteration (Frémand et al., 2023, their Fig. 1; Pritchard et al., 2025). However, those maps and associated papers focus only on where the RES data were used to pick an echo at the bed, and do not provide information on whether the constituent surveys also imaged internal architecture. Here, therefore, we will outline the sequential development of airborne RES systems and surveys across Antarctica focussing on their attributes and availability for imaging and analysing internal architecture (Section 4.1). We will then briefly introduce some wide-ranging *ground-based* RES surveys that complement the overall database available for interrogating internal architecture (Section 4.2), and conclude with a "progress report" of existing traced radiostratigraphy across Antarctica (Section 4.3).

### 4.1 Evolution and availability of airborne RES for internal architecture

Airborne RES surveying across Antarctica has undergone three key technology-led developments as follows. Firstly, there has been a transition from initially recording RES data onto analogue tape recorders or film to inputting data directly into more sophisticated digital recording systems. Secondly, there has been the introduction of Global Navigation Satellite System (GNSS) systems to onboard flight navigation. Thirdly, there has been a progression from all datasets being acquired incoherently, wherein RES data receipt and recording were not phase-matched, to RES acquisition with coherent RES systems, for which the phase of the transmitted signal is preserved in a reference signal with which the received signal is compared, greatly increasing the clarity and quality of the imaging, which is especially pertinent for the analysis of internal architecture. The following subsections and Fig. 6 describe what may accordingly be termed three main eras of airborne RES surveying over the Antarctic ice sheets.

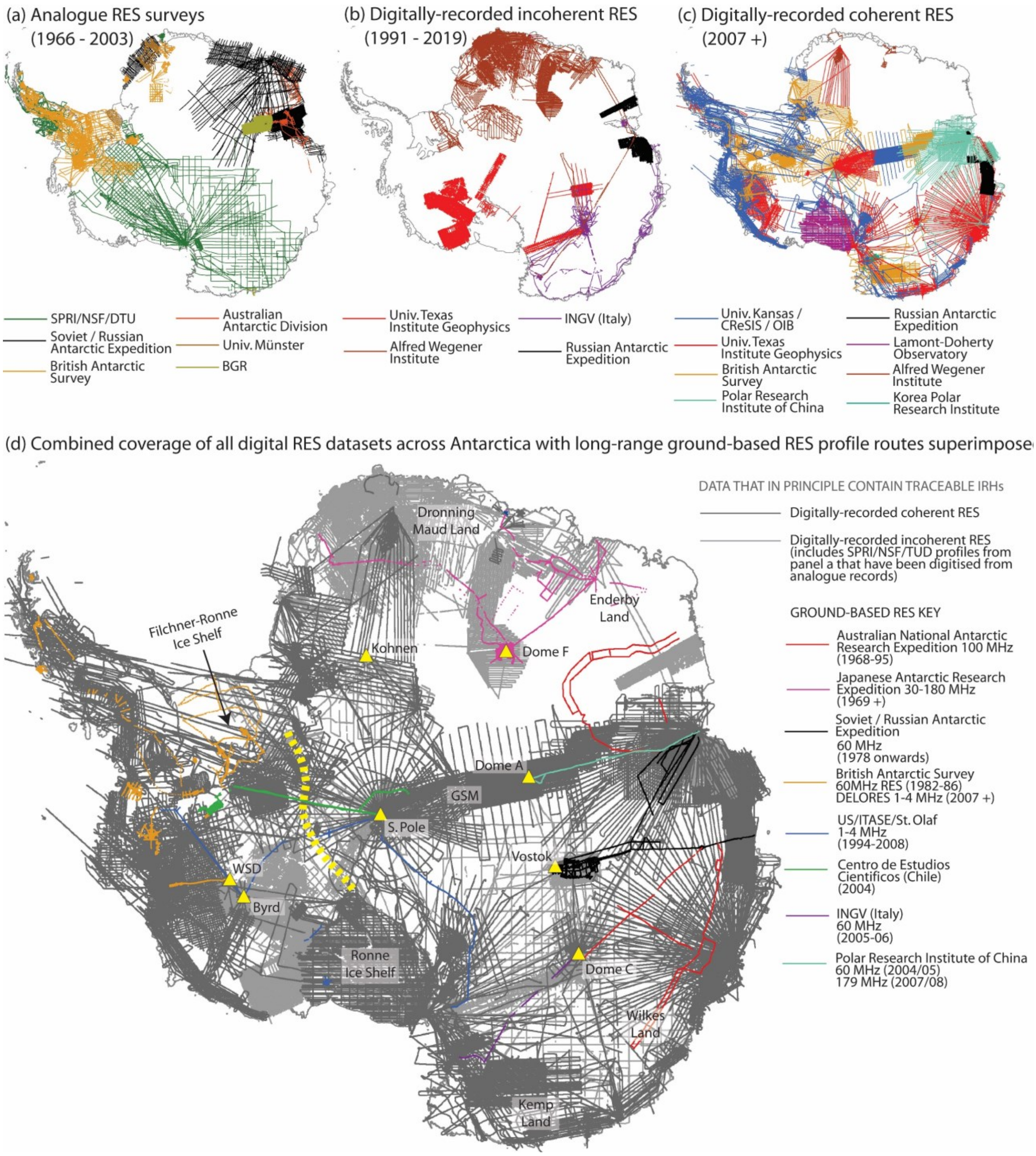


**Figure 6.** RES coverage and suitability for tracing internal architecture across Antarctica. (a) Airborne RES profiles acquired with analogue RES systems between 1966 and 2003. SPRI/NSF/DTU = Scott Polar Research Institute/National Science Foundation/Technical University of Denmark; BGR = Bundesanstalt für Geowissenschaften und Rohstoffe (Germany's Federal Institute for Geosciences and Natural Resources). (b) Airborne RES profiles acquired digitally but incoherently between 1991 and 2019. INGV = Istituto Nazionale di Geofisica e Vulcanologia (Italy's National Institute of Geophysics and Volcanology). (c) Airborne RES profiles acquired digitally and coherently since 2007. Univ. Kansas / CReSIS / OIB = data acquired using systems designed by University of Kansas, often under the auspices of the USA's Centre for Remote Sensing and Integrated Systems and/or NASA's Operation IceBridge. (d) Map of all digitally-acquired airborne RES profiles (two shades of grey) and long-range ground-based RES profiles (coloured tracks) that collectively represent all data presently available for analysing internal architecture through Antarctica. The coverage of digitally-recorded incoherent RES (light grey) includes the originally analogue but now digitised SPRI/NSF/TUD data collected between 1971 and 1974. RES profile locations depicted in this map from Frémand et al. (2023, Tables S1 and S2). US/ITASE/St. Olaf = data acquired by radar system and operators from St. Olaf College, USA, often under the auspices of the International Trans-Antarctic Expedition (Mayewski et al., 2005). Also annotated in panel (d) are key locations mentioned in this paper, with yellow triangles
408 marking key deep-ice-core sites. The yellow dashed line marks the nominal divide between the West Antarctic and

### 4.1.1 Analogue data recording

Before the 2000s, the majority of airborne RES data across Antarctica were recorded onto analogue tape recorders or film, and most of these data, including all data acquired prior to the 1990s, were acquired without GNSS being available for accurate navigation. Due to the analogue recording, all such systems recorded data incoherently. The coverage of these analogue surveys is shown in Fig. 6a.

Continent-spanning RES surveying was pioneered across West Antarctica and around half of East Antarctica by the UK-based Scott Polar Research Institute (SPRI), with key logistical support from the USA's National Science Foundation and, from 1971, using antennas designed and installed by engineers from the Technical University of Denmark (DTU), which fundamentally improved the reflection of IRHs (Swithinbank, 1969; Evans and Smith, 1970; Gudmandsen et al., 1975; Drewry, 2023). Also through the late 1960s and 1970s, and continuing through the 1980s, the Soviet Antarctic Expedition conducted airborne surveying across parts of East Antarctica (Popov, 2020) (Fig. 6a). Both the SPRI-NSF-TUD and Soviet campaigns used a 60 MHz centre-frequency RES system, inspiring the British Antarctic Survey (BAS) to adopt the same centre frequency as it commenced progressive regional RES surveys through the 1980s (Fig. 6a).

The 1990s saw a step-change improvement in flight navigation and concomitant RES-dataset positioning with the introduction of GNSS. The 1990s was also a period of transition, with some RES operators developing the capacity to acquire data digitally and coherently (as expanded in Sections 4.1.2 and 4.1.3), but other major data providers, such as the British Antarctic Survey and Russian (formerly Soviet) groups continuing to record data only in analogue format, hence also incoherently. These analogue surveys, supplemented by some regional surveys across East Antarctica over the same era by groups from Australia (e.g., Morgan et al., 1982) and Germany (e.g., Thyssen and Grosfeld (1988); Damaske and McLean (2005)), are depicted in Fig. 6a.

### 4.1.2 Digital data recording, incoherent RES

Digital recording systems were first implemented in Antarctic airborne RES surveying in the early 1990s by the USA-based University of Texas Institute of Geophysics (UTIG). UTIG's surveys through the 1990s, principally of West Antarctica, used adapted versions of the 60 MHz SPRI-NSF-DTU incoherent RES system (Blankenship et al., 2001; Carter et al., 2007; Young et al., 2016). In the mid-1990s, national operators from Germany and Italy also commenced digital acquisition of incoherent RES surveys across parts of East Antarctica, both using RES systems operating around a higher centre frequency of 150 MHz (Steinhage et al., 2001; Eisen et al., 2007; Tabacco et al., 2008; Zirizzoti et al., 2008). The full coverage of airborne RES data acquired digitally with incoherent RES systems is depicted in Fig. 6b. It includes data acquired broadly from the early 1990s to the mid 2000s, although some operators continued to acquire data incoherently into the mid 2010s.

#### 4.1.3 Digital data recording, coherent RES

Fully coherent RES systems were first operated in Antarctica by the USA-based University of Kansas on a joint USA (NASA; National Aeronautics and Space Administration) / Chile (CECs; Centro de Estudios Científícos) mission to survey fast-changing regions of West Antarctica (Rignot et al., 2004). In 2005, Kansas became host to the USA's Center for Remote Sensing and Integrated Systems (previously Center for Remote Sensing of Ice Sheets; CReSIS), an NSF-designated national Science and Technology Centre with a focus on ice-sheet sounding; and began to operate an upgraded series of deep-looking RES systems with centre frequencies of ~190-194 MHz named Multichannel Coherent Radar Depth Sounders (MCoRDS), which were deployed widely across Antarctica between 2009 and 2019 as part of NASA's Operation IceBridge programme (Fig. 6c; Rodriguez-Morales et al., 2013; MacGregor et al., 2021).

From 2004 onwards, both BAS and UTIG transitioned their RES systems into coherent data acquisition, with this year also marking BAS' first implementation of digital data recording. BAS' Polarimetric Radar Airborne Science Instrument (PASIN) has a centre frequency of 150 MHz, and transmits two waveforms, a narrow pulse (0.1 µs) for detecting shallow radiostratigraphy in the upper 2 km of the ice column, and a deep-sounding chirp (4 µs) for detecting deeper radiostratigraphy and the bed (Corr et al., 2007; Hélière et al., 2007; see Fig. 2 for examples of each). PASIN was upgraded in the mid-2010s to enable the acquisition of swaths (i.e. wide strips) of RES data to map the ice-sheet bed (Arenas-Pingarrón et al., 2023). UTIG integrated a coherent 60 MHz centre-frequency RES system (Moussessian et al., 2000) with radio-frequency hardware from DTU to allow high-power coherent recording, which enabled synthetic-aperture-radar (SAR) processing of acquired data (Peters et al., 2005; Peters et al., 2007; refer back to Sect. 3.1 for description of SAR processing). This initial High-Capability Radar Sounder (HiCARS) system was translated to commercially available components (HiCARSII) which were incorporated from the mid-2010s into the subsequent Multifrequency Airborne Radar-sounder for Full-phase Assessment (MARFA), capable of cross-track interferometry for clutter discrimination (Castelletti et al., 2017; Scanlan et al., 2020).

Other airborne RES operators transitioned into coherent RES across Antarctica during the mid-2010s. Alongside continuing surveying by BAS, CReSIS and UTIG, large volumes of coherent RES data have been acquired across Antarctica over the last decade by the Russian Antarctic Expedition (Popov, 2020; Popov, 2022), Germany's AWI using an improved version of CReSIS' MCoRDS system (Humbert et al., 2018; Karlsson et al., 2018; Winter et al., 2019a; Wang et al., 2023; Franke et al., 2025), as well as the Polar Research Institute of China (PRIC; Cui et al., 2020ba; 2020b; 2020c) and the Korean Polar Research Institute (KOPRI; Lindzey et al., 2020; Lee et al., 2021) (Fig. 6c).

### 4.2 Ground-based RES datasets

Since the 1960s, groups from at least twelve institutions have acquired ground-based RES datasets focussed on sounding Antarctica's subglacial bed and have also typically imaged internal architecture in the process. Typically, ground-based surveys have been confined to smaller regions or shorter profiles than covered by the airborne RES surveys, befitting the more common application of ground-based RES to detailed site surveys in preparation for retrieving ice cores, or for accessing the ice bed or subglacial lakes (e.g., Frezzotti et al., 2004; Laird et al., 2010; Christianson et al., 2012; Ross et al., 2020). From these surveys, several local radiostratigraphies have been published (e.g., Eisen et al., 2005; Jacobel and Welch, 2005; Koutnik et al., 2016; Cavitte et al., 2023; Chung et al., 2023). These detailed studies provide invaluable seeding points for extending radiostratigraphies much more widely across the ice sheets (e.g., Winter et al., 2019a) and for understanding better ice-sheet history and glaciological processes.

Supplementing the more local surveys, some ground-based profiles have been acquired over traverses of multiple 100s of km over the Antarctic ice sheets, and these traverses, marked on Fig. 6d, merit special attention as potential resources for analysing pan-continental radiostratigraphy. A particularly extensive programme of ground-based surveys has been conducted since 1969 by the Japanese Antarctic Research Expedition (JARE) connecting coastal East Antarctica in Dronning Maud and Enderby Land to Dome F, with data from some of these traverses conducted in the 1990s underpinning seminal work on the origins of IRHs (Fujita et al., 1999; Matsuoka et al., 2003). Today, data from JARE represent some of the most spatially extensive of Antarctica's ground-based RES datasets and a rich repository of internal architecture (Fujita et al., 2011; Van Liefferinge et al., 2021; Tsutaki et al., 2022). Further long ground-based RES traverses were acquired by several national and international teams in the 2000s under the auspices of the International Trans-Antarctic Scientific Expedition (ITASE). RES profiles containing particularly rich internal architecture were acquired by the USA-NSF's ITASE traverses across both West (Welch and Jacobel, 2003; Jacobel and Welch, 2005) and East Antarctica (Welch et al., 2009), with findings from Arcone et al. (2012a) suggesting that in some parts of East Antarctica the radiostratigraphy is unconformable and may present significant challenges to tracking radiostratigraphy.

### 4.3 Progress report

#### 4.3.1 Summary of available data

Fig. 6d shows the coverage of RES profiles acquired across Antarctica that are, in principle, available for developing a pan-Antarctic stratigraphy. This includes all RES data acquired digitally, whether coherent or incoherent. Generally, RES data that are acquired coherently are the highest quality for tracing unbroken IRHs over long distances, but incoherent data can also be utilised for IRH tracing. Fig. 6d therefore also only includes data that were acquired by GNSS navigation, with one exception: the 1970s SPRI-NSF-TUD data are included because they imaged IRHs across Antarctica with a clarity that rivals many modern RES surveys and form potentially vital links across otherwise unsurveyed regions, and consequently have been "revived" by a dedicated fine-resolution digitisation and distribution programme (Schroeder et al., 2019; Schroeder et al., 2022). Navigational uncertainties inherent to pre-GNSS navigation remain with these data (of the order of several kms), but there is a prospect of using crossovers with more modern datasets to reconstruct the navigation with improved accuracy (Teisberg and Schroeder, 2023).

#### 4.3.2 Existing dated radiostratigraphy across Antarctica

Prior to the inception of *AntArchitecture* in 2018, several studies had produced radiostratigraphies spanning the last 17.5 ka across West Antarctica and 352 ka for East Antarctica (e.g., Hodgkins et al., 2000; Siegert and Hodgkins, 2000; Siegert, 2003; Siegert and Payne, 2004; Jacobel and Welch, 2005; Leysinger Vieli et al., 2011; Steinhage et al., 2013; Karlsson et al., 2014; Wang et al., 2016). However, the spatial extents of these radiostratigraphies were relatively limited. Through *AntArchitecture*, a more coordinated and focused approach to characterising Antarctic radiostratigraphy has been conducted, as depicted in Fig. 7 and detailed in Table 1. This programme has facilitated the recovery and characterisation of several isochrones with ages up to 25 ka across much of the Amundsen and Weddell Sea sectors of West Antarctica (Muldoon et al., 2018; Ashmore et al., 2020; Bodart et al., 2021; Bodart et al., 2023). Over East Antarctica, a much older record has been extracted, owing to the more stable and slow-flowing ice conditions in the area, including isochrones dating back to the last 705 ka (Cavitte et al., 2016; Winter et al., 2019a; Beem et al., 2021; Cavitte et al., 2021; Chung et al., 2023; Wang et al., 2023; Sanderson et al., 2024; Franke et al., 2025).

A notable finding is the presence of widespread and ubiquitous isochrones that have been imaged by different RES systems and are found in several ice-core records. Across West Antarctica, the most prevalent isochrone, dated precisely and independently at Byrd and WAIS Divide ice cores to ~4.7 ka, has been identified by several studies (Jacobel and Welch, 2005; Karlsson et al., 2014; Holschuh et al., 2018; Muldoon et al., 2018; Ashmore et al., 2020; Bodart et al., 2021; Bodart et al., 2023). There is evidence that this same isochrone may also be found widely across East Antarctica, based on sulphate concentrations in ice cores and findings from individual RES surveys across the region (Steinhage et al., 2013; Winski et al., 2019; Beem et al., 2021; Cole-Dai et al., 2021; Sigl et al., 2022). Additionally, across much of the West Antarctic Ice Sheet an isochrone dated at 17.5 ka has been observed in both ground-based and airborne RES data (Jacobel and Welch, 2005; Muldoon et al., 2018; Bodart et al., 2021). This 17.5 ka RES isochrone has been identified and linked to an eruption from West Antarctica's Mount Takahe in both the Byrd (Hammer et al., 1997) and WAIS Divide (McConnell et al., 2017) ice cores. Over East Antarctica, packages of closely spaced isochrones of ages ~38 ka, ~73 ka, ~128 ka, ~160 ka, and ~170 ka have been traced from ice cores (Leysinger Vieli et al., 2011; Winter et al., 2019a; Cavitte et al., 2021; Wang et al., 2023; Sanderson et al., 2024; Franke et al., 2025); notably, the ~73 ka isochrone has been linked by ice-core profiling to the Toba Eruption in Indonesia

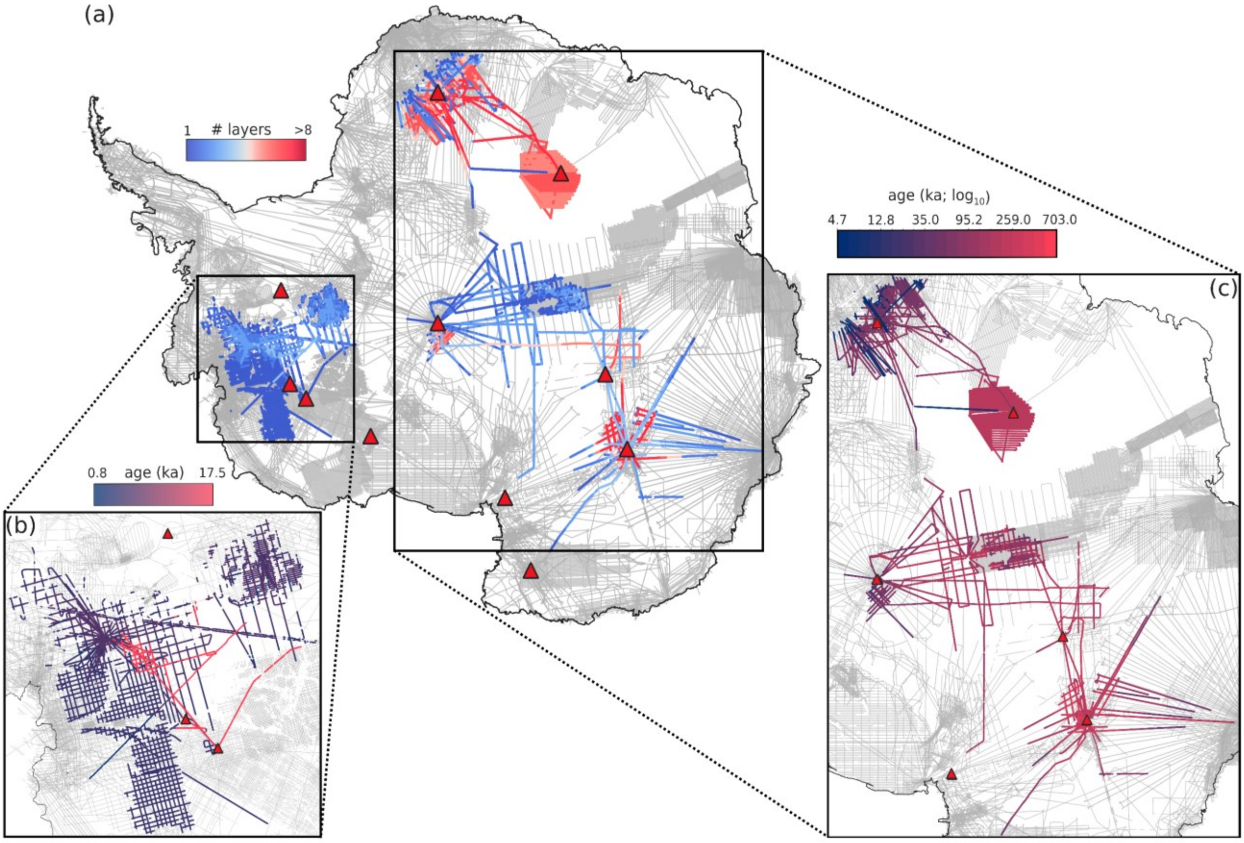


**Figure 7.** Existing open-access dated stratigraphies across Antarctica obtained from the Digital Object Identifiers (DOIs) provided in Table 1, with RES profiles for Bedmap-2 and Bedmap-3 products shown in the background (grey; Frémand et al., 2023). Existing deep ice cores (defined here as ice cores that have been drilled to near the ice-bed interface and that provide a multi-millennial record) are shown as red triangles. (a) Maximum number of isochrones traced through each dataset (from 1 to >8); see Table 1 for full details (b-c) Age of the deepest (oldest) isochrone across each dataset for the WAIS (b) and EAIS (c) regions respectively. Note that the scale used for (c) is logarithmic.

(Svensson et al., 2013). Together, such distinct isochrones, imaged by and from multiple RES systems and platforms, provide important regional or continental-wide time markers, equivalent to Greenland's highly recognisable "three sisters" (Fahnestock et al., 2001a; MacGregor et al., 2015a; 2025) for inferring past changes at specific time intervals.

Despite the advances discussed here, the established radiostratigraphy across the Antarctic ice sheets currently represents only a small subset of the total available RES data (Fig. 7, and refer back to Sect. 4.3 and Fig. 6). The establishment of the *AntArchitecture* community, and its commitment to establish protocols for sharing and processing internal architecture across the multiple datasets, is expected to facilitate further isochrone tracing, which will in turn contribute to the development of the first three-dimensional age-depth model of the ice sheet.

**Table 1.** Inventory of expansive radiostratigraphic datasets for the Antarctic ice sheets, ordered by region and cumulative distance of dataset (cumulative distance here corresponds to the total km of isochrone profiles summed for each isochrone where the data are openly available (via use of a DOI), or approximated value where datasets are not publicly available). Openly available datasets are shown in Figure 7; locations of ice cores are marked on Fig. 6d. Data-provider acronyms provided at foot of table; in most cases we also list here a specific project acronym for each survey which can be cross-referenced through the reference and/or dataset listed in each row.

(For EGUsphere formatting, this 10-column table is presented across two pages.)

| **Region** | **Survey dates** | **Data provider (acronyms expanded at foot of table)** | **Survey name / acronym** | **Ice-core intersection(s)** | **No. of traced isochrones** |
|---|---|---|---|---|---|
| EAIS | 1996 – 2023 | AWI / CReSIS | EPICA / DML | Kohnen / Dome F | 9 |
| EAIS | 2016 - 2017 | AWI | Beyond EPICA Dome Fuji | Dome F | 7 |
| EAIS | 1998 - 2008 | AWI / CReSIS | DoCo / EPICA / AGAP | Kohnen / Dome F / Vostok / Dome C | 5 |
| EAIS | 2007 - 2016 | BAS | AGAP / PolarGap | South Pole | 3 |
| EAIS | 1974 – 1979 | SPRI-NSF-DTU | - | Vostok / Dome C | 12 |
| EAIS | 2016 – 2018 | BAS | Beyond EPICA Little Dome C | Dome C | 20 |
| EAIS | 2008 - 2018 | UTIG | ICECAP | Dome C | 26 |
| EAIS | 1974 – 1979 | SPRI/NSF/DTU | - | Vostok | 15 |
| EAIS | 1974 – 1979 | SPRI/NSF/DTU | - | Vostok / Dome C / Dome A / South Pole | 15 |
| EAIS | 2016 – 2017 | PRIC | South Pole Corridor | South Pole | 8 |
| EAIS | 2002 – 2003 | AWI | - | Kohnen / Dome F | 8 |
| EAIS | 2019 – 2020 | UA / AWI | Beyond EPICA Little Dome C | Dome C | 19 |
| EAIS | 2004 – 2005 | PRIC | Dome A (CHINARE-21) | Vostok | 6 |
| WAIS | 2004 – 2018 | BAS / CReSIS | BBAS / OIB | WAIS Divide | 4 |
| WAIS | 1991 – 2014 | UTIG | CASERTZ / SOAR / AGASEA / GIMBLE | Byrd / WAIS Divide | 1 |
| WAIS | 2010 – 2011 | BAS | IMAFI | - | 3 |
| WAIS | 1977 – 1978 | SPRI-NSF-DTU | - | Byrd | 5 |
| WAIS | 2000 – 2001 | NSF | ITASE | Byrd | 1 |

**Table 1** continued: Columns 6-10.

| Isochrone age range (ka) | Cumulative distance of traced IRHs (km) | Dataset Reference | Dataset DOI |
|---|---|---|---|
| 4.8 – 91.0 | 203 500 | Franke et al. (2025) | 10.1594/PANGAEA.973266 |
| 31.4 – 232.7 | 110 000 | Wang et al. (2023) | 10.1594/PANGAEA.958462 |
| 38.0 – 161.0 | 40 000 | Winter et al. (2019a) | 10.1594/PANGAEA.895528 |
| 38.0 – 162.0 | 30 400 | Sanderson et al. (2024) | 10.5285/cfafb639-991a-422f-9caa-7793c195d316 |
| 17.5 – 352.4 | 30 245 | Leysinger Vieli et al. (2011) | 10.1029/2010JF001785 |
| 10.5 – 414.6 | 24 820 | Chung et al. (2023) | 10.1594/PANGAEA.963470 |
| 10.0 – 705.0 | 15 500 | Cavitte et al. (2021) | 10.15784/601411 |
| 17.0 – 211.0 | 15 000 | Leysinger Vieli et al. (2004) | - |
| 45.9 – 169.7 | 13 300 | Siegert (2003) | - |
| 4.7 – 93.9 | 12 100 | Beem et al. (2021) | 10.15784/601437 |
| 4.7 – 72.4 | 9 700 | Steinhage et al. (2013) | - |
| 73.7 - 476.4 | 3 000 | Chung et al. (2023) | 10.1594/PANGAEA.957176 |
| 34.3 – 161.4 | 1 300 | Wang et al. (2016) | - |
| 2.3 – 16.5 | 30 700 | Bodart et al. (2021) | 10.5285/f2de31af-9f83-44f8-9584-f0190a2cc3eb |
| 4.7 | 19 000 | Muldoon et al. (2018) | 10.15784/601673 |
| 1.9 – 8.1 | 13 700 | Ashmore et al. (2020) | 10.5281/zenodo.4945301 |
| 0.8 – 16.0 | 2 400 | Siegert and Payne (2004) | 10.1002/esp.1238 |
| 17.5 | 1 000 | Jacobel and Welch (2005) | 10.7265/N5R20Z9T |

Data providers:
AWI = Alfred-Wegener Institute, Germany
BAS = British Antarctic Survey, UK
CReSIS = Centre for Remote Sensing and Integrated Systems, USA
NSF = National Science Foundation, USA
PRIC = Polar Research Institute of China
SPRI/NSF/DTU = Scott Polar Research Institute/National Science Foundation/Technical University of Denmark
UA = University of Alabama, USA
UTIG = University of Texas Institute of Geophysics, USA

## 5 Applications of internal architecture to wider Antarctic science

Here, we now review to what scientific purposes internal architecture has already been exploited. Sect. 5.1 to 5.4, supported by Fig. 8, exemplify four primary applications of RES-imaged isochrones, Sect. 5.5 explores the scientific applications of other forms of internal architecture, and Sect. 5.6 discusses how radiostratigraphic data have been incorporated into numerical modelling, and their use in calibrating ice-sheet models of varying complexity. This section contextualises the following Sect. 6 which then suggests priorities for future research that will be enabled as Antarctica's internal architecture, and particularly its radiostratigraphy, continue to be explored and made available.

### 5.1 Radiostratigraphy and ice cores

Ice cores from Antarctica provide fundamental palaeoclimate records (e.g., EPICA Community Members, 2004; WAIS Divide Project Members, 2015). The layering found in ice cores is also visible in radiostratigraphy, as a function of the RES-system resolution (Section 2), and we have already introduced the concept that RES records tied to existing ice cores provide a basis for extending these "point-source" age-depth chronologies into 3-D age-depth fields that extend widely across the Antarctic ice sheets (cf. Sect. 3.4 and 4.3.2). Conversely, RES-imaged radiostratigraphy can be used to guide the best locations for recovering future ice cores. Accumulation rate, ice dynamics and age-depth relationships extracted from isochrones have previously informed the appropriateness of coring sites (e.g., Neumann et al., 2008; Parrenin et al., 2017; Beem et al., 2021; Wang et al., 2023) and have been essential for pre-site survey of potential future ice coring, e.g. for the *Oldest Ice* endeavour of the International Partnerships for Ice Core Sciences (IPICS; e.g., Fischer et al., 2013; Van Liefferinge and Pattyn, 2013; Karlsson et al., 2018; Lilien et al., 2021; Chung et al., 2023).

Radiostratigraphy has also provided opportunities for synchronising and reducing uncertainties in ice-core chronologies by facilitating the direct tracing of isochrones between two or more ice cores in order to correlate ice-core chronologies (as achieved for the Greenland Ice Sheet by MacGregor et al., 2015a; see Fig. 8b). In Antarctica, previous studies that have used isochrones to correlate chronologies between ice cores include Siegert et al. (1998), Steinhage et al. (2013), Cavitte et al. (2016), Le Meur et al. (2018) and Winter et al. (2019a) for East Antarctica, and Muldoon et al. (2018) for West Antarctica. These studies have provided confidence that ice cores obtained from locations separate by 100s of km capture analogous variations in palaeoclimate at regional scales, and that the signals recorded by RES correspond to genuine physical variations in the ice (typically variations in electrical conductivity, often related to fallout from past volcanic eruptions; as noted in Sect. 4.5).

The key challenge in synchronising ice-core records between distant sites using RES has been in resolving the radiostratigraphically- and ice-core-derived chronologies between each ice-core site, given the order-of-magnitude difference in resolution of chronologies recoverable from RES (on the order of metres) versus ice-core records (on the order of centimetres). This has typically been dealt with using forward modelling based on electrical-conductivity measurements or dielectric profiling of the ice cores to provide a transfer function (e.g., Miners et al., 1997; Hempel et al., 2000; Eisen et al., 2003; Eisen et al., 2006; Winter et al., 2017; Mojtabavi et al., 2022), or by adopting Bayesian frameworks which provide a probability distribution of the age of the isochrones (Muldoon et al., 2018). Thus, while the age-depth fields compiled from isochrones will never match the precision and accuracy of ice-core age-depth relationships (MacGregor et al., 2015a; Winter et al., 2017), they provide the spatial context that 'point-source' ice cores cannot. Through isochrone-constraint modelling (see Sect. 5.6), the age of the ice and its spatial distribution can be more effectively constrained in regions distant from the current drilling sites (Born and Robinson, 2021; Sutter et al., 2021).

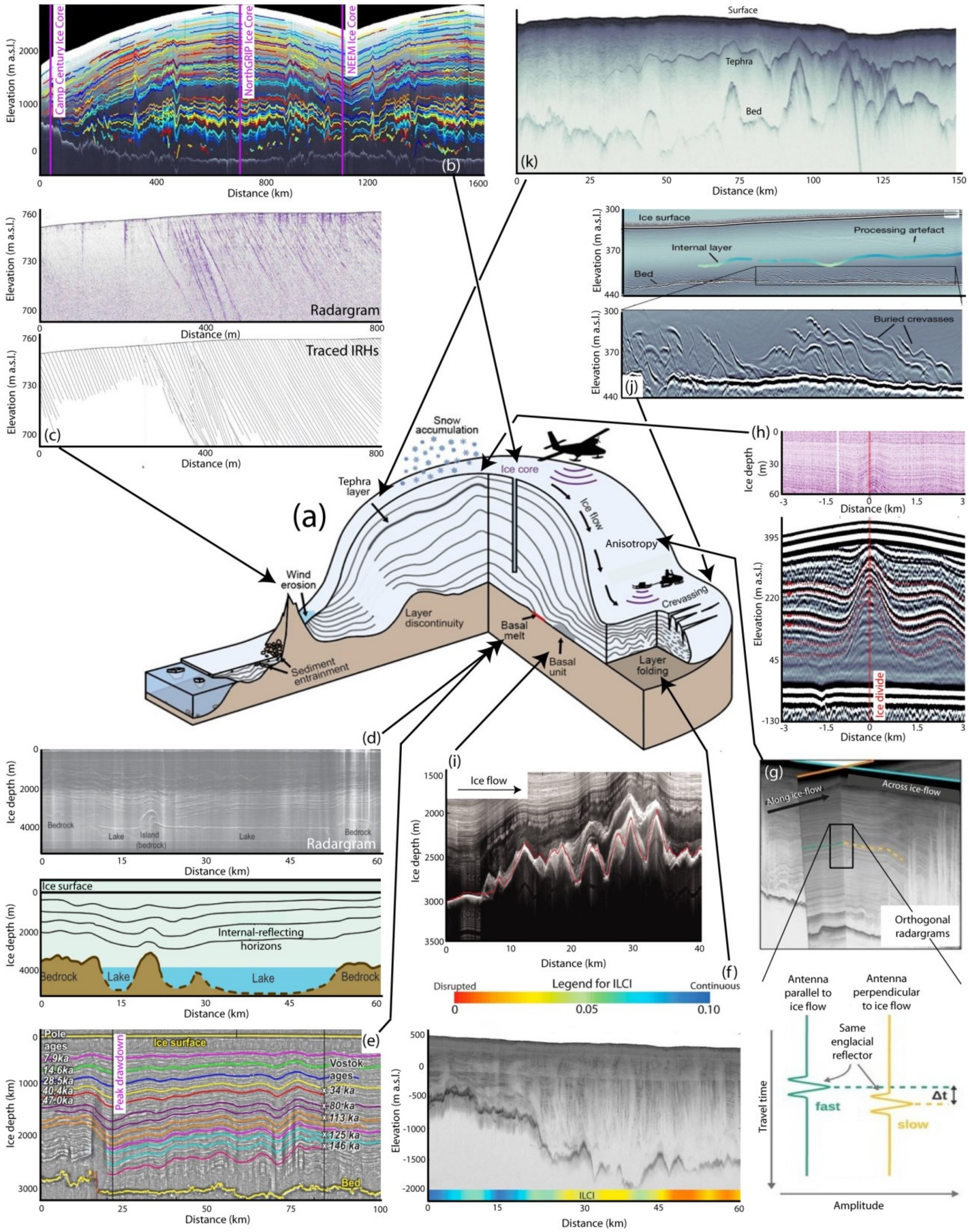

**Figure 8.** Schematic illustration of radiostratigraphic observations within an ice sheet and their scientific applications; (a), in the centre, depicts typical ice-sheet locations for applications shown in subsequent panels. (b) Connecting and validating ice cores in Greenland (after MacGregor et al., 2015a). (c) Imaging intersections of IRHs with ice surface in region of surface wind scouring (after Winter et al., 2016). (d) Using isochrones to calculate basal melting across Subglacial Lake Vostok (after Siegert et al., 2001). (e) Using isochrone drawdown to locate region of elevated geothermal heat flux near South Pole (after Jordan et al., 2018). (f) Application of "Internal Layering Continuity Index" (ILCI) to quantify disruption (folding/warping) to otherwise continuous isochrones (after Bingham et al., 2015). (g) Using intersecting RES profiles to explore ice anisotropy (after Gerber et al., 2023). (h) Raymond Arch imaged in near-surface (top panel) and deep RES across Derwael Ice Rise, Dronning Maud Land (after Drews et al., 2015). (i) Basal-ice units and suggested accreted basal ice in East Antarctica (after Bell et al., 2011). (j) Basal crevasses imaged in West Antarctica and used to date regrounding of previously floating ice (after Kingslake et al., 2018). (k) Prominent tephra horizon imaged by RES across Pine Island Glacier, West Antarctica (after Corr and Vaughan, 2008).

In marginal locations of the ice sheets, or around nunataks, where persistent pronounced surface scouring is co-located with upward ice flow over subglacial topography – i.e., in regions of so-called "blue ice" – very old ice may outcrop obliquely to the ice surface and hence allow the recovery of a "horizontal ice core" along the ice surface (Spaulding et al., 2013). Dated isochrones have been used to trace the age-depth model recovered from horizontal ice cores back into the ice sheet (Reeh et al., 2002; Siegert et al., 2003a; Winter et al., 2016; Fogwill et al., 2017; Baggenstos et al., 2018; see Fig. 8c). However, shearing and folding can disrupt the stratigraphic order of the outcropping IRHs, rendering the interpretation of their radiostratigraphy more complex than for most vertical ice cores.

### 5.2 Surface mass balance

Successive snowfall events create a record of progressively buried isochrones which can be observed in radargrams. In slow-flowing ice and especially around ice divides, the depth of isochrones is largely controlled by surface mass balance and therefore dated radiostratigraphy has made it possible to reconstruct past surface mass balance over millennial timescales across spatially extensive regions (e.g., Nereson et al., 2000; Siegert, 2003; Siegert and Payne, 2004; Eisen et al., 2005; Waddington et al., 2007; Neumann et al., 2008; MacGregor et al., 2009; Leysinger Vieli et al., 2011; Karlsson et al., 2014; Koutnik et al., 2016; Cavitte et al., 2018; Bodart et al., 2023). Such records have fundamentally informed us about how mass balance has changed with time over past millenia, for example showing that accumulation rates changed significantly over central (Siegert and Payne, 2004; Neumann et al., 2008; Koutnik et al., 2016; Bodart et al., 2023) and coastal (Karlsson et al., 2014) West Antarctica throughout the Holocene. Typically, vertical strain rates must be corrected for the whole ice column, particularly in regions of (present or past) fast flow, or there is a need to account for basal processes such as enhanced basal melting (e.g., Leysinger Vieli et al., 2011; Chung et al., 2023), because in such cases the isochrone depths will be dynamically modified and therefore will not represent the surface mass balance at the time of deposition (e.g., Koutnik et al., 2016). Where the radiostratigraphy has not been impacted significantly by strain, the shallow-layer approximation can be applied, which allows us to ignore these strain-rate corrections (Waddington et al., 2007). If horizontal advection influences the stratigraphy 2D, 2.5D or 3-D modelling is required (see Sect. 5.6).

Regions of unconformable radiostratigraphy occurring throughout the ice column in parts of Antarctica have partly limited the extent to which some surface mass balance records could be more widely extrapolated (Arcone et al., 2012b; Cavitte et al., 2016). RES surveys of the upper ~100 m of the ice column in the affected regions typically reveal widespread conformal, annual horizons modified by local variations in accumulation or ice flow (Eisen, 2008), and the majority of them have been ascribed to wind scouring out surface deposits and forming "megadunes" (Das et al., 2013; Traversa et al., 2023) that then become progressively buried as sets of unconformable IRHs. Studies have identified such unconformities in several locations in East

Antarctica (Welch and Jacobel, 2005; Traversa et al., 2023) and West Antarctica (Woodward and King, 2009; Holschuh et al., 2018).

### 5.3 Basal melting and geothermal heat flux

The presence of a subglacial water body or enhanced geothermal heat flux draws isochrones down towards the ice base. Exploiting this principle, isochrones have been used to calculate melting at the base of the ice. Mismatches between surface-accumulation-driven modelled isochrones and traced isochrones have been used to infer regions of enhanced basal melting in Greenland (Dahl-Jensen et al., 1997; Fahnestock et al., 2001b) and Antarctica (Carter et al., 2009) on the principle that removal of ice at the base by basal melting thins annual layers above. However, for locating areas of enhanced geothermal heat flux (or subglacial lakes, which may sometimes owe their existence to enhanced geothermal heat flux) researchers now typically rely more on analysing the reflectivity or specularity of the ice-bed echo in RES data (e.g., Young et al., 2016; Chu et al., 2021), and only use isochrones to guide derivations of basal melting where such more direct data are lacking.

Isochrones have been analysed in more detail over parts of Antarctica to constrain basal melting in more localised settings. For example, Siegert et al. (2000) used deviations in the dip of deep isochrones away from parallelism with the ice-bed/subglacial-lake surface over Subglacial Lake Vostok to calculate basal melting and water exchange between the lake and the overlying ice sheet (Fig. 8d). Jordan et al. (2018) identified isochrones dipping towards the bed ~200 km from the South Pole (Fig. 8e), and used these to model how much basal melt would be required to draw the isochrones down towards the bed. By assuming that minimal frictional melting would be generated by the slow ice flow in this region, they showed that the most likely cause of the isochrones being drawn down towards the bed must be enhanced geothermal heat flux in this region. Ross and Siegert (2020) undertook a detailed survey of isochrone geometry over Subglacial Lake Ellsworth, West Antarctica, and showed that the isochrones were preferentially drawn down over the NW shoreline of the lake, rather than the lake itself. This conclusion was in agreement with the pattern of basal mass balance derived from previous numerical modelling of water circulation in the lake and indicated very high basal melting of ~16 cm $a^{-1}$ on its northern shoreline.

### 5.4 Ice-flow dynamics

Moving ice causes IRHs that were originally deposited flat at the surface to deform through folding, tilting and disruption. Therefore, deformed isochrones may be analysed to interpret past ice-flow dynamics. Present-day (last ~35 years) information on ice-flow dynamics is derived from satellite monitoring of ice-surface flow (Rignot et al., 2017), but to understand fully where and how ice-flow dynamics have changed over the past several thousand years, and hence may be likely to do so again, researchers have interrogated how changes to ice-flow dynamics have been imprinted into the RES-imaged internal architecture. The most common methodology has been to explore and classify where the radiostratigraphy diverges from relatively flat isochrones to profiles that show folding (a.k.a. buckling, warping or disruption) of the isochrones (Fig. 8f). Wherever there is folding of isochrones, it is an indication that the ice has experienced considerable strain, often as a result of flowing around or over significant bedrock obstacles (Robin and Millar, 1982; Hindmarsh et al., 2006; Tang et al., 2022) or becoming variously stretched and compressed as it flows through an ice-stream onset region or through ice-stream shear margins (Jacobel et al., 1993; Bell et al., 1998; Ng and Conway, 2004; King, 2011). Overall, isochrone folding can indicate convergent ice flow, anisotropic rheology, basal freeze-on, basal sliding, non-negligible transverse velocity gradients, or the abutting of units of contrasting rheology. Importantly, the signature recorded by these processes is often advected downstream, so that where it is observed does not necessarily indicate where the folding took place (Weertman, 1976; Jacobel et al., 1993; Leysinger Vieli et al., 2004; NEEM Community Members, 2013; Wolovick et al., 2014; Bons et al., 2016; Leysinger Vieli et al., 2018; Ross et al., 2020; Franke et al., 2021; Jennings and Hambrey, 2021; Jansen et al., 2024). In certain cases, relict folds that do not correspond to the current ice-flow direction indicate a past change in ice-flow direction (Conway et al., 2002; Siegert et al., 2004; Rippin et al., 2006; Franke et al., 2022).

While, therefore, there are multiple origins for isochrone folding, their geographical association with fast ice flow has led to their presence being used as a broad diagnostic of the long-term stability (or otherwise) of ice flow around Antarctica (e.g., Rippin et al., 2003; Siegert et al., 2003b; Bingham et al., 2007; Karlsson et al., 2009; Ross et al., 2011; Bingham et al., 2015; Winter et al., 2015; Sanderson et al., 2023). In areas where isochrones are strongly disrupted by (past or present) enhanced flow, extracting ILCI or isochrone-slope products from the radiostratigraphy (as introduced in Sect. 3.3) has helped to complement reconstructions of past or present ice-flow dynamics (e.g., Karlsson et al., 2012; Bingham et al., 2015; Holschuh et al., 2017; Ashmore et al., 2020; Luo et al., 2020; Sanderson et al., 2023). In some cases, sequences of folded isochrones have been observed beneath sequences of conformable isochrones, indicative of a past sudden change from fast to slow ice flow (e.g., Conway et al., 2002; Siegert et al., 2013; Kingslake et al., 2016). To obtain more complex information on past ice-dynamic changes falls into the realm of applying numerical modelling, which is taken up in Sect. 5.6.

An important outcome of most ice flow is that the ice crystals themselves develop a preferred orientation, typically termed anisotropic crystal-orientation fabric, which may then influence the direction-dependent propagation speed of radio waves through ice (Gow and Williamson, 1976; Robin and Millar, 1982; Fujita et al., 1999; Matsuoka et al., 2003; Eisen et al., 2007; Drews et al., 2012; Jordan et al., 2020; Jordan et al., 2022). Studies have reconstructed and constrained the mechanical anisotropy of ice and histories of ice deformation by calculating the travel-time difference for IRHs across intersecting RES profiles where the radio waves have been polarised in different directions (e.g., Fig. 8g; Ershadi et al., 2022; Jordan et al., 2022; Gerber et al., 2023; Zeising et al., 2023). A special case of isochrone folding due to changes in ice-crystal fabric occurs at ice divides, where upward-pointing folds termed Raymond Arches (Fig. 8h) form due to the interplay of the strain-rate dependence of ice viscosity, which leads to stiffer ice beneath the divide, slowing isochrone thinning down relative to the flanks (Raymond, 1983; Vaughan et al., 1999; Martín et al., 2009; Hindmarsh et al., 2011; Matsuoka et al., 2015). The special geometry of these isochrone arches has been used to infer local ice-flow history including the onset of divide flow (Conway et al., 1999; Kingslake et al., 2016), divide migration (Nereson et al., 1998; Martín et al., 2009; Schannwell et al., 2019) and ice-thickness changes (Drews et al., 2015). With stable ice-divide positions over extended periods of time, these arches can evolve further into double-peaked Raymond Arches, as observed (Drews et al., 2013) and simulated by incorporating anisotropy into the ice-flow models (Pettit et al., 2007; Martín and Gudmundsson, 2012; Martín et al., 2014). In terms of efforts to trace isochrones widely across the Antarctic ice sheets, Raymond Arches have the greatest relevance in how they affect site selection for deep ice cores that are ideally used to assign ages to Antarctic-wide isochrones (as introduced in Sect. 3.4). The relative thinness of isochrones at the apex of Raymond Arches implies that better resolution age-depth records reaching further back in time would be obtained around the flanks, rather than on the apexes, of ice divides where arches are present.

### 5.5 Applications of internal architecture complementary to radiostratigraphy

Ice located near to the bed of an ice sheet is typically expected to have undergone strong deformation due to shear, or to originate from processes other than earlier surface accumulation. The basal ice of Antarctica and Greenland is typically characterised by an echo-free or low-backscatter zone lacking coherent layered reflections, termed an *echo-free zone* (EFZ) in early observations (Drewry and Meldrum, 1978; Robin and Millar, 1982; Fujita et al., 1999). With modern RES systems, this zone now appears as a basal unit in which IRHs are often warped, folded and pinched out, and consequently lack coherent reflections (Drews et al., 2009), but even without traceable radiostratigraphy this architecture contains useful information about ice properties and origins. With the progressive enhancement of RES-system range resolution, a variety of reflection sub-units distinctly standing out from the otherwise low-backscatter zone have been identified (e.g., Fig 8i; Bell et al., 2011; Bell et al., 2014; Wrona et al., 2018; Ross et al., 2020; Lilien et al., 2021; Franke et al., 2024b). Some of these features manifest as zones with nearly continuous high backscatter spanning several hundred metres in thickness. Some features drape over mountainous subglacial regions (e.g., in Antarctica's Gamburtsev Mountains and Jutulstraumen drainage basin; Bell et al., 2011; Wrona et al., 2018; Franke et al., 2024b), while others build plume-like structures within the cores of englacial folds (e.g., in northern Greenland and Antarctica's Institute Ice Stream; Bell et al., 2014; Ross et al., 2020). These basal units are likely of different origins and exhibit different dielectric properties compared to their low-backscatter surroundings, offering insights into potential formation mechanisms. Current hypotheses include strong deformation on the micro-scale by ice dynamics (Drews et al., 2009), freeze-on of subglacial water at the ice base (Bell et al., 2011; Creyts et al., 2014; Leysinger Vieli et al., 2018), and the incorporation of point reflectors (e.g., basal sediment; Winter et al., 2019b; Franke et al., 2024b), as well as ice flowing over regions with changes in basal friction (Wolovick et al., 2014; Wolovick and Creyts, 2016) or convergent flow (Bons et al., 2016; Ross et al., 2020). The presence of these basal units can influence the rheological properties and fabric structure of the ice column, as well as impact the continuity of climatic records, highlighting their significance for ice-core drilling projects and ice-flow-modelling endeavours (Bell et al., 2014; MacGregor et al., 2015a; Panton and Karlsson, 2015).

Buried surface crevasses imaged in RES data have been used as key evidence for timing the shutdown of Kamb Ice Stream (Retzlaff et al., 1993; Jacobel et al., 2000; Smith et al., 2002; Catania et al., 2006) and the reorganisation of flow through Whillans Ice Stream (Conway et al., 2002). The locations and geometry of basal crevasses formed near the grounding line (Fig. 8j) have also been used to identify previously floating ice, and time the formation of ice rises and ice-flow reorganisation during the Holocene in Antarctica's Weddell Sea Sector (Kingslake et al., 2018; Wearing and Kingslake, 2019).

Finally, some particularly bright isochrones have been used to constrain the timing of past volcanic eruptions and constrain the ranges of their tephra fallout. Most such reflectors are relatively bright through chemical signatures alone (e.g., Welch and Jacobel, 2003), but a particularly prominent isochrone, ~30 dB stronger than other typical isochrone-reflection strengths, and thus interpreted as containing physical tephra fragments in addition to chemical residues, was mapped and interpreted by Corr and Vaughan (2008) to demonstrate a volcanic eruption occurred ~2000 years ago in West Antarctica and covered much of the Pine Island Glacier basin (Fig 8k).

### 5.6 Using isochrones in ice-sheet models

Ice-flow models of different complexities comprise the foremost tools for projecting future ice-sheet and glacier evolution (e.g., Gagliardini et al., 2013; Cornford et al., 2015; DeConto and Pollard, 2016; Seroussi et al., 2020; 2024). Incorporating radiostratigraphic data into ice-sheet models provides a means for validation, improves their calibration and might be essential for making more robust projections by models seeking to constrain ice-sheet evolution over the past few centuries to the late Quaternary (Hindmarsh et al., 2009; Leysinger Vieli et al., 2011; Holschuh et al., 2017; Born and Robinson, 2021; Sutter et al., 2021). Palaeo-proxy records such as exposure-age dating (Brook and Kurz, 1993; Mackintosh et al., 2014; Hillebrand et al., 2021), grounding-line reconstructions (Bentley et al., 2014; Wearing and Kingslake, 2019) or estimates of past sea-level highstands (Dutton et al., 2015) provide invaluable snapshots of ice-sheet variability on local, regional and continental scales (Lecavalier et al., 2023, present a state-of-the-art database), but their interpretation remains challenging in terms of attribution of ice volume, and changes to the grounding zone and ice elevation. Dated radiostratigraphy, on the other hand, contains detailed information on the evolution of ice flow on the relevant timescales (as compiled for today in Sect. 4.5) and thus provides a much-refined calibration target bridging gaps in between snapshot proxy data. Although the theoretical link between ice flow and isochrone geometry has been established for steady tube flow of an ice sheet (Parrenin and

Hindmarsh, 2007), the general 3D and transient case remains far more challenging. In this section, we overview recent developments in ice-sheet modelling that incorporate or exploit isochronal data from RES surveys.

### 5.6.1 Modelling past climate and ice-dynamic changes

Radiostratigraphy is an ideal tuning target for ice-sheet models on continental, regional (catchment) and local scales, because it inherently records the history of the ice flow as well as its response to changing climate conditions in its geometry. As opposed to traditionally-employed tuning targets such as surface flow, ice-sheet geometry or ice volume, which only represent snapshots of ice-sheet evolution, radiostratigraphy provides a 3-D structure which has been formed by the transient palaeo-evolution of the ice sheet. Modelling isochronal geometry and age is technically relatively straightforward, with the main challenge being pervasive uncertainties in boundary conditions (e.g. climate forcing and geothermal heat flux) and the intrinsic uncertainties of ice-sheet models due to their parameterisations of physical processes (Sutter et al., 2021). Isochrones in RES data, age-depth profiles in ice cores and the isotopic content of ice sheets have been modelled either by employing Lagrangian (Sutter et al., 2021) or semi-Lagrangian (Tarasov and Peltier, 2003; Clarke et al., 2005; Goelles et al., 2014) advection or isochronal models (Born, 2017; Rieckh et al., 2024). Models that simulate stratigraphy can thus be used to explore the effects of palaeoclimate evolution on ice-dynamic changes, such as marine ice-sheet instabilities or the evolution of ice-sheet drainage systems.

Continental-scale ice-sheet models employing approximations of the full-Stokes equations have allowed the computation of ice flow on time scales of centuries to millions of years, albeit at the cost of resolution, which is usually ~5–40 km (Pollard and DeConto, 2009; Golledge et al., 2015; Sutter et al., 2019; Albrecht et al., 2020; Seroussi et al., 2024). While these relatively coarse grid sizes (compared to applications of full-Stokes models; e.g. Zhao et al., 2018) preclude a meaningful interpretation of small-scale processes that influence radiostratigraphy (e.g. local freezing, melting, bedrock features etc.), large-scale models have the advantage that they incorporate the whole thermomechanically-coupled ice-sheet system and its response to changing climate conditions. Consequently, large-scale models are also the main tools for projections of sea-level contributions from the Antarctic and Greenland ice sheets (e.g., Goelzer et al., 2020; Seroussi et al., 2020; 2024).

The analysis of isochrones to inform on past ice flow need not be limited to the grounded parts of an ice sheet and has been extended to ice shelves (Višnjević et al., 2022; Moss et al., 2023), ice rises (Goel et al., 2018; Goel et al., 2024), and the ice-rise/ice-shelf system (Henry et al., 2024). In these studies, isochrones have served as valuable resources for reconstructing both the surface and/or basal mass balance of ice shelves and ice rises using forward and inverse modelling along the flowline (in 2D), and for investigating rheological properties of ice rise/ice shelf systems in 3D (Henry et al., 2024). Extending this approach to include the past ice-shelf evolution and linking the isochronal structure to its grounded counterparts remains challenging due to the lack of tie points to dated isochrones and a lack of observable isochronal structure across the grounding line.

### 5.6.2 Model integration of isochronal data

A range of models has been used to calculate the age-depth relationship in ice over both large and small portions of Antarctica and compare this with existing radiostratigraphies; an exercise that can offer valuable insights into ice-sheet processes and how these are represented in ice-sheet models (Fig. 9). When integrating isochronal data in models, multiple factors play a role in the choice of model set up, such as the size of the area of interest (e.g. regional or continental) and the type of flow regime present (e.g. dome, vertical shearing, extension). Various types of flow regime are found in Antarctica, ranging from vertical compression at domes moving to vertical shear and finally to longitudinal extension in ice streams and ice shelves. Consequently, it is important to use a model with the most suitable dimensionality (1D, 2D or 3D) for the specific glaciological conditions in the area being studied. 2.5D models, i.e. 2D models that take into account some aspects of a third dimension, provide another option (Chung et al., 2024).

1D models typically assume negligible horizontal flow, making simplifying assumptions such as a steady-state velocity field and the local layer approximation (Waddington et al., 2007, provide guidelines on its applicability) and have predominantly been used at domes such as Dome C (Parrenin et al., 2017; Lilien et al., 2021; Chung et al., 2023) and Dome F (Obase et al., 2023; Wang et al., 2023), where vertical compression dominates. Dated isochrones have been used in multiple studies to constrain 1D age-depth models of different complexity to determine millennial-scale accumulation rates in Antarctica (e.g., Leysinger Vieli et al., 2004; Siegert and Payne, 2004; MacGregor et al., 2009; Karlsson et al., 2014; Koutnik et al., 2016; Cavitte et al., 2018; Zhao et al., 2018; Ashmore et al., 2020; Bodart et al., 2023; Sanderson et al., 2024) and retrieve horizontal flow velocity from 2D isochrone architecture (Eisen, 2008). While most such studies have been restricted to using steady-state due to temporal limitations in available data, some models have allowed for temporal changes in boundary conditions (Callens et al., 2016; Parrenin et al., 2017; Chung et al., 2023).

3D modelling of ice-rise stratigraphy (Henry et al., 2024) has provided a step towards constraining long-term simulations in coastal areas. The influence of model physics on this stratigraphy was first investigated in 2D idealised studies of Raymond arches (Pettit and Waddington, 2003; Pettit et al., 2007; Martín and Gudmundsson, 2012), with Hindmarsh et al. (2011) extending this work in 3D idealised simulations. Modelling studies have examined the influence of Glen's flow law exponent on Raymond-arch amplitude (Pettit and Waddington, 2003; Martín et al., 2006; Martín and Gudmundsson, 2012). This methodology has been extended to 2D simulations of real-world ice rises and domes in coastal Antarctica with the comparison of modelled and observed Raymond arches at ice divides (Martín et al., 2009; Hindmarsh et al., 2011; Pettit et al., 2011; Martín et al., 2014; Drews et al., 2015; Goel et al., 2018; Goel et al., 2024).

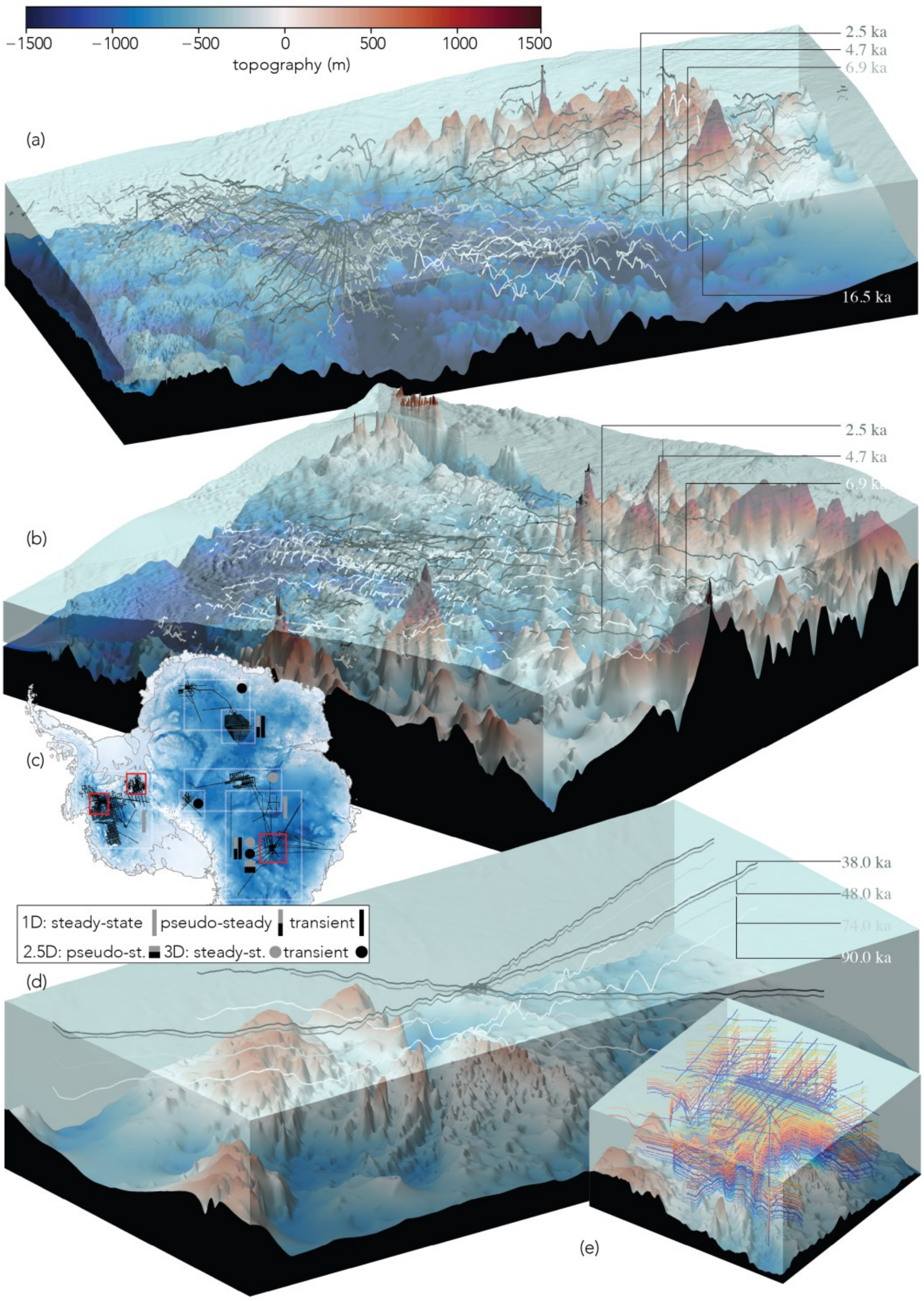


832 **Figure 9.** 3D visualisation of selected traced and dated isochrones in East And West Antarctica, and locations where different modelling applications have been conducted. (a) 2.5 ka (black lines) and 16.5 ka (grey lines) isochrones across the Pine Island/Thwaites Glacier catchment area (Bodart et al., 2021). (b) 2.5, 4.7 and 6.9 ka isochrones spanning Institute Ice Stream (Ashmore et al., 2020). (c) Map of Antarctic traced and dated isochrone transects (black lines) and areas where at least one modelling study is available (grey boxes); red boxes denote areas of the 3D visualisations. (d) Traced and dated (38, 48, 90, 160 ka) isochronal structure around Dome C from Winter et al. (2019a) and (e) Cavitte et al. (2021).

Isochrones have also been used to estimate ice temperature on catchment- to continent-wide scales. Because the electrical conductivity of ice varies exponentially with temperature, resulting in higher dielectric attenuation in warmer ice (MacGregor et al., 2007), temperature variability across the ice sheets leaves a signature in the returned power of measured radio waves. To date, studies have concentrated on using thermomechanical ice-sheet models to improve interpretation of RES data by using modelled temperature fields to remove attenuation effects and strengthen interpretations of bed properties based on basal reflectivity (Matsuoka et al., 2012; MacGregor et al., 2015b; Chu et al., 2021; Dawson et al., 2022). This approach assumes that thermomechanical models can estimate the ice temperature field to high confidence. Additionally, 1D age-depth models that incorporate a thermomechanical component (Parrenin et al., 2017; Passalacqua et al., 2017; Obase et al., 2023) have been used to infer basal melt rates in Antarctica close to domes. Temperature modelling, however, can be challenging in fast-flowing areas where heat production by viscous dissipation is substantial, such as along shear margins or ice streams. As efforts to reduce ambiguity in the direct inference of temperature from RES reflection strength develop, it will become possible to assimilate RES measurements of temperature to improve model performance, as has been done with other direct and indirect observations of subsurface temperature (Pattyn, 2010; Van Liefferinge and Pattyn, 2013). While a combined evaluation of model temperature and velocity data from RES data has been performed qualitatively (Holschuh et al., 2019), there is a growing desire to incorporate *both* radiometric and structural information in a formal modelling framework.

## 6 Future directions

In this review, we have considered how the internal architecture of the Antarctic ice sheets, and in particular their radiostratigraphy, is increasingly being exploited to elucidate ice and climate history. The ultimate aim of these endeavours is to constrain in ever finer detail the rates, locations and underlying processes of past ice-sheet changes in response to climate forcing. This is crucial to inform and reduce uncertainties in models projecting future ice-sheet changes and concomitant global sea-level rise. Yet, despite the progress reported above, Antarctica's internal architecture remains an underutilised resource for this purpose. In this final section, we set out recommendations for future research activities to be underpinned by an expanded and accessible database of Antarctica's internal architecture. Firstly (Sect. 6.1), we present a pathway towards expanding the volume of radiostratigraphy across Antarctica towards the goal of building a 3-D age-depth model of the ice; secondly (Sect. 6.2), we set out a number of future science challenges that a comprehensive database of Antarctica's englacial architecture can help to address; and finally (Sect. 6.3), we make some recommendations for community actions to facilitate the delivery of these goals.

### 6.1 Pathway to expanding Antarctic radiostratigraphy

We have identified throughout this review a clear need to expand significantly the traced radiostratigraphy across the Antarctic ice sheets, covering both more area and a greater depth range through the ice. To achieve this requires the following steps:

#### *6.1.1 Numerical modelling to guide where radiostratigraphic constraints are most needed*

We recommend that future targets for tracing radiostratigraphy across different regions of Antarctica, from existing RES data or guiding new RES surveys, are informed directly by the needs of the ice-sheet modelling community to benchmark and constrain their models. Modelling can guide location-based suggestions (e.g. to recover more radiostratigraphy away from ice divides and into more dynamic regions where simple model heuristics may misrepresent englacial conditions), or require targeting of particular time periods (e.g. targeting older isochrones that could advance understanding of glacial-interglacial transitions, amongst others).

#### *6.1.2 Systematic assessment of the potential of existing data for tracing radiostratigraphy*

For this review, we have compiled the spatial coverage of existing published RES data across Antarctica that have high-quality (GNSS) navigation and were acquired digitally, and often coherently (Fig. 6d). In principle, this demonstrates the present coverage of RES data from which radiostratigraphy could be extracted and mapped, and indicates that RES datasets range and interconnect widely across both the East and West Antarctic ice sheets. While this presents a positive message of the potential for pan-Antarctic tracing of radiostratigraphy, whether and how much radiostratigraphy *can* be extracted so widely across the ice sheets from all of these profiles remains unknown. Not all of the RES tracks necessarily contain traceable radiostratigraphy, for reasons that range from inherent RES-system limitations upon data acquisition, decisions made in the processing of the data that are available (see Sect. 3), to the presence of physical phenomena in the ice that disrupt radiostratigraphy or steeply sloping basal topography that makes isochrones too steep to be traced (Sect. 5).

A community effort is therefore required to investigate the full potential for mapping radiostratigraphy through these existing datasets. A useful first step, which was beyond the scope of this paper, would be to apply the ILCI to all of the modern datasets presented in Fig. 6d to assess their viability for tracing isochrones across different regions, i.e., to produce a more comprehensive version of Fig. 5 expanded to all the datasets discussed in Sect. 4.

#### *6.1.3 Reprocessing of existing datasets to accentuate internal architecture*

While the visibility of internal architecture is partly determined by the initial acquisition parameters and varies across Antarctica, the information visible in RES data is also influenced significantly by the processing applied to the data *after* they have been acquired (Sect. 3.1). Where the raw data exist, the data can be reprocessed, which may significantly enhance the value of some existing datasets for tracing their radiostratigraphy. For much of Antarctica's RES data, the only processing that has been applied was implemented to emphasise and pick the bed echo. In some cases, the same processing accentuated radiostratigraphy in parallel but, in others, it has suppressed the imaging of isochrones or induced artefacts in the radargrams that have hampered or precluded any tracing of radiostratigraphy. Therefore, where existing data lack distinct isochrones in locations identified by numerical modelling as optimal candidates for radiostratigraphy, we recommend, where feasible, firstly reprocessing the raw data to enhance internal architecture. Such an initiative is currently being trialled as part of the Open Polar Radar project using AWI, BAS and USA-acquired RES data across Antarctica (Paden et al., 2021).

#### *6.1.4 New data acquisition*

Importantly, new RES data for radiostratigraphic constraints need only be acquired where the processes described above have highlighted that existing data cannot provide the radiostratigraphic constraints required by modelling applications. Such areas will fall into three categories:

(a) Regions that are still unsurveyed or undersurveyed. Clear examples of this situation, from Fig. 6d, comprise data gaps > 100 km wide in East Antarctica in Enderby Land; between South Pole and Vostok; and between Wilkes and Kemp lands; and we also note that the Filchner-Ronne Ice Shelf does not have dense survey cover.

(b) Regions where RES surveys have occurred but where the existing data – even after reprocessing – do not contain any internal architecture. These regions typically comprise those last surveyed by RES several decades ago with less sophisticated RES systems. From Fig. 6d, we identify the Siple Coast region of West Antarctica as one such data gap. Although this region was intensively studied and surveyed during the 1980s and 1990s, its last major RES surveys predate widespread use of coherent RES systems.

(c) Regions where RES surveys have occurred but where the existing data – even after reprocessing – contain some internal architecture, but which does not meet modelling needs. Likely scenarios here are that age-depth information is needed at finer resolution than is retrievable in the existing data, or there is a requirement to recover radiostratigraphy deeper into the ice than has been imaged by the existing survey. This situation is common amongst existing datasets that were acquired for projects focussed on other scientific priorities. For example, where some airborne RES datasets have been acquired in combination with potential-field data (gravity and magnetics), the requirement to fly the aircraft at a stable elevation has sometimes led to poor-quality radiostratigraphy where the range from aircraft to ice surface was too large.

These cases should fundamentally guide the locations, nature and platforms of any new RES data acquisition for internal architecture. As reviewed in Sect. 4, modern airborne RES systems and processing algorithms are adept at detecting multiple isochrones over large regions. In some cases, such as through regions of complex topography, complex flow dynamics or a requirement for very fine resolution of isochrones over regional scales, ground-based RES systems that can typically sound more IRHs and deeper into the underlying ice may still represent the optimal tool and justify the resources required to emplace deep-field parties. However, uncrewed aerial vehicles capable of carrying RES systems (Arnold et al., 2020; Teisberg et al., 2022), when routinely operationalised, may offer a cheaper and safer solution over remote and challenging terrains.

#### *6.1.5 Advances in deep learning to expedite the extraction of internal architecture from RES data*

As reviewed in Sect. 3, all of the present radiostratigraphy mapped across Antarctica (Fig. 7) has been generated in the absence of a fully automated isochrone-picking algorithm. Although substantial progress has been made, the need for frequent manual intervention has slowed the generation of pan-Antarctic radiostratigraphy. The greatest promise for a step-change in our ability to trace radiostratigraphy significantly faster lies in the application of deep-learning methods to the challenge. As we discussed in Sect. 3.2, deep-learning applications for isochrone tracing are in their infancy, but have already shown great promise for the fast extraction of both near-surface and (more recently) deeper isochrones. While surface-conformable isochrones are relatively more straightforward to trace by machine-learning models, tracing isochrones deeper in the ice column is challenged by IRH fading, unconformities, and/or merging and splitting of isochrones as ice flows over or around large bedrock obstacles. The significant volume of traced radiostratigraphic data now assembled to date across Antarctica (Fig. 7) may now contribute training data to facilitate the advance and wider application of deep learning to tracing Antarctica's deeper isochrones. However, for recently-established machine-learning pipelines (e.g., Moqadam et al., 2025) to use Antarctic radiostratigraphies most effectively, ideally the number of isochrones traced through different regions would need to be increased significantly. A further limitation to this goal is that machine-learning models are highly data-dependent, such that it is still challenging to analyse in parallel datasets derived from different RES systems and/or derived through diverse processing flows. Despite these challenges, the fast progress made towards successful implementation of such applications and the growing availability of traced radiostratigraphy and underlying RES data now being available, are collectively expected to facilitate a step-change in the growing coverage of Antarctic radiostratigraphy in the years to come.

## 6.2 Scientific challenges to be addressed using internal architecture

### *6.2.1 Identification of optimal areas for retrieving new palaeoclimate records*

As outlined in Sect. 5.1, Antarctica's deep ice cores have provided invaluable palaeoclimate records from both West and East Antarctica and yet there remain two outstanding directives in the quest for augmenting these existing datasets. One, presently the primary focus of the SCAR IPICS *Oldest Ice* programme, is to identify where a potential climate record extending further back in time than Antarctica's current record (back to ~800,000 k.a. from Dome C; Bouchet et al., 2023) can be sampled. This would address the substantial unknown of whether Antarctica's ice holds a direct continuous record of the mid-Pleistocene transition switch from 41-kyr to 100-kyr glacial-interglacial cycles that is inferred to have occurred between ~1.25-0.8 M k.a. from marine-sediment oxygen-isotope records (Hays et al., 1976; Clark et al., 2006; Legrain et al., 2023). A second requirement is to locate sites in the Antarctic ice sheets that preserve higher-resolution palaeoclimate records of epochs than are currently represented in the already-sampled sites. In particular, regions with relatively high present or past accumulation rates can potentially preserve high-resolution climate records of the last millenia. We contend that the development of a pan-continental radiostratigraphy could form a crucial tool for identifying most future ice-core locations around Antarctica.

We further recommend that attention is placed on tracing radiostratigraphy around Antarctica's blue-ice zones which, as discussed in Sect. 5.1, have and can represent sites for retrieving ice older than 800 k.a. Targeted studies on their radiostratigraphy could improve understanding of how ice deforms to produce the sampled structures, and hence better contextualise how the ice outcropping in such regions is related to ice buried at depth in interior Antarctica.

These initiatives may be complemented by the strategic deployment of rapid-access drilling techniques that could be deployed, alongside intersections with ice cores (discussed in Sect. 5.1), to date and validate the radiostratigraphy. Rapid-access drilling (e.g., Goodge and Severinghaus, 2016; Rix et al., 2019; Goodge et al., 2021; Schwander et al., 2023) can provide borehole access into the ice for deploying sensors to record physical characteristics that correlate with RES isochrones (IceCube Collaboration, 2013; Goodge et al., 2021; Schwander et al., 2023). Additionally, rapid-access drilling allows direct sampling of ice that can be used for radiometric-age dating that can validate the radiostratigraphy (e.g., Bender et al., 2008; Rowell et al., 2023). A dedicated programme of rapid-access ice drilling coordinated with *AntArchitecture* could therefore both help to validate radiostratigraphic age-depth models, and provide a relatively quick and cost-effective methodology for targeting potential future sites for both vertical and horizontal ice coring.

### *6.2.2 Reconstruction of surface mass balance – millennial timescales*

In Sect. 5.2, we discussed that tracing deep (>200 m below the ice surface) isochrones across the Antarctic ice sheets enables reconstruction of changes in surface mass balance over the past several millenia. While the few existing studies have mostly focussed at or near ice divides, where horizontal flow and its associated complexities can mostly be neglected, an expanded pan-continental radiostratigraphy that more comprehensively spans and connects all of Antarctica's central divide regions will enable these simple applications to be expanded, and can provide a spatially widespread record of how surface mass balance has varied regionally at millennial timescales. Such a record would help us to understand the pervasiveness of synoptic snow-accumulation patterns (e.g., Le Meur et al., 2018; Pauling et al., 2023), and could inform scenarios of future plausible surface-mass-balance variability to be incorporated into model projections (see Lenaerts et al., 2019, for a review). In turn, such refined surface-mass-balance reconstructions would greatly improve the climate forcings employed by palaeo-ice-sheet-modelling studies and increase confidence in their conclusions.

### *6.2.3 Reconstruction of surface mass balance – historical timescales*

To reduce uncertainties in near-term (i.e., ~next 200 years) projections of Antarctica's future evolution, and thereby improve global sea-level projections, there is a critical need to constrain further the regional climate models (e.g., Pratap et al., 2022) that are fundamental to forcing ice-sheet models. Important validation for these models comes from the historical record provided primarily by ice cores, but also by near-surface radiostratigraphy sounded in the upper few 100 m of the ice sheet. Neither this review, nor the *AntArchitecture* community to date, has focussed on near-surface IRHs. However, the majority of RES surveys depicted in Fig. 6 also detected near-surface radiostratigraphy, and many additional surveys have been undertaken over the past decades across Antarctica using a range of airborne and ground-based platforms that focussed on detecting shallow isochrones, often for local, but sometimes also for more regional, scientific applications (e.g., Medley et al., 2013; Medley et al., 2014; Konrad et al., 2019; Kowalewski et al., 2021; Cavitte et al., 2022). We therefore propose that an important future activity should be the development of a "near-surface" pan-Antarctic radiostratigraphy complementary to the deeper version that has primarily formed the focus of this review. In parallel with the techniques and philosophy we have discussed for dating deep isochrones across Antarctica, near-surface radiostratigraphy can be dated from intersections with near-surface ice-core records; and the product could be progressively refined by using it to identify where future near-surface ice cores should be drilled to provide finer dating control. The overall task of tracing near-surface isochrones across Antarctica should benefit from the application of machine learning to isochrone tracing, as already exemplified byseveral studies (e.g., Dong et al., 2021; Rahnemoonfar et al., 2021; Yari et al., 2021).

#### *6.2.4 Estimate geothermal heat flux from radiostratigraphy*

The studies mentioned in Sect. 5.3 speak to the significant potential for Antarctica's radiostratigraphy to be used as a resource for constraining variations to the continent's geothermal heat flux, which remains enigmatic (Burton-Johnson et al., 2020). As exemplified by Fahnestock et al. (2001b) across the Greenland Ice Sheet, and more locally in Antarctica by Jordan et al. (2018), it is possible to quantify basal melt with isochrones by calculating how much melting is required to draw isochrones down towards the base. However, the relationship between isochrone geometry and basal melting is complex, multi-dimensional and partly controversial (Leysinger Vieli et al., 2007; Carter et al., 2009; Bons et al., 2021; Wolovick et al., 2021b; Wolovick et al., 2021a). For a continental-scale application of this technique, a more detailed pan-Antarctic radiostratigraphy is needed. The optimal data product to invert for geothermal heat flux would be the most widespread tracings of the deepest undisrupted isochrones across the ice sheets, which is challenging because deeper isochrones are harder to image and significant drawdown of isochrones where basal melting is high can prohibit widespread tracing (e.g., Ross and Siegert, 2020). Nevertheless, there is significant potential to use deep isochrone geometry as further calibration for numerical models seeking to invert geothermal heat flux (Pattyn, 2010; Van Liefferinge and Pattyn, 2013; Burton-Johnson et al., 2020).

#### *6.2.5 Comprehensive mapping of basal-ice units and deep-isochrone geometry*

In Sect. 5.5, we noted that in some regions of the Antarctic ice sheets, RES data indicate that the deeper ice has distinctive physical characteristics compared with the ice above, i.e., where this deeper ice obscures or precludes imaging of IRHs, and where distinct basal-ice units exist around which the overlying IRHs have become folded or warped. An improved understanding of the distribution of these features across Antarctica is important for several reasons. Firstly, it would identify where deep-ice palaeoclimate records would be compromised by ice deformation or basal melting, thus critically informing ice-core site identification. Secondly, it would act as an observationally-informed broad-scale indicator of which areas of the ice sheet are prone to basal melting and hence inform mapping of geothermal heat flux. Thirdly, it would provide information towards a better understanding of how the rheology of Antarctica's ice varies, what are the causes of this variation, and how these effects impact on Antarctica's ice dynamics. Some of these issues would be informed by some specific rapid-access drilling into basal-ice units, and a comprehensive mapping exercise of basal-unit distribution would inform which targets might be most easily accessed. In addition to mapping basal units themselves, a complementary activity could be to map the degree to which deep-ice radiostratigraphy follows or diverges from the ice-bed interface across Antarctica. This exercise would inform modelling aimed to deconvolve how much isochrone geometry is affected by basal topography versus ice dynamics versus basal melt. This, in turn, will better inform projections of the ice sheets' future with radiostratigraphic constraints.

#### *6.2.6 Advance knowledge of volcanic activity and fallout across Antarctica*

Given that most isochrones traced across the Antarctic ice sheets manifest changes to acidity, and that some of the brightest have been linked to precipitated fallout from volcanic eruptions within and beyond Antarctica, there is significant potential to use isochrones across Antarctica more comprehensively to trace the spatial distribution of volcanic fallout from the numerous past eruptions that have been identified by chemical analyses of Antarctica's ice cores (Narcisi and Petit, 2021). Despite many tephra and cryptotephra (microscopic layers of volcanic ash) having been detected in Antarctica's ice cores, few have explicitly been traced widely beyond the ice cores using radiostratigraphy, and most isochrones that have been linked to past volcanic events have been used as time markers for other purposes, e.g. calculating past accumulation, rather than having been traced to focus on the origins and properties of the volcanic events themselves (e.g., Jacobel and Welch, 2005; Bodart et al., 2023). There is therefore significant potential, already with existing data, to use Antarctica's radiostratigraphy to trace the geographical distribution of volcanic fallout from numerous eruptions that have been detected in ice-core records, and this information may be used to help trace further the origins and nature of past eruptions beyond that which can be gleaned solely from the ice-core chemistry. This objective would complement the ongoing activities and recent recommendations for future research on volcanism presented by the SCAR AntVolc group (Geyer et al., 2023).

#### *6.2.7 Development of a new model benchmark for the Antarctic ice sheets*

As reviewed in Sect. 5.6, the vast majority of ice-sheet models presently employed for ice-sheet reconstruction and future projections are initialised with present-day snapshots of the ice-sheet state (e.g., surface velocity, ice thickness). An Antarctic-wide radiostratigraphy would provide a much better initialisation and tuning target for ice-sheet models, as it inherently records both ice-flow history and the ice sheet's response to changing external forcings (e.g., atmospheric and ocean conditions) – all within a tangible set of physical horizons that can be reproduced by existing models. The development of an Antarctic-wide radiostratigraphically-calibrated model benchmark is therefore a primary scientific objective for SCAR's *AntArchitecture* community.

### 6.3 Community actions

The greatest challenge for attaining the outcomes described above is how to foster and maintain engagement between scientists working across numerous different disciplines and operating at institutions spread across Earth. Even within the scientific community who self-describe as RES, radar, or even radioglaciology specialists, this challenge is innate. As we have reviewed, the history and ongoing practices of Antarctic RES surveying encompass multiple agencies whose foci are typically on medium-term projects of a few years' duration. The intent of this review was to communicate to a wider audience (both within and beyond the radioglaciology community) the baseline availability and potential of the present archive of existing RES data spanning both East and West Antarctica's ice sheets, and to showcase their value for tackling major science questions concerning Antarctica's ice and climate history and future.

A major challenge to greater progress in the study of Antarctica's internal architecture has been the lack of a common framework for archiving RES data and metadata between different operators and potential users. The establishment of the FAIR (Findable, Accessible, Interoperable, and Reusable; Wilkinson et al., 2016) data-exchange guidelines has provided a clear framework making possible the release of RES data in open-access repositories, facilitating open-access releases of some of the datasets discussed in Sect. 4.3.2. These releases have been accompanied by interactive data portals and FAIR-compliant data standards, including rich metadata relating to the acquisition, processing and quality of the data, and provide examples for releasing further data in the future. We recommend that the next significant community data focus should be on developing common protocols for processing RES data, formatting and sharing raw data files, and in some cases reprocessing existing data to facilitate much greater interoperability of the data moving into the future. This recommendation falls into the remit of the Open Polar Radar project currently being trialled with AWI, BAS and USA-acquired RES data (Paden et al., 2021) but, specifically with regards to publishing and sharing future radiostratigraphy datasets, there remains a need to set a common standard. We suggest a standardised structure here in Appendix 1.

A core principle moving forwards with our science must also be on improving sustainability, given the significant resource and carbon impact of using aircraft and establishing deep-field camps in Antarctica. When proposing new Antarctic RES acquisition, we suggest that it first be demonstrated that it is needed, following the procedures laid out in Sect. 6.1. Although crewed airborne and ground-based RES platforms currently presently continue to provide the most reliable options, where new data are clearly needed n pathways for improving the sustainability of data collection are opening up with the development of uncrewed aerial vehicles capable of hosting RES systems (Arnold et al., 2020; Teisberg et al., 2022).

## 7. Conclusions

In this review we have highlighted the vast scientific potential that is contained in Radio-Echo Sounding (RES) data that have been acquired across the Antarctic ice sheets. The majority of these data have been analysed only to measure ice thickness, using only the bed echoes which are just one component of the complex data that RES surveys routinely acquire. However, Antarctic RES surveys, conducted for the last six decades, have also generated vast archives of "internal architecture" (typically 3-D fields of RES-imaged isochrones) that record the depositional, deformational and melting histories of ice around Antarctica. Until recently, this vast archive has been relatively little utilised, for reasons ranging from the challenges of working with datasets acquired with differing RES systems by multiple operators from different countries, to limitations with processing big datasets and limited capacity, to trace many 10s to 100s of RES-imaged isochrones through hundreds of thousands of km of RES profiles. We have detailed how RES data are processed and can be optimised to make them scientifically useful for a wide range of scientific applications exploring the past and future evolution of the Antarctic ice sheets (Sect. 3); inventoried where RES data are available to analyse (Sect. 4.1, 4.2 and Fig. 6) and detailed where this process has begun (Sect. 4.3, Fig. 7 and Table 1); and reviewed how internal architecture has been applied so far to make progress in linking between and verifying ice-core chronologies, reconstruct surface mass balance, basal melting and ice-flow dynamics, and been integrated into numerical modelling of ice-sheet evolution (Sect. 5). We have presented a vision for future research in Antarctic science that can be underpinned by RES-imaged internal architecture of the ice (Sect. 6), which can inform (1) Identification of optimal sites for retrieving new ice-core palaeoclimate records targeting different periods; (2) Reconstruction of surface mass balance on millennial or historical timescales; (3) Estimates of basal melting and geothermal heat flux from radiostratigraphy and comprehensively mapping basal-ice units, to complement inferences from other geophysical and geological methods; (4) Advancing knowledge of volcanic activity and fallout across Antarctica; and (5) The refinement of numerical models that leverage radiostratigraphy to tune time-varying accumulation, basal melting and ice flow, firstly to reconstruct past behaviour, and then to reduce uncertainties in projecting future ice-sheet behaviour.

To address our scientific goals, we call for continued efforts to build and enhance the inclusion and diversity of researchers involved in acquiring and analysing RES datasets towards understanding better Antarctica's past and future. This paper has benefitted immeasurably from including perspectives from authors spread across the world, navigating different stages of their careers, and identifying as different genders, ethnicities, nationalities and religions; and from including the expertise of field- and data-focussed scientists in the same space as the expertise of practitioners whose focus is on applying the data and integrating them into numerical models. We conclude by reiterating our core scientific ambitions for *AntArchitecture* above: to build a pan-Antarctic database of isochrones that are accessible, sustainable over the long term, and useful for multiple scientific applications across multiple users, for example ice-sheet modellers and the substantial ice-core community. Alongside this, and of equal importance, the community that is active both in acquiring and analysing Antarctica's internal architecture must continue to diversify.

## Author contributions

The paper was jointly written by RGB, JAB, MGPC, AC, RJS and JCRS (the lead-writing team). All co-authors contributed ideas, perspectives and edits. The review was conceptualised by RGB, OE, NBK, JAM, NR and DAY as a deliverable for the SCAR *AntArchitecture* 2018-2022 Action Group. RGB coordinated the writing process. DWA, RGB, JAB, AB, MGPC, WC, OE, NH, NBK, MRK, GJMCLV, JAM, EJM, EM, CM, FP, NR, JCRS, KW & DAY made significant contributions to first draft compiled during the covid-19 pandemic in 2020-21, forming the framework for the current version handled by the lead-writing team since 2023. Original figures were drawn by KW, NBK & JAB (Fig. 1), DWA (Fig. 2), SF (Fig. 3), JAB (Fig. 5 & 7), RGB(Fig. 6), , MGCP & RJS (Fig. 8), and JCRS (Fig. 9), and Table 1 was assembled by JAB. Prior to submission, DWA, AB, RD, JWG, MRK, CM, FN, SVP, DMS, TOT, XC & XT provided substantive edits; SF, VG, ACJC, AH, BHH, FMO, TR & SY led detailed reviews of each section of the manuscript which shaped further edits; and OE, NBK, GJMCLV, JAM, FSLN, NR, RS, MJS & DAY contributed final checks and perspectives informing the final version of the paper.

## Competing interests

Nanna Karlsson is Co-Editor-in-Chief, Olaf Eisen is Advisory Editor, and Reinhard Drews, Joseph MacGregor, Elisa Mantelli, Carlos Martín and Johannes Sutter are Editors of *The Cryosphere*.

## Disclaimer

The views and opinions expressed here are those of the author(s) only and do not necessarily reflect those of the European Union or the European Research Council Executive Agency. Neither the European Union nor the granting authority can be held responsible for them.

## Acknowledgements

This research is a contribution to the Scientific Committee for Antarctic Research's *AntArchitecture* Action Group, and we thank members of SCAR's Physical Sciences and Geosciences Divisions for ongoing support of the group since 2018. All of the UK-based authors acknowledge research funding support from the UK Natural Environment Research Council, including Doctoral Training Scholarships to CJN (Edinburgh E4), RJS (One Planet) and HD (SENSE). JCRS, JAB, AH, and VV acknowledge funding from the Swiss National Science Foundation (grant no. 211542). MGPC is a postdoctoral researcher of the FRS-FNRS. AC, OE, EM and FP acknowledge funding from the European Union: AC, OE and FP via the Horizon 2020 Marie Skłodowska-Curie grant agreement no. 955750 (DEEPICE), EM from European Research Council Starting Grant 101076793. JAM, DAY, TOT, SY and SS acknowledge support from the US National Aeronautical and Space Administration; TOT was supported by a NASA FINESST Grant (80NSSC23K0271) and the TomKat Center for Sustainable Energy. DAY, BHH, NH, MK, EJM, DMS, SY, MR and SS acknowledge funding from the US National Science Foundation:

for DAY, NH, MK, SY and SS through the Center for Oldest Ice Exploration, an NSF Science and Technology Center (NSF 2019719); for DAY, SY and SS additionally from Earthcube (NSF 2127606); for BHH from an Office of Polar Programs Postdoctoral Research Fellowship (NSF 2317927); for EJM from Geosciences Open System Ecosystem Award NSF 2324092; for DMS from Office of Polar Programs Award NSF 1745137; and for MR from BIGDATA (IIS-1838230, 2308649) and NSF Leadership Class Computing (OAC-2139536) awards. DAY, SY and SS were also supported by the G. Unger Vetlesen Foundation. This paper is University of Texas Institute for Geophysics contribution ####. AB and TR acknowledge funding from the Norwegian Research Council Grant 314614 (Simulating Ice Cores and Englacial Tracers in the Greenland Ice Sheet). RD was supported by an Emmy Noether Grant from the Deutsche Forschungsgemeinschaft (DR 822/3-1). SF was funded by the Walter Benjamin Programme of the German Research Foundation (DFG; project number 506043073). ACJH is supported by the Wallenberg Foundation (KAW 2021.0275). FMO acknowledges support from the German Academic Scholarship Foundation. XC (Grant 42376253) and XT (Grant 42276257) were supported by National Natural Science Foundation of China. CFD was funded by the Natural Sciences and Engineering Research Council of Canada (NSERC; RGPIN-03761-2017) and the Canada Research Chairs Program (950-231237).

## References


Albrecht, T., R. Winkelmann & A. Levermann (2020) Glacial-cycle simulations of the Antarctic Ice Sheet with the Parallel Ice Sheet Model (PISM) – Part 2: Parameter ensemble analysis. *The Cryosphere,* 14**,** 633-656.

Allen, C. (2008) A brief history of radio-echo sounding of ice. *Earthzine Monthly Newsletter*. https://earthzine.org/a-brief-history-of-radio-echo-sounding-of-ice-2/ (last accessed 21 May 2024).

Arcone, S. A., R. Jacobel & G. Hamilton (2012a) Unconformable stratigraphy in East Antarctica: Part I. Large firn cosets, recrystallized growth, and model evidence for intensified accumulation. *Journal of Glaciology,* 58**,** 240-252.

Arcone, S. A., R. Jacobel & G. Hamilton (2012b) Unconformable stratigraphy in East Antarctica: Part II. Englacial cosets and recrystallized layers. *Journal of Glaciology,* 58**,** 253-264.

Arenas-Pingarrón, Á., H. F. J. Corr, C. Robinson, T. A. Jordan & P. V. Brennan (2023) Polarimetric Airborne Scientific Instrument, Mark 2: An ice-sounding airborne synthetic-aperture radar for subglacial 3D imagery. *IET Radar, Sonar & Navigation,* 17**,** 1391-1404.

Arnold, E., C. Leuschen, F. Rodriguez-Morales, J. Li, J. Paden, R. Hale, et al. (2020) CReSIS airborne radars and platforms for ice and snow sounding. *Annals of Glaciology,* 61**,** 58-67.

Ashmore, D. W., R. G. Bingham, N. Ross, M. J. Siegert, T. A. Jordan & D. W. F. Mair (2020) Englacial architecture and age-depth constraints across the West Antarctic Ice Sheet. *Geophysical Research Letters,* 47**,** e2019GL086663.

Baggenstos, D., J. P. Severinghaus, R. Mulvaney, J. R. McConnell, M. Sigl, O. J. Maselli, et al. (2018) A horizontal ice core from Taylor Glacier, its implications for Antarctic climate history, and an improved Taylor Dome Ice Core time scale. *Paleoceanography and Paleoclimatology,* 33**,** 778-794.

Beem, L. H., D. A. Young, J. S. Greenbaum, D. D. Blankenship, M. G. P. Cavitte, J. Guo, et al. (2021) Aerogeophysical characterization of Titan Dome, East Antarctica, and potential as an ice-core target. *The Cryosphere,* 15**,** 1719-1730.

Bell, R. E., D. D. Blankenship, C. A. Finn, D. L. Morse, T. A. Scambos, J. M. Brozena, et al. (1998) Influence of subglacial geology on the onset of a West Antarctic ice stream from aerogeophysical observations. *Nature,* 394**,** 58-62.

Bell, R. E., F. Ferraccioli, T. T. Creyts, D. Braaten, H. Corr, I. Das, et al. (2011) Widespread persistent thickening of the East Antarctic Ice Sheet by freezing from the base. *Science,* 331**,** 1592-1595.

Bell, R. E., K. Tinto, I. Das, M. Wolovick, W. Chu, T. T. Creyts, et al. (2014) Deformation, warming and softening of Greenland's ice by refreezing meltwater. *Nature Geoscience,* 7**,** 497-502.

Bender, M. L., B. Barnett, G. Dreyfus, J. Jouzel & D. Porcelli (2008) The contemporary degassing rate of $^{40}$Ar from the solid Earth. *Proceedings of the National Academy of Sciences,* 105**,** 8232-8237.

Bentley, M. J., C. Ó Cofaigh, J. B. Anderson, H. Conway, B. Davies, A. G. C. Graham, et al. (2014) A community-based geological reconstruction of Antarctic Ice Sheet deglaciation since the Last Glacial Maximum. *Quaternary Science Reviews,* 100**,** 1-9.

Bingham, R. G., D. M. Rippin, N. B. Karlsson, H. F. J. Corr, F. Ferraccioli, T. A. Jordan, et al. (2015) Ice-flow structure and ice-dynamic changes in the Weddell Sea sector of West Antarctica from radar-imaged internal layering. *Journal of Geophysical Research: Earth Surface,* 120**,** 655-670.

Bingham, R. G. & M. J. Siegert (2007) Radio-echo sounding over polar ice masses. *Journal of Environmental and Engineering Geophysics,* 12**,** 47-62.

Bingham, R. G., M. J. Siegert, D. A. Young & D. D. Blankenship (2007) Organized flow from the South Pole to the Filchner-Ronne Ice Shelf: An assessment of balance velocities in interior East Antarctica using radio-echo sounding data. *Journal of Geophysical Research: Earth Surface,* 112**,** F03S26.

Blankenship, D. D., D. L. Morse, C. A. Finn, R. E. Bell, M. E. Peters, S. D. Kempf, et al. (2001) Geologic controls on the initiation of rapid basal motion for West Antarctic ice streams: A geophysical perspective including new airborne radar sounding and laser altimetry results. In *The West Antarctic Ice Sheet: Behavior and Environment*, 105-121.

Blankenship, D. D., S. D. Kempf, D. A. Young, T. G. Richter, D. M. Schroeder, J. S. Greenbaum, et al. (2017a) IceBridge HiCARS 1 L1B Time-Tagged Echo Strength Profiles, Version 1. [Indicate subset used]. Boulder, Colorado USA. NASA National Snow and Ice Data Center Distributed Active Archive Center.

Bodart, J. A., R. G. Bingham, D. W. Ashmore, N. B. Karlsson, A. S. Hein & D. G. Vaughan (2021) Age-depth stratigraphy of Pine Island Glacier inferred from airborne radar and ice-core chronology. *Journal of Geophysical Research: Earth Surface,* 126**,** e2020JF005927.

Bodart, J. A., R. G. Bingham, D. A. Young, J. A. MacGregor, D. W. Ashmore, E. Quartini, et al. (2023) High mid-Holocene accumulation rates over West Antarctica inferred from a pervasive ice-penetrating radar reflector. *The Cryosphere,* 17**,** 1497-1512.

Bons, P. D., T. de Riese, S. Franke, M. G. Llorens, T. Sachau, N. Stoll, et al. (2021) Comment on "Exceptionally high heat flux needed to sustain the Northeast Greenland Ice Stream" by Smith-Johnsen et al. (2020). *The Cryosphere,* 15, 2251-2254.

Bons, P. D., D. Jansen, F. Mundel, C. C. Bauer, T. Binder, O. Eisen, et al. (2016) Converging flow and anisotropy cause large-scale folding in Greenland's ice sheet. *Nature Communications,* 7, 11427.

Born, A. (2017) Tracer transport in an isochronal ice-sheet model. *Journal of Glaciology,* 63, 22-38.

Born, A. & A. Robinson (2021) Modeling the Greenland englacial stratigraphy. *The Cryosphere,* 15, 4539-4556.

Bouchet, M., A. Landais, A. Grisart, F. Parrenin, F. Prié, R. Jacob, et al. (2023) The Antarctic Ice Core Chronology 2023 (AICC2023) chronological framework and associated timescale for the European Project for Ice Coring in Antarctica (EPICA) Dome C ice core. *Climate of the Past,* 19, 2257-2286.

Brook, E. J. & C. Buizert (2018) Antarctic and global climate history viewed from ice cores. *Nature,* 558, 200-208.

Brook, E. J. & M. D. Kurz (1993) Surface-exposure chronology using in situ cosmogenic $^{3}$He in Antarctic quartz sandstone boulders. *Quaternary Research,* 39, 1-10.

Burton-Johnson, A., R. Dziadek & C. Martín (2020) Geothermal heat flow in Antarctica: Current and future directions. *The Cryosphere,* 14, 3843-3873.

Callens, D., R. Drews, E. Witrant, M. Philippe & F. Pattyn (2016) Temporally stable surface mass balance asymmetry across an ice rise derived from radar internal-reflection horizons through inverse modeling. *Journal of Glaciology,* 62, 525-534.

Carter, S. P., D. D. Blankenship, M. E. Peters, D. A. Young, J. W. Holt & D. L. Morse (2007) Radar-based subglacial-lake classification in Antarctica. *Geochemistry, Geophysics, Geosystems,* 8, Q03016.

Carter, S. P., D. D. Blankenship, D. A. Young & J. W. Holt (2009) Using radar-sounding data to identify the distribution and sources of subglacial water: Application to Dome C, East Antarctica. *Journal of Glaciology,* 55, 1025-1040.

Castelletti, D., D. M. Schroeder, S. Hensley, C. Grima, G. Ng, D. Young, et al. (2017) An interferometric approach to cross-track clutter detection in two-channel VHF radar sounders. *IEEE Transactions on Geoscience and Remote Sensing,* 55, 6128-6140.

Castelletti, D., D. M. Schroeder, T. M. Jordan & D. Young (2021) Permanent scatterers in repeat-pass airborne VHF radar sounder for layer-velocity estimation. *IEEE Geoscience and Remote Sensing Letters,* 18, 1766-1770.

Castelletti, D., D. M. Schroeder, E. Mantelli & A. Hilger (2019) Layer-optimized SAR processing and slope estimation in radar-sounder data. *Journal of Glaciology,* 65, 983-988.

Catania, G., C. Hulbe & H. Conway (2010) Grounding-line basal melt rates determined using radar-derived internal stratigraphy. *Journal of Glaciology,* 56, 545-554.

Catania, G. A., T. A. Scambos, H. Conway & C. F. Raymond (2006) Sequential stagnation of Kamb Ice Stream, West Antarctica. *Geophysical Research Letters,* 33, L14502.

Cavitte, M. G. P., D. D. Blankenship, D. A. Young, D. M. Schroeder, F. Parrenin, E. Le Meur, et al. (2016) Deep radiostratigraphy of the East Antarctic plateau: Connecting the Dome C and Vostok ice-core sites. *Journal of Glaciology,* 62, 323-334.

Cavitte, M. G. P., H. Goosse, K. Matsuoka, S. Wauthy, V. Goel, R. Dey, et al. (2023) Investigating the spatial representativeness of East Antarctic ice cores: A comparison of ice core and radar-derived surface mass balance over coastal ice rises and Dome Fuji. *The Cryosphere,* 17, 4779-4795.

Cavitte, M. G. P., H. Goosse, S. Wauthy, T. Kausch, J.-L. Tison, B. Van Liefferinge, et al. (2022) From ice core to ground-penetrating radar: Representativeness of SMB at three ice rises along the Princess Ragnhild Coast, East Antarctica. *Journal of Glaciology,* 68, 1221-1233.

Cavitte, M. G. P., F. Parrenin, C. Ritz, D. A. Young, B. Van Liefferinge, D. D. Blankenship, et al. (2018) Accumulation patterns around Dome C, East Antarctica, in the last 73 kyr. *The Cryosphere,* 12, 1401-1414.

Cavitte, M. G. P., D. A. Young, R. Mulvaney, C. Ritz, J. S. Greenbaum, G. Ng, et al. (2021) A detailed radiostratigraphic data set for the central East Antarctic Plateau spanning from the Holocene to the mid-Pleistocene. *Earth System Science Data,* 13, 4759-4777.

Christianson, K., R. W. Jacobel, H. J. Horgan, S. Anandakrishnan & R. B. Alley (2012) Subglacial Lake Whillans: Ice-penetrating radar and GPS observations of a shallow active reservoir beneath a West Antarctic ice stream. *Earth and Planetary Science Letters,* 331-332, 237-245.

Chu, W., A. M. Hilger, R. Culberg, D. M. Schroeder, T. M. Jordan, H. Seroussi, et al. (2021) Multisystem synthesis of radar sounding observations of the Amundsen Sea Sector from the 2004–2005 field season. *Journal of Geophysical Research: Earth Surface,* 126, e2021JF006296.

Chung, A., F. Parrenin, R. Mulvaney, L. Vittuari, M. Frezzotti, A. Zanutta, et al. (2024) Age, thinning and spatial origin of the Beyond EPICA ice from a 2.5D ice flow model. *EGUsphere,* 2024, 1-21.

Chung, A., F. Parrenin, D. Steinhage, R. Mulvaney, C. Martín, M. G. P. Cavitte, et al. (2023) Stagnant ice and age modelling in the Dome C region, Antarctica. *The Cryosphere,* 17, 3461-3483.

Clark, P. U., D. Archer, D. Pollard, J. D. Blum, J. A. Rial, V. Brovkin, et al. (2006) The middle Pleistocene transition: Characteristics, mechanisms, and implications for long-term changes in atmospheric pCO2. *Quaternary Science Reviews,* 25**,** 3150-3184.

Clarke, G. K. C., N. Lhomme & S. J. Marshall (2005) Tracer transport in the Greenland Ice Sheet: Three-dimensional isotopic stratigraphy. *Quaternary Science Reviews,* 24**,** 155-171.

Clough, J. W. (1977) Radio-echo sounding: Reflections from internal layers in ice sheets. *Journal of Glaciology,* 18**,** 3-14.

Cole-Dai, J., D. G. Ferris, J. A. Kennedy, M. Sigl, J. R. McConnell, T. J. Fudge, et al. (2021) Comprehensive record of volcanic eruptions in the Holocene (11,000 years) from the WAIS Divide, Antarctica, ice core. *Journal of Geophysical Research: Atmospheres,* 126**,** e2020JD032855.

Conway, H., G. Catania, C. F. Raymond, A. M. Gades, T. A. Scambos & H. Engelhardt (2002) Switch of flow direction in an Antarctic ice stream. *Nature,* 419**,** 465-467.

Conway, H., B. L. Hall, G. H. Denton, A. M. Gades & E. D. Waddington (1999) Past and future grounding-line retreat of the West Antarctic Ice Sheet. *Science,* 286**,** 280-283.

Cook, C. P., T. van de Flierdt, T. Williams, S. R. Hemming, M. Iwai, M. Kobayashi, et al. (2013) Dynamic behaviour of the East Antarctic Ice Sheet during Pliocene warmth. *Nature Geoscience,* 6**,** 765-769.

Cornford, S. L., D. F. Martin, A. J. Payne, E. G. Ng, A. M. Le Brocq, R. M. Gladstone, et al. (2015) Century-scale simulations of the response of the West Antarctic Ice Sheet to a warming climate. *The Cryosphere,* 9**,** 1579-1600.

Corr, H., F. Ferraccioli, N. Frearson, T. Jordan, C. Robinson, E. Armadillo, et al. (2007) Airborne radio-echo sounding of the Wilkes Subglacial Basin, the Transantarctic Mountains, and the Dome C region. *Terra Antartica Reports,* 13**,** 55-63.

Corr, H. F. J. & D. G. Vaughan (2008) A recent volcanic eruption beneath the West Antarctic Ice Sheet. *Nature Geoscience,* 1**,** 122-125.

.

Creyts, T. T., F. Ferraccioli, R. E. Bell, M. Wolovick, H. Corr, K. C. Rose, et al. (2014) Freezing of ridges and water networks preserves the Gamburtsev Subglacial Mountains for millions of years. *Geophysical Research Letters,* 41**,** 8114-8122.

Cui, X., J. S. Greenbaum, S. Lang, X. Zhao, L. Li, J. Guo, et al. (2020a) The scientific operations of Snow Eagle 601 in Antarctica in the past five austral seasons. *Remote Sensing,* 12**,** 2994.

Cui, X., H. Jeofry, J. S. Greenbaum, J. Guo, L. Li, L. E. Lindzey, et al. (2020b) Bed topography of Princess Elizabeth Land in East Antarctica. *Earth System Science Data,* 12**,** 2765-2774.

Cui, X. B., W. J. Du, H. Xie & B. Sun (2020c) The ice flux to the Lambert Glacier and Amery Ice Shelf along the Chinese inland traverse and implications for mass balance of the drainage basins, East Antarctica. *Polar Research,* 39**,** 3582.

Dahl-Jensen, D., N. S. Gundestrup, K. Keller, S. J. Johnsen, S. P. Gogineni, C. T. Allen, et al. (1997) A search in north Greenland for a new ice-core drill site. *Journal of Glaciology,* 43**,** 300-306.

Damaske, D. & M. McLean (2005) An aerogeophysical survey south of the Prince Charles Mountains, East Antarctica. *Terra Antartica,* 12**,** 87-98.

Dansgaard, W. & S. J. Johnsen (1969) A flow model and a time scale for the ice core from Camp Century, Greenland. *Journal of Glaciology,* 8**,** 215 - 223.

Das, I., R. E. Bell, T. A. Scambos, M. Wolovick, T. T. Creyts, M. Studinger, et al. (2013) Influence of persistent wind scour on the surface mass balance of Antarctica. *Nature Geoscience,* 6**,** 367-371.

Das, I., L. Padman, R. E. Bell, H. A. Fricker, K. J. Tinto, C. Hulbe, et al. (2020) Multidecadal basal-melt rates and structure of the Ross Ice Shelf, Antarctica, using airborne ice-penetrating radar. *Journal of Geophysical Research: Earth Surface,* 125**,** e2019JF005241.

Dawson, E. J., D. M. Schroeder, W. Chu, E. Mantelli & H. Seroussi (2022) Ice mass-loss sensitivity to the Antarctic Ice Sheet basal thermal state. *Nature Communications,* 13**,** 4957.

DeConto, R. M. & D. Pollard (2016) Contribution of Antarctica to past and future sea-level rise. *Nature,* 531**,** 591-597.

DeConto, R. M., D. Pollard, R. B. Alley, I. Velicogna, E. Gasson, N. Gomez, et al. (2021) The Paris Climate Agreement and future sea-level rise from Antarctica. *Nature,* 593**,** 83-89.

Delf, R., D. M. Schroeder, A. Curtis, A. Giannopoulos & R. G. Bingham (2020) A comparison of automated approaches to extracting englacial-layer geometry from radar data across ice sheets. *Annals of Glaciology,* 61**,** 234-241.

Dome Fuji Ice Core Project Members (2017) State dependence of climatic instability over the past 720,000 years from Antarctic ice cores and climate modeling. *Science Advances,* 3**,** e1600446.

Dong, S., X. Tang, J. Guo, L. Fu, X. Chen & B. Sun (2021) EisNet: Extracting bedrock and internal layers from radiostratigraphy of ice sheets with machine learning. *IEEE Transactions on Geoscience and Remote Sensing,* 60**,** 4303212.

Dowdeswell, J. A. & S. Evans (2004) Investigations of the form and flow of ice sheets and glaciers using radio-echo sounding. *Reports on Progress in Physics,* 67**,** 1821-1861.

Drewry, D. J. (1975) Terrain units in eastern Antarctica. *Nature,* 256**,** 194-195.

Drewry, D. J. (Ed.) (1983) Antarctica: Glaciological and Geophysical Folio. Cambridge: Cambridge University Press.

Drewry, D. J. (2023) *The Land Beneath the Ice: The Pioneering Years of Radar Exploration in Antarctica*. Princeton: Princeton University Press.

Drewry, D. J. & D. T. Meldrum (1978) Antarctic airborne radio-echo sounding, 1977–78. *Polar Record,* 19**,** 267-273.

Drews, R., O. Eisen, D. Steinhage, I. Weikusat, S. Kipfstuhl & F. Wilhelms (2012) Potential mechanisms for anisotropy in ice-penetrating radar data. *Journal of Glaciology,* 58**,** 613-624.

Drews, R., O. Eisen, I. Weikusat, S. Kipfstuhl, A. Lambrecht, D. Steinhage, et al. (2009) Layer disturbances and the radio-echo free zone in ice sheets. *The Cryosphere,* 3**,** 195-203.

Drews, R., C. Martín, D. Steinhage & O. Eisen (2013) Characterizing the glaciological conditions at Halvfarryggen Ice Dome, Dronning Maud Land, Antarctica. *Journal of Glaciology,* 59**,** 9-20.

Drews, R., K. Matsuoka, C. Martín, D. Callens, N. Bergeot & F. Pattyn (2015) Evolution of Derwael Ice Rise in Dronning Maud Land, Antarctica, over the last millennia. *Journal of Geophysical Research: Earth Surface,* 120**,** 564-579.

Dutton, A., A. E. Carlson, A. J. Long, G. A. Milne, P. U. Clark, R. DeConto, et al. (2015) Sea-level rise due to polar ice-sheet mass loss during past warm periods. *Science,* 349**,** aaa4019.

Eisen, O. (2008) Inference of velocity pattern from isochronous layers in firn, using an inverse method. *Journal of Glaciology,* 54**,** 613-630.

Eisen, O., I. Hamann, S. Kipfstuhl, D. Steinhage & F. Wilhelms (2007) Direct evidence for continuous radar reflector originating from changes in crystal-orientation fabric. *The Cryosphere,* 1**,** 1-10.

Eisen, O., U. Nixdorf, F. Wilhelms & H. Miller (2002) Electromagnetic wave speed in polar ice: Validation of the common-midpoint technique with high-resolution dielectric-profiling and γ-density measurements. *Annals of Glaciology,* 34**,** 150-156.

Eisen, O., W. Rack, U. Nixdorf & F. Wilhelms (2005) Characteristics of accumulation around the EPICA deep-drilling site in Dronning Maud Land, Antarctica. *Annals of Glaciology,* 41**,** 41-46.

Eisen, O., F. Wilhelms, U. Nixdorf & H. Miller (2003) Revealing the nature of radar reflections in ice: DEP-based FDTD forward modeling. *Geophysical Research Letters,* 30**,** 1218.

Eisen, O., F. Wilhelms, D. Steinhage & J. Schwander (2006) Improved method to determine radio-echo sounding reflector depths from ice-core profiles of permittivity and conductivity. *Journal of Glaciology,* 52**,** 299-310.

EPICA Community Members (2004) Eight glacial cycles from an Antarctic ice core. *Nature,* 429**,** 623-628.

Ershadi, M. R., R. Drews, C. Martín, O. Eisen, C. Ritz, H. Corr, et al. (2022) Polarimetric radar reveals the spatial distribution of ice fabric at domes and divides in East Antarctica. *The Cryosphere,* 16**,** 1719-1739.

Escutia, C., M. A. Bárcena, R. G. Lucchi, O. Romero, A. M. Ballegeer, J. J. Gonzalez, et al. (2009) Circum-Antarctic warming events between 4 and 3.5 Ma recorded in marine sediments from the Prydz Bay (ODP Leg 188) and the Antarctic Peninsula (ODP Leg 178) margins. *Global and Planetary Change,* 69**,** 170-184.

Evans, S. & B. M. E. Smith (1970) Radio-echo exploration of the Antarctic Ice Sheet, 1969–70. *Polar Record,* 15**,** 336-338.

Fahnestock, M., W. Abdalati, S. Luo & S. Gogineni (2001a) Internal-layer tracing and age-depth-accumulation relationships for the northern Greenland Ice Sheet. *Journal of Geophysical Research: Atmospheres,* 106**,** 33789-33797.

Fahnestock, M. A., W. Abdalati, I. R. Joughin, J. M. Brozena & P. Gogineni (2001b) High geothermal heat flow, basal melt, and the origin of rapid ice flow in central Greenland. *Science,* 294**,** 2338 - 2342.

Fischer, H., J. Severinghaus, E. Brook, E. Wolff, M. Albert, O. Alemany, et al. (2013) Where to find 1.5 million yr old ice for the IPICS "Oldest-Ice" ice core. *Climate of the Past,* 9**,** 2489-2505.

Fogwill, C. J., C. S. M. Turney, N. R. Golledge, D. M. Etheridge, M. Rubino, D. P. Thornton, et al. (2017) Antarctic ice-sheet discharge driven by atmosphere-ocean feedbacks at the Last Glacial Termination. *Scientific Reports,* 7**,** 39979.

Fox-Kemper, B., H. T. Hewitt, C. Xiao, G. Aðalgeirsdóttir, S. S. Drijfhout, T. L. Edwards, et al. 2021. Ocean, cryosphere and sea-level change. In *Climate Change 2021: The Physical Science Basis. Contribution of Working Group I to the Sixth Assessment Report of the Intergovernmental Panel on Climate Change,* eds. V. Masson-Delmotte, P. Zhai, A. Pirani, S. L. Connors, C. Péan, S. Berger, N. Caud, Y. Chen, L. Goldfarb, M. I. Gomis, M. Huang, K. Leitzell, E. Lonnoy, J. B. R. Matthews, T. K. Maycock, T. Waterfield, O. Yelekçi, R. Yu & B. Zhou, 1211-1362. Cambridge: Cambridge University Press.

Franke, S., H. Eisermann, W. Jokat, G. Eagles, J. Asseng, H. Miller, et al. (2021) Preserved landscapes underneath the Antarctic Ice Sheet reveal the geomorphological history of Jutulstraumen Basin. *Earth Surface Processes and Landforms,* 46**,** 2728-2745.

Franke, S., T. Gerber, C. Warren, D. Jansen, O. Eisen & D. Dahl-Jensen (2023) Investigating the radar response of englacial-debris-entrained basal-ice units in East Antarctica using electromagnetic forward modeling. *IEEE Transactions on Geoscience and Remote Sensing,* 61**,** 4301516.

Franke, S., D. Jansen, T. Binder, J. D. Paden, N. Dörr, T. A. Gerber, et al. (2022) Airborne ultra-wideband radar sounding over the shear margins and along flow lines at the onset region of the Northeast Greenland Ice Stream. *Earth System Science Data,* 14, 763-779.

Franke, S., D. Steinhage, V. Helm, A. M. Zuhr, J. A. Bodart, O. Eisen & P. Bons (2025) Age-depth distribution in western Dronning Maud Land, East Antarctica, and Antarctic-wide comparisons of internal refllection horizons. *The Cryosphere*, 19, 1153-1180.

Franke, S., M. Wolovick, R. Drews, D. Jansen, K. Matsuoka & P. D. Bons (2024b) Sediment freeze-on and transport near the onset of a fast-flowing glacier in East Antarctica. *Geophysical Research Letters,* 51, e2023GL107164.

Frémand, A. C., J. A. Bodart, T. A. Jordan, F. Ferraccioli, C. Robinson, H. F. J. Corr, et al. (2022) British Antarctic Survey's aerogeophysical data: Releasing 25 years of airborne gravity, magnetic, and radar datasets over Antarctica. *Earth System Science Data,* 14, 3379-3410.

Frémand, A. C., P. Fretwell, J. A. Bodart, H. D. Pritchard, A. Aitken, J. L. Bamber, et al. (2023) Antarctic Bedmap data: Findable, Accessible, Interoperable, and Reusable (FAIR) sharing of 60 years of ice bed, surface, and thickness data. *Earth System Science Data,* 15, 2695-2710.

Frezzotti, M., G. Bitelli, P. De Michelis, A. Deponti, A. Forieri, S. Gandolfi, et al. (2004) Geophysical survey at Talos Dome, East Antarctica: The search for a new deep-drilling site. *Annals of Glaciology,* 39, 423-432.

Fudge, T. J., B. H. Hills, A. N. Horlings, N. Holschuh, J. E. Christian, L. Davidge, et al. (2023) A site for deep ice coring at West Hercules Dome: Results from ground-based geophysics and modeling. *Journal of Glaciology,* 69, 538-550.

Fujita, S., P. Holmlund, I. Andersson, I. Brown, H. Enomoto, Y. Fujii, et al. (2011) Spatial and temporal variability of snow accumulation rate on the East Antarctic ice divide between Dome Fuji and EPICA DML. *The Cryosphere,* 5, 1057-1081.

Fujita, S., H. Maeno, S. Uratsuka, T. Furukawa, S. Mae, Y. Fujii, et al. (1999) Nature of radio-echo layering in the Antarctic Ice Sheet detected by a two-frequency experiment. *Journal of Geophysical Research: Solid Earth,* 104, 13013-13024.

Fujita, S., T. Matsuoka, T. Ishida, K. Matsuoka & S. Mae (2000) A summary of the complex dielectric permittivity of ice in the megahertz range and its applications for radar sounding of polar ice sheets. In *International Symposium on Physics of Ice Core Records*, 185 - 212. Shikotsukohan, Hokkaido, Japan.

Gagliardini, O., T. Zwinger, F. Gillet-Chaulet, G. Durand, L. Favier, B. de Fleurian, et al. (2013) Capabilities and performance of Elmer/Ice, a new-generation ice-sheet model. *Geoscientific Model Development,* 6, 1299-1318.

Gasson, E., R. DeConto, D. Pollard & R. H. Levy (2016) Dynamic Antarctic ice sheet during the early to mid-Miocene. *Proceedings of the National Academy of Sciences,* 113, 3459-3464.

Gerber, T. A., D. A. Lilien, N. M. Rathmann, S. Franke, T. J. Young, F. Valero-Delgado, et al. (2023) Crystal-orientation-fabric anisotropy causes directional hardening of the Northeast Greenland Ice Stream. *Nature Communications,* 14, 2653.

Geyer, A., A. Di Roberto, J. L. Smellie, M. Van Wyk de Vries, K. S. Panter, A. P. Martin, et al. (2023) Volcanism in Antarctica: An assessment of the present state of research and future directions. *Journal of Volcanology and Geothermal Research,* 444, 107941.

Goel, V., C. Martín & K. Matsuoka (2018) Ice-rise stratigraphy reveals changes in surface mass balance over the last millennia in Dronning Maud Land. *Journal of Glaciology,* 64, 932-942.

Goel, V., C. Martín & K. Matsuoka (2024) Evolution of ice rises in the Fimbul Ice Shelf, Dronning Maud Land, over the last millennium. *Antarctic Science,* 36, 110-124.

Goelles, T., K. Grosfeld & G. Lohmann (2014) Semi-Lagrangian transport of oxygen isotopes in polythermal ice sheets: implementation and first results. *Geoscientific Model Development,* 7, 1395-1408.

Goelzer, H., S. Nowicki, A. Payne, E. Larour, H. Seroussi, W. H. Lipscomb, et al. (2020) The future sea-level contribution of the Greenland Ice Sheet: A multi-model ensemble study of ISMIP6. *The Cryosphere,* 14, 3071-3096.

Gogineni, P., T. Chuah, C. Allen, K. Jezek & R. K. Moore (1998) An improved coherent radar depth sounder. *Journal of Glaciology,* 44, 659-669.

Golledge, N. R., E. D. Keller, N. Gomez, K. A. Naughten, J. Bernales, L. D. Trusel, et al. (2019) Global environmental consequences of twenty-first-century ice-sheet melt. *Nature,* 566, 65-72.

Golledge, N. R., D. E. Kowalewski, T. R. Naish, R. H. Levy, C. J. Fogwill & E. G. W. Gasson (2015) The multi-millennial Antarctic commitment to future sea-level rise. *Nature,* 526, 421-425.

Goodge, J. W. & J. P. Severinghaus (2016) Rapid Access Ice Drill: A new tool for exploration of the deep Antarctic ice sheets and subglacial geology. *Journal of Glaciology,* 62, 1049-1064.

Goodge, J. W., J. P. Severinghaus, J. Johnson, D. Tosi & R. Bay (2021) Deep ice drilling, bedrock coring and dust logging with the Rapid Access Ice Drill (RAID) at Minna Bluff, Antarctica. *Annals of Glaciology,* 62, 324-339.

Gow, A. J. & T. Williamson (1976) Rheological implications of the internal structure and crystal fabrics of the West Antarctic Ice Sheet as revealed by deep core drilling at Byrd Station. *Geological Society of America Bulletin,* 87, 1665-1677.

Gudmandsen, P., E. Nilsson, M. Pallisgaard, N. Skou & F. Søndergaard (1975) New equipment for radio-echo sounding. *Antarctic Journal of the United States,* 10, 234-236.

Gulick, S. P. S., A. E. Shevenell, A. Montelli, R. Fernandez, C. Smith, S. Warny, et al. (2017) Initiation and long-term instability of the East Antarctic Ice Sheet. *Nature,* 552, 225-229.

Hammer, C. U. (1980) Acidity of polar ice cores in relation to absolute dating, past volcanism, and radio–echoes. *Journal of Glaciology,* 25, 359-372.

Hammer, C. U., H. B. Clausen & C. C. Langway (1997) 50,000 years of recorded global volcanism. *Climatic Change,* 35, 1-15.

Harrison, C. H. (1973) Radio-echo sounding of horizontal layers in ice. *Journal of Glaciology,* 12, 383-397.

Hays, J. D., J. Imbrie & N. J. Shackleton (1976) Variations in the Earth's orbit: Pacemaker of the ice ages. *Science,* 194, 1121-1132.

Hein, A., S. M. Marrero, J. Woodward, S. A. Dunning, K. Winter, M. J. Westoby, et al. (2016) Mid-Holocene pulse of thinning in the Weddell Sea sector of the West Antarctic ice sheet. Nature Communications, 7, 12511.

Heister, A. & R. Scheiber (2018) Coherent large-beamwidth processing of radio-echo sounding data. *The Cryosphere,* 12, 2969-2979.

Hélière, F., C.-C. Lin, H. F. J. Corr & D. G. Vaughan (2007) Radio-echo sounding of Pine Island Glacier, West Antarctica: Aperture-synthesis processing and analysis of feasibility from space. *IEEE Transactions on Geoscience and Remote Sensing,* 45, 2573-2582.

Hempel, L., F. Thyssen, N. Gundestrup, H. B. Clausen & H. Miller (2000) A comparison of radio-echo sounding data and electrical conductivity of the GRIP Ice Core. *Journal of Glaciology,* 46, 369-374.

Henry, A. C. J., C. Schannwell, V. Višnjević, J. Millstein, P. D. Bons, O. Eisen, et al. (2024) Predicting the three-dimensional age-depth field of an ice rise. *Authorea*, DOI: 10.22541/essoar.169230234.44865946/v1.

Higgins, J. A., A. V. Kurbatov, N. E. Spaulding, E. Brook, D. S. Introne, L. M. Chimiak, et al. (2015) Atmospheric composition 1 million years ago from blue ice in the Allan Hills, Antarctica. *Proceedings of the National Academy of Sciences,* 112, 6887-6891.

Hillebrand, T. R., J. O. Stone, M. Koutnik, C. King, H. Conway, B. Hall, et al. (2021) Holocene thinning of Darwin and Hatherton glaciers, Antarctica, and implications for grounding-line retreat in the Ross Sea. *The Cryosphere,* 15, 3329-3354.

Hillenbrand, C.-D., J. A. Smith, D. A. Hodell, M. Greaves, C. R. Poole, S. Kender, et al. (2017) West Antarctic Ice Sheet retreat driven by Holocene warm water incursions. *Nature,* 547, 43-48.

Hills, B. H., K. Christianson, A. O. Hoffman, T. J. Fudge, N. Holschuh, E. C. Kahle, et al. (2022) Geophysics and thermodynamics at South Pole Lake indicate stability and a regionally thawed bed. *Geophysical Research Letters,* 49, e2021GL096218.

Hindmarsh, R. C. A., E. C. King, R. Mulvaney, H. F. J. Corr, G. Hiess & F. Gillet-Chaulet (2011) Flow at ice-divide triple junctions: 2. Three-dimensional views of isochrone architecture from ice-penetrating radar surveys. *Journal of Geophysical Research: Earth Surface,* 116, F02024.

Hindmarsh, R. C. A., G. J.-M. C. Leysinger Vieli & F. Parrenin (2009) A large-scale numerical model for computing isochrone geometry. *Annals of Glaciology,* 50, 130-140.

Hindmarsh, R. C. A., G. J.-M. C. Leysinger Vieli, M. J. Raymond & G. H. Gudmundsson (2006) Draping or overriding: The effect of horizontal stress gradients on internal layer architecture in ice sheets. *Journal of Geophysical Research: Earth Surface,* 111, F02018.

Hodgkins, R., M. J. Siegert & J. A. Dowdeswell (2000) Geophysical investigations of ice-sheet internal layering and deformation in the Dome C region of central East Antarctica. *Journal of Glaciology,* 46, 161-166.

Holland, P. R., H. F. J. Corr, D. G. Vaughan, A. Jenkins & P. Skvarca (2009) Marine ice in Larsen Ice Shelf. *Geophysical Research Letters,* 36, L11604.

Holschuh, N., K. Christianson & S. Anandakrishnan (2014) Power loss in dipping internal reflectors, imaged using ice-penetrating radar. *Annals of Glaciology,* 55, 49-56.

Holschuh, N., K. Christianson, H. Conway, R. Jacobel & B. Welch (2018) Persistent tracers of historic ice flow in glacial stratigraphy near Kamb Ice Stream, West Antarctica. *The Cryosphere,* 12, 2821 - 2829.

Holschuh, N., D. A. Lilien & K. Christianson (2019) Thermal weakening, convergent flow, and vertical heat transport in the Northeast Greenland Ice Stream shear margins. *Geophysical Research Letters,* 46, 8184-8193.

Holschuh, N., B. R. Parizek, R. B. Alley & S. Anandakrishnan (2017) Decoding ice-sheet behavior using englacial layer slopes. *Geophysical Research Letters,* 44, 5561-5570.

Humbert, A., D. Steinhage, V. Helm, S. Beyer & T. Kleiner (2018) Missing evidence of widespread subglacial lakes at Recovery Glacier, Antarctica. *Journal of Geophysical Research: Earth Surface,* 123, 2802-2826.

IceCube Collaboration (2013) South Pole glacial climate reconstruction from multi-borehole laser particulate stratigraphy. *Journal of Glaciology,* 59**,** 1117-1128.

Jacobel, R. W., A. M. Gades, D. L. Gottschling, S. M. Hodge & D. L. Wright (1993) Interpretation of radar-detected internal layer folding in West Antarctic ice streams. *Journal of Glaciology,* 39**,** 528-537.

Jacobel, R. W., T. A. Scambos, N. A. Nereson & C. F. Raymond (2000) Changes in the margin of Ice Stream C, Antarctica. *Journal of Glaciology,* 46**,** 102-110.

Jacobel, R. W. & B. C. Welch (2005) A time marker at 17.5 kyr BP detected throughout West Antarctica. *Annals of Glaciology,* 41**,** 47-51.

Jansen, D., S. Franke, C. C. Bauer, T. Binder, D. Dahl-Jensen, J. Eichler, et al. (2024) Shear margins in upper half of Northeast Greenland Ice Stream were established two millennia ago. *Nature Communications,* 15**,** 1193.

Jennings, S. J. A. & M. J. Hambrey (2021) Structures and deformation in glaciers and ice sheets. *Reviews of Geophysics,* 59**,** e2021RG000743.

Johnson, J. S., M. J. Bentley & K. Gohl (2008) First exposure ages from the Amundsen Sea Embayment, West Antarctica: The Late Quaternary context for recent thinning of Pine Island, Smith, and Pope Glaciers. Geology, 36, 223-226.

Jordan, T. A., C. Martín, F. Ferraccioli, K. Matsuoka, H. Corr, R. Forsberg, et al. (2018) Anomalously high geothermal flux near the South Pole. *Scientific Reports,* 8**,** 16785.

Jordan, T. M., C. Martín, A. M. Brisbourne, D. M. Schroeder & A. M. Smith (2022) Radar characterization of ice-crystal-orientation fabric and anisotropic viscosity within an Antarctic ice stream. *Journal of Geophysical Research: Earth Surface,* 127**,** e2022JF006673.

Jordan, T. M., D. M. Schroeder, C. W. Elsworth & M. R. Siegfried (2020) Estimation of ice fabric within Whillans Ice Stream using polarimetric phase-sensitive radar sounding. *Annals of Glaciology,* 61**,** 74-83.

Jouzel, J., V. Masson-Delmotte, O. Cattani, G. Dreyfus, S. Falourd, G. Hoffmann, et al. (2007) Orbital and millennial Antarctic climate variability over the past 800,000 years. *Science,* 317**,** 793-796.

Karlsson, N. B., T. Binder, G. Eagles, V. Helm, F. Pattyn, B. Van Liefferinge, et al. (2018) Glaciological characteristics in the Dome Fuji region and new assessment for "Oldest Ice". *The Cryosphere,* 12**,** 2413-2424.

Karlsson, N. B., R. G. Bingham, D. M. Rippin, R. C. A. Hindmarsh, H. F. J. Corr & D. G. Vaughan (2014) Constraining past accumulation in the central Pine Island Glacier basin, West Antarctica, using radio-echo sounding. *Journal of Glaciology,* 60**,** 553-562.

Karlsson, N. B., D. M. Rippin, R. G. Bingham & D. G. Vaughan (2012) A 'continuity-index' for assessing ice-sheet dynamics from radar-sounded internal layers. *Earth and Planetary Science Letters,* 335-336**,** 88-94.

Karlsson, N. B., D. M. Rippin, D. G. Vaughan & H. F. J. Corr (2009) The internal layering of Pine Island Glacier, West Antarctica, from airborne radar-sounding data. *Annals of Glaciology,* 50**,** 141-146.

King, E. C. (2011) Ice stream or not? Radio-echo sounding of Carlson Inlet, West Antarctica. *The Cryosphere,* 5**,** 907-916.

Kingslake, J., R. C. A. Hindmarsh, G. Aðalgeirsdóttir, H. Conway, H. F. J. Corr, F. Gillet-Chaulet, et al. (2014) Full-depth englacial vertical ice-sheet velocities measured using phase-sensitive radar. *Journal of Geophysical Research: Earth Surface,* 119**,** 2604-2618.

Kingslake, J., C. Martín, R. J. Arthern, H. F. J. Corr & E. C. King (2016) Ice-flow reorganization in West Antarctica 2.5 kyr ago dated using radar-derived englacial flow velocities. *Geophysical Research Letters,* 43**,** 9103-9112.

Kingslake, J., R. P. Scherer, T. Albrecht, J. Coenen, R. D. Powell, R. Reese, et al. (2018) Extensive retreat and re-advance of the West Antarctic Ice Sheet during the Holocene. *Nature,* 558**,** 430-434.

Koch, I., R. Drews, O. Eisen, S. Franke, D. Jansen, K. Matsuoka, et al. (2023) Radar internal reflection horizons from multisystem data reflect ice dynamic and surface accumulation history along the Princess Ragnhild Coast, Dronning Maud Land, East Antarctica. *Journal of Glaciology***,** 70, e18.

Konrad, H., A. E. Hogg, R. Mulvaney, R. Arthern, R. J. Tuckwell, B. Medley, et al. (2019) Observations of surface mass balance on Pine Island Glacier, West Antarctica, and the effect of strain history in fast-flowing sections. *Journal of Glaciology,* 65**,** 595-604.

Koutnik, M. R., T. J. Fudge, H. Conway, E. D. Waddington, T. A. Neumann, K. M. Cuffey, et al. (2016) Holocene accumulation and ice flow near the West Antarctic Ice Sheet Divide ice-core site. *Journal of Geophysical Research: Earth Surface,* 121**,** 907-924.

Kovacs, A., A. J. Gow & R. M. Morey (1995) The in-situ dielectric constant of polar firn revisited. *Cold Regions Science and Technology,* 23**,** 245-256.

Kowalewski, S., V. Helm, E. M. Morris & O. Eisen (2021) The regional-scale surface mass balance of Pine Island Glacier, West Antarctica, over the period 2005–2014, derived from airborne radar soundings and neutron probe measurements. *The Cryosphere,* 15**,** 1285-1305.

Laird, C. M., W. A. Blake, K. Matsuoka, H. Conway, C. T. Allen, C. J. Leuschen, et al. (2010) Deep ice stratigraphy and basal conditions in central West Antarctica revealed by coherent radar. *IEEE Geoscience and Remote Sensing Letters,* 7, 246-250.

Le Meur, E., O. Magand, L. Arnaud, M. Fily, M. Frezzotti, M. Cavitte, et al. (2018) Spatial and temporal distributions of surface mass balance between Concordia and Vostok stations, Antarctica, from combined radar and ice-core data: First results and detailed error analysis. *The Cryosphere,* 12, 1831-1850.

Lecavalier, B. S., L. Tarasov, G. Balco, P. Spector, C. D. Hillenbrand, C. Buizert, et al. (2023) Antarctic Ice Sheet paleo-constraint database. *Earth System Science Data,* 15, 3573-3596.

Lee, H., H. Seo, H. Han, H. Ju & J. Lee (2021) Velocity anomaly of Campbell Glacier, East Antarctica, observed by double-differential interferometric SAR and ice-penetrating radar. *Remote Sensing,* 13, 2691.

Legrain, E., F. Parrenin & E. Capron (2023) A gradual change is more likely to have caused the Mid-Pleistocene Transition than an abrupt event. *Communications Earth & Environment,* 4, 90.

Lenaerts, J. T. M., B. Medley, M. R. van den Broeke & B. Wouters (2019) Observing and modeling ice-sheet surface mass balance. *Reviews of Geophysics,* 57, 376-420.

Leysinger Vieli, G. J.-M. C., R. C. A. Hindmarsh & M. J. Siegert (2007) Three-dimensional flow influences on radar layer stratigraphy. *Annals of Glaciology,* 46, 22-28.

Leysinger Vieli, G. J.-M. C., R. C. A. Hindmarsh, M. J. Siegert & B. Sun (2011) Time-dependence of the spatial pattern of accumulation rate in East Antarctica deduced from isochronic radar layers using a 3-D numerical ice flow model. *Journal of Geophysical Research: Earth Surface,* 116, F02018.

Leysinger Vieli, G. J.-M. C., C. Martín, R. C. A. Hindmarsh & M. P. Lüthi (2018) Basal freeze-on generates complex ice-sheet stratigraphy. *Nature Communications,* 9, 4669.

Leysinger Vieli, G. J.-M. C., M. J. Siegert & A. J. Payne (2004) Reconstructing ice-sheet accumulation rates at Ridge B, East Antarctica. *Annals of Glaciology,* 39, 326-330.

Lilien, D. A., D. Steinhage, D. Taylor, F. Parrenin, C. Ritz, R. Mulvaney, et al. (2021) New radar constraints support presence of ice older than 1.5 Myr at Little Dome C. *The Cryosphere,* 15, 1881-1888.

Lindzey, L. E., L. H. Beem, D. A. Young, E. Quartini, D. D. Blankenship, C. K. Lee, et al. (2020) Aerogeophysical characterization of an active subglacial lake system in the David Glacier catchment, Antarctica. *The Cryosphere,* 14, 2217-2233.

Luo, K., S. Liu, J. Guo, T. Wang, L. Li, X. Cui, et al. (2020) Radar-derived internal structure and basal roughness characterization along a traverse from Zhongshan Station to Dome A, East Antarctica. *Remote Sensing,* 12, 1079.

Luo, K., X. Tang, S. Liu, J. Guo, J. S. Greenbaum, L. Li, et al. (2022) Deep radiostratigraphy constraints support the presence of persistent wind scouring behavior for more than 100 ka in the East Antarctic Ice Sheet. *IEEE Transactions on Geoscience and Remote Sensing,* 60, 4306213.

MacGregor, J. A., L. N. Boisvert, B. Medley, A. A. Petty, J. P. Harbeck, R. E. Bell, et al. (2021) The scientific legacy of NASA's Operation IceBridge. *Reviews of Geophysics,* 59, e2020RG000712.

MacGregor, J. A., W. T. Colgan, M. A. Fahnestock, M. Morlighem, G. A. Catania, J. D. Paden, et al. (2016) Holocene deceleration of the Greenland Ice Sheet. *Science,* 351, 590-593.

MacGregor, J. A., M. A. Fahnestock, G. A. Catania, J. D. Paden, S. P. Gogineni, S. K. Young, et al. (2015a) Radiostratigraphy and age structure of the Greenland Ice Sheet. *Journal of Geophysical Research: Earth Surface,* 120, 212-241.

MacGregor, J. A., M. A. Fahnestock, J. D. Paden, J, Li, J. P. Harbeck & A. Aschwanden (2025) A revised and expanded deep radiostratigraphy of the Greenland Ice Sheet from airborne radar sounding surveys between 1993–2019. *Earth System Science Data Discussions,* https://doi.org/10.5194/essd-2024-578, in review, 2025.

MacGregor, J. A., J. L. Li, J. D. Paden, G. A. Catania, G. D. Clow, M. A. Fahnestock, et al. (2015b) Radar attenuation and temperature within the Greenland Ice Sheet. *Journal of Geophysical Research: Earth Surface,* 120, 983-1008.

MacGregor, J. A., K. Matsuoka, M. R. Koutnik, E. D. Waddington, M. Studinger & D. P. Winebrenner (2009) Millennially averaged accumulation rates for the Vostok Subglacial Lake region inferred from deep internal layers. *Annals of Glaciology,* 50, 25-34.

MacGregor, J. A., D. P. Winebrenner, H. Conway, K. Matsuoka, P. A. Mayewski & G. D. Clow (2007) Modeling englacial radar attenuation at Siple Dome, West Antarctica, using ice chemistry and temperature data. *Journal of Geophysical Research: Earth Surface,* 112, F03008.

Mackintosh, A. N., E. Verleyen, P. E. O'Brien, D. A. White, R. S. Jones, R. McKay, et al. (2014) Retreat history of the East Antarctic Ice Sheet since the Last Glacial Maximum. *Quaternary Science Reviews,* 100, 10-30.

Martín, C. & G. H. Gudmundsson (2012) Effects of nonlinear rheology, temperature and anisotropy on the relationship between age and depth at ice divides. *The Cryosphere,* 6, 1221-1229.

Martín, C., G. H. Gudmundsson & E. C. King (2014) Modelling of Kealey Ice Rise, Antarctica, reveals stable ice-flow conditions in East Ellsworth Land over millennia. *Journal of Glaciology,* 60, 139-146.

Martín, C., R. C. A. Hindmarsh & F. J. Navarro (2006) Dating ice flow change near the flow divide at Roosevelt Island, Antarctica, by using a thermomechanical model to predict radar stratigraphy. *Journal of Geophysical Research: Earth Surface,* 111**,** F01011.

Martín, C., R. C. A. Hindmarsh & F. J. Navarro (2009) On the effects of divide migration, along-ridge flow, and basal sliding on isochrones near an ice divide. *Journal of Geophysical Research: Earth Surface,* 114**,** F02006.

Matsuoka, K., T. Furukawa, S. Fujita, H. Maeno, S. Uratsuka, R. Naruse, et al. (2003) Crystal-orientation fabrics within the Antarctic Ice Sheet revealed by a multipolarization plane and dual-frequency radar survey. *Journal of Geophysical Research: Solid Earth,* 108**,** 2499.

Matsuoka, K., A. Gades, H. Conway, G. Catania & C. F. Raymond (2009) Radar signatures beneath a surface topographic lineation near the outlet of Kamb Ice Stream and Engelhardt Ice Ridge, West Antarctica. *Annals of Glaciology,* 50**,** 98-104.

Matsuoka, K., R. C. A. Hindmarsh, G. Moholdt, M. J. Bentley, H. D. Pritchard, J. Brown, et al. (2015) Antarctic ice rises and rumples: Their properties and significance for ice-sheet dynamics and evolution. *Earth-Science Reviews,* 150**,** 724-745.

Matsuoka, K., J. A. MacGregor & F. Pattyn (2012) Predicting radar attenuation within the Antarctic Ice Sheet. *Earth and Planetary Science Letters,* 359-360**,** 173-183.

Mayewski, P. A., M. Frezzotti, N. Bertler, T. van Ommen, G. Hamilton, T. H. Jacka, et al. (2005) The International Trans-Antarctic Scientific Expedition (ITASE): an overview. Annals of Glaciology, 41, 180-185.

McConnell, J. R., A. Burke, N. W. Dunbar, P. Köhler, J. L. Thomas, M. M. Arienzo, et al. (2017) Synchronous volcanic eruptions and abrupt climate change ~17.7 ka plausibly linked by stratospheric ozone depletion. *Proceedings of the National Academy of Sciences,* 114**,** 10035-10040.

Medley, B., I. Joughin, S. B. Das, E. J. Steig, H. Conway, S. Gogineni, et al. (2013) Airborne-radar and ice-core observations of annual snow accumulation over Thwaites Glacier, West Antarctica, confirm the spatiotemporal variability of global and regional atmospheric models. *Geophysical Research Letters,* 40**,** 3649-3654.

Medley, B., I. Joughin, B. E. Smith, S. B. Das, E. J. Steig, H. Conway, et al. (2014) Constraining the recent mass balance of Pine Island and Thwaites glaciers, West Antarctica, with airborne observations of snow accumulation. *The Cryosphere,* 8**,** 1375-1392.

Millar, D. H. M. (1981) Radio-echo layering in polar ice sheets and past volcanic activity. *Nature,* 292**,** 441-443.

Millar, D. H. M. (1982) Acidity levels in ice sheets from radio echo-sounding. *Annals of Glaciology,* 3**,** 199-203.

Miners, W. D., A. Hildebrand, S. Gerland, N. Blindow, D. Steinhage & E. W. Wolff (1997) Forward modeling of the internal layers in radio-echo sounding using electrical and density measurements from ice cores. *Journal of Physical Chemistry B,* 101**,** 6201-6204.

Mojtabavi, S., O. Eisen, S. Franke, D. Jansen, D. Steinhage, J. Paden, et al. (2022) Origin of englacial stratigraphy at three deep ice core sites of the Greenland Ice Sheet by synthetic radar modelling. *Journal of Glaciology,* 68**,** 799-811.

Moqadam, H., D. Steinhage, A. Wilhelm & O. Eisen (2025) Going deeper with deep learning: Automatically tracing internal reflection horizons in ice sheets. In review for *Machine Learning and Computation*, https://doi.org/10.22541/essoar.172987463.39597493/v1.

Morgan, V., T. Jacka, G. Akerman & A. Clarke (1982) Outlet glacier and mass-budget studies in Enderby, Kemp, and Mac. Robertson Lands, Antarctica. *Annals of Glaciology,* 3**,** 204-210.

Morlighem, M. (2020) MEaSUREs BedMachine Antarctica, Version 2. NASA National Snow and Ice Data Center Distributed Active Archive Center.

Moss, G., V. Višnjević, O. Eisen, F. M. Oraschewski, C. Schröder, J. H. Macke, et al. (2023) Simulation-based inference of surface accumulation and basal-melt rates of an Antarctic ice shelf from isochronal layers. *ArXiv,* abs/2312.02997.

Moussessian, A., R. L. Jordan, E. Rodriguez, A. Safaeinili, T. L. Akins, W. N. Edelstein, et al. (2000) A new coherent radar for ice sounding in Greenland. In *International Geoscience and Remote Sensing Symposium (IGARRS) Proceedings*, 484-486 vol.2.

Muldoon, G. R., C. S. Jackson, D. A. Young & D. D. Blankenship (2018) Bayesian estimation of englacial radar chronology in Central West Antarctica. *Dynamics and Statistics of the Climate System,* 3**,** dzy004.

Naish, T., R. Powell, R. Levy, G. Wilson, R. Scherer, F. Talarico, et al. (2009) Obliquity-paced Pliocene West Antarctic ice sheet oscillations. *Nature,* 458**,** 322-328.

Narcisi, B. & J. R. Petit (2021) Englacial tephras of East Antarctica. *Geological Society, London, Memoirs,* 55**,** 649-664.

NEEM Community Members (2013) Eemian interglacial reconstructed from a Greenland folded ice core. *Nature,* 493**,** 489-494.

Nereson, N. A., C. F. Raymond, R. W. Jacobel & E. D. Waddington (2000) The accumulation pattern across Siple Dome, West Antarctica, inferred from radar-detected internal layers. *Journal of Glaciology,* 46**,** 75-87.

Nereson, N. A., C. F. Raymond, E. D. Waddington & R. W. Jacobel (1998) Migration of the Siple Dome ice divide, West Antarctica. *Journal of Glaciology,* 44, 643-652.

Neumann, T. A., H. Conway, S. F. Price, E. D. Waddington, G. A. Catania & D. L. Morse (2008) Holocene accumulation and ice-sheet dynamics in central West Antarctica. *Journal of Geophysical Research: Earth Surface,* 113, F02018.

Ng, F. & H. Conway (2004) Fast-flow signature in the stagnated Kamb Ice Stream, West Antarctica. *Geology,* 32, 481-484.

Ng, F. & E. C. King (2011) Kinematic waves in polar firn stratigraphy. *Journal of Glaciology,* 57, 1119-1134.

Nicholls, K. W., H. F. J. Corr, C. L. Stewart, L. B. Lok, P. V. Brennan & D. G. Vaughan (2015) A ground-based radar for measuring vertical strain rates and time-varying basal melt rates in ice sheets and shelves. *Journal of Glaciology,* 61, 1079-1087.

Nye, J. (1957) The distribution of stress and velocity in glaciers and ice sheets. *Proceedings of the Royal Society A: Mathematical, Physical and Engineering Sciences,* 239, 113-133.

Obase, T., A. Abe-Ouchi, F. Saito, S. Tsutaki, S. Fujita, K. Kawamura, et al. (2023) A one-dimensional temperature and age modeling study for selecting the drill site of the oldest ice core near Dome Fuji, Antarctica. *The Cryosphere,* 17, 2543-2562.

Oppenheimer, M., B. C. Glavovic, J. Hinkel, R. van de Wal, A. K. Magnan, A. Abd-Elgawad, et al. 2019. Sea-level rise and implications for low-lying islands, coasts and communities. In *IPCC Special Report on the Ocean and Cryosphere in a Changing Climate,* eds. H.-O. Pörtner, D. C. Roberts, V. Masson-Delmotte, P. Zhai, M. Tignor, E. Poloczanska, K. Mintenbeck, A. Alegría, M. Nicolai, A. Okem, J. Petzold, B. Rama & N. M. Weyer, 321-445. Cambridge: Cambridge University Press.

Oraschewski, F. M., I. Koch, M. R. Ershadi, J. Hawkins, O. Eisen & R. Drews (2023) Layer-optimized SAR processing with a mobile phase-sensitive radar for detecting the deep englacial stratigraphy of Colle Gnifetti, Switzerland/Italy. *The Cryosphere,* 18, 3875-3889.

Otosaka, I. N., A. Shepherd, E. R. Ivins, N. J. Schlegel, C. Amory, M. R. van den Broeke, et al. (2023) Mass balance of the Greenland and Antarctic ice sheets from 1992 to 2020. *Earth System Science Data,* 15, 1597-1616.

Paden, J., K. Tinto, D. Young, K. Christianson, D. Schroeder, M. Rahnemoonfar, et al. (2021) Open Polar Radar software and services to standardize radar echograms and integrate into a geospatial database. . In *AGU Fall Meeting 2021*, 2021AGUFM.C51A.08P.

Panton, C. (2014) Automated mapping of local layer slope and tracing of internal layers in radio echograms. *Annals of Glaciology,* 55, 71-77.

Panton, C. & N. B. Karlsson (2015) Automated mapping of near-bed radio-echo layer disruptions in the Greenland Ice Sheet. *Earth and Planetary Science Letters,* 432, 323-331.

Parrenin, F., M. G. P. Cavitte, D. D. Blankenship, J. Chappellaz, H. Fischer, O. Gagliardini, et al. (2017) Is there 1.5-million-year-old ice near Dome C, Antarctica? *The Cryosphere,* 11, 2427-2437.

Parrenin, F. & R. Hindmarsh (2007) Influence of a non-uniform velocity field on isochrone geometry along a steady flowline of an ice sheet. *Journal of Glaciology,* 53, 612-622.

Passalacqua, O., C. Ritz, F. Parrenin, S. Urbini & M. Frezzotti (2017) Geothermal flux and basal melt rate in the Dome C region inferred from radar reflectivity and heat modelling. *The Cryosphere,* 11, 2231-2246.

Pattyn, F. (2010) Antarctic subglacial conditions inferred from a hybrid ice-sheet/ice-stream model. *Earth and Planetary Science Letters,* 295, 451-461.

Pauling, A. G., C. M. Bitz & E. J. Steig (2023) Linearity of the climate-system response to raising and lowering West Antarctic and coastal Antarctic topography. *Journal of Climate,* 36, 6195-6212.

Peters, M. E., D. D. Blankenship, S. P. Carter, S. D. Kempf, D. A. Young & J. W. Holt (2007) Along-track focusing of airborne radar sounding data from West Antarctica for improving basal reflection analysis and layer detection. *IEEE Transactions on Geoscience and Remote Sensing,* 45, 2725-2736.

Peters, M. E., D. D. Blankenship & D. L. Morse (2005) Analysis techniques for coherent airborne radar sounding: Application to West Antarctic ice streams. *Journal of Geophysical Research: Solid Earth,* 110, B06303.

Pettit, E. C., T. Thorsteinsson, H. P. Jacobson & E. D. Waddington (2007) The role of crystal fabric in flow near an ice divide. *Journal of Glaciology,* 53, 277-288.

Pettit, E. C. & E. D. Waddington (2003) Ice flow at low deviatoric stress. *Journal of Glaciology,* 49, 359-369.

Pettit, E. C., E. D. Waddington, W. D. Harrison, T. Thorsteinsson, D. Elsberg, J. Morack, et al. (2011) The crossover stress, anisotropy and the ice flow law at Siple Dome, West Antarctica. *Journal of Glaciology,* 57, 39-52.

Pittard, M. L., P. L. Whitehouse, M. J. Bentley & D. Small (2022) An ensemble of Antarctic deglacial simulations constrained by geological observations. *Quaternary Science Reviews,* 298, 107800.

Pollard, D. & R. M. DeConto (2009) Modelling West Antarctic Ice Sheet growth and collapse through the past five million years. *Nature,* 458, 329-332.

Popov, S. (2020) Fifty-five years of Russian radio-echo sounding investigations in Antarctica. *Annals of Glaciology,* 61, 14-24.

Popov, S. (2022) Ice cover, subglacial landscape, and estimation of bottom melting of Mac. Robertson, Princess Elizabeth, Wilhelm II, and western Queen Mary Lands, East Antarctica. *Remote Sensing,* 14, 241.

Pratap, B., R. Dey, K. Matsuoka, G. Moholdt, K. Lindbäck, V. Goel, et al. (2022) Three-decade spatial patterns in surface mass balance of the Nivlisen Ice Shelf, central Dronning Maud Land, East Antarctica. *Journal of Glaciology,* 68, 174-186.

Pritchard, H. D., P. T. Fretwell, A. C. Frémand, J. A. Bodart, J. D. Kirkham, et al. (2025) Bedmap3 updated ice bed, surface and thickness datasets for Antarctica. *Scientific Data*, 12, 414.

Rahnemoonfar, M., M. Yari, J. Paden, L. Koenig & O. Ibikunle (2021) Deep multi-scale learning for automatic tracking of internal layers of ice in radar data. *Journal of Glaciology,* 67, 39-48.

Raymond, C. F. (1983) Deformation in the vicinity of ice divides. *Journal of Glaciology,* 29, 357-373.

Reeh, N., H. Oerter & H. H. Thomsen (2002) Comparison between Greenland ice-margin and ice-core oxygen-18 records. *Annals of Glaciology,* 35, 136-144.

Retzlaff, R., N. Lord & C. R. Bentley (1993) Airborne-radar studies: Ice Streams A, B and C, West Antarctica. *Journal of Glaciology,* 39, 495-506.

Rieckh, T., A. Born, A. Robinson, R. Law & G. Gülle (2024) Introducing ELSA v2.0: An isochronal model for ice-sheet layer tracing. *Geoscientific Model Development*, 17, 6987-7000.

Rignot, E., J. Mouginot & B. Scheuchl (2017) MEaSUREs InSAR-Based Antarctica Ice Velocity Map, Version 2. NASA National Snow and Ice Data Center Distributed Active Archive Center.

Rignot, E., R. H. Thomas, P. Kanagaratnam, G. Casassa, E. Frederick, S. Gogineni, et al. (2004) Improved estimation of the mass balance of glaciers draining into the Amundsen Sea sector of West Antarctica from the CECS/NASA 2002 campaign. *Annals of Glaciology,* 39, 231-237.

Rippin, D. M., M. J. Siegert & J. L. Bamber (2003) The englacial stratigraphy of Wilkes Land, East Antarctica, as revealed by internal radio-echo sounding layering, and its relationship with balance velocities. *Annals of Glaciology,* 36, 189-196.

Rippin, D. M., M. J. Siegert, J. L. Bamber, D. G. Vaughan & H. F. J. Corr (2006) Switch-off of a major enhanced ice-flow unit in East Antarctica. *Geophysical Research Letters,* 33, L15501.

Rivera, A., J. Uribe, R. Zamora & J. Oberreuter (2015) Subglacial Lake CECs: Discovery and in situ survey of a privileged research site in West Antarctica. *Geophysical Research Letters,* 42, 3944-3953.

Rix, J., R. Mulvaney, J. Hong & D. A. N. Ashurst (2019) Development of the British Antarctic Survey Rapid-Access Isotope Drill. *Journal of Glaciology,* 65, 288-298.

Robin, G. d. Q., S. Evans & J. T. Bailey (1969) Interpretation of radio echo sounding in polar ice sheets. *Philosophical Transactions of the Royal Society of London Series A - Mathematical and Physical Sciences,* 265, 437-505.

Robin, G. d. Q. & D. H. M. Millar (1982) Flow of ice sheets in the vicinity of subglacial peaks. *Annals of Glaciology,* 3, 290-294.

Rodriguez-Morales, F., S. Gogineni, C. J. Leuschen, J. D. Paden, J. Li, C. C. Lewis, et al. (2013) Advanced multifrequency radar instrumentation for polar research. *IEEE Transactions on Geoscience and Remote Sensing,* 52, 2824-2842.

Ross, N., H. Corr & M. Siegert (2020) Large-scale englacial folding and deep-ice stratigraphy within the West Antarctic Ice Sheet. *The Cryosphere,* 14, 2103-2114.

Ross, N. & M. Siegert (2020) Basal melting over Subglacial Lake Ellsworth and its catchment: Insights from englacial layering. *Annals of Glaciology,* 61, 198-205.

Ross, N., M. J. Siegert, J. Woodward, A. M. Smith, H. F. J. Corr, M. J. Bentley, et al. (2011) Holocene stability of the Amundsen-Weddell ice divide, West Antarctica. *Geology,* 39, 935-938.

Rowell, I. F., R. Mulvaney, J. Rix, D. R. Tetzner & E. W. Wolff (2023) Viability of chemical and water isotope ratio measurements of RAID ice chippings from Antarctica. *Journal of Glaciology,* 69, 623-638.

Sanderson, R. J., N. Ross, K. Winter, R. G. Bingham, S. L. Callard, T. A. Jordan, et al. (2024) Dated radar-stratigraphy between Dome A and South Pole, East Antarctica: Old-ice potential and ice-sheet history. *Journal of Glaciology*.

Sanderson, R. J., K. Winter, S. L. Callard, F. Napoleoni, N. Ross, T. A. Jordan, et al. (2023) Englacial architecture of Lambert Glacier, East Antarctica. *The Cryosphere,* 17, 4853-4871.

Scambos, T. A., R. E. Bell, R. B. Alley, S. Anandakrishnan, D. H. Bromwich, K. Brunt, et al. (2017) How much, how fast?: A science review and outlook for research on the instability of Antarctica's Thwaites Glacier in the 21st century. *Global and Planetary Change,* 153, 16-34.

Scanlan, K. M., A. Rutishauser, D. A. Young & D. D. Blankenship (2020) Interferometric discrimination of cross-track bed clutter in ice-penetrating radar sounding data. *Annals of Glaciology,* 61, 68-73.

Schannwell, C., R. Drews, T. A. Ehlers, O. Eisen, C. Mayer & F. Gillet-Chaulet (2019) Kinematic response of ice-rise divides to changes in ocean and atmosphere forcing. *The Cryosphere,* 13, 2673-2691.

Schroeder, D. M., R. G. Bingham, D. D. Blankenship, K. Christianson, O. Eisen, G. E. Flowers, et al. (2020) Five decades of radioglaciology. *Annals of Glaciology,* 61, 1-13.

Schroeder, D. M., A. L. Broome, A. Conger, A. Lynch, E. J. Mackie & A. Tarzona (2022) Radiometric analysis of digitized Z-scope records in archival radar sounding film. *Journal of Glaciology,* 68, 733-740.

Schroeder, D. M., J. A. Dowdeswell, M. J. Siegert, R. G. Bingham, W. N. Chu, E. J. MacKie, et al. (2019) Multidecadal observations of the Antarctic Ice Sheet from restored analog radar records. *Proceedings of the National Academy of Sciences,* 116**,** 18867-18873.
Schwander, J., T. F. Stocker, R. Walther & S. Marending (2023) Progress of the RADIX (Rapid Access Drilling and Ice eXtraction) fast-access drilling system. *The Cryosphere,* 17**,** 1151-1164.
Seroussi, H., S. Nowicki, A. J. Payne, H. Goelzer, W. H. Lipscomb, A. Abe-Ouchi, et al. (2020) ISMIP6 Antarctica: a multi-model ensemble of the Antarctic Ice Sheet evolution over the 21st century. *The Cryosphere,* 14**,** 3033-3070.
Seroussi, H., T. Pelle, W. H. Lipscomb, et al. (2024) Evolution of the Antarctic Ice Sheet over the next three centuries from an ISMIP6 model ensemble. *Earth's Future*, 12, e2024EF004561.
Siegert, M., N. Ross, H. Corr, J. Kingslake & R. Hindmarsh (2013) Late Holocene ice-flow reconfiguration in the Weddell Sea sector of West Antarctica. *Quaternary Science Reviews,* 78**,** 98-107.
Siegert, M. J. (2003) Glacial–interglacial variations in central East Antarctic ice accumulation rates. *Quaternary Science Reviews,* 22**,** 741-750.
Siegert, M. J., J. C. Ellis-Evans, M. Tranter, C. Mayer, J.-R. Petit, A. Salamatin, et al. (2001) Physical, chemical and biological processes in Lake Vostok and other Antarctic subglacial lakes. *Nature,* 414**,** 603-609.
Siegert, M. J., R. C. A. Hindmarsh & G. S. Hamilton (2003a) Evidence for a large surface ablation zone in central East Antarctica during the last Ice Age. *Quaternary Research,* 59**,** 114-121.
Siegert, M. J. & R. Hodgkins (2000) A stratigraphic link across 1100 km of the Antarctic Ice Sheet between the Vostok ice-core site and Titan Dome (near South Pole). *Geophysical Research Letters,* 27**,** 2133-2136.
Siegert, M. J., R. Hodgkins & J. A. Dowdeswell (1998) A chronology for the Dome C deep ice-core site through radio-echo layer correlation with the Vostok Ice Core, Antarctica. *Geophysical Research Letters,* 25**,** 1019-1022.
Siegert, M. J., R. Kwok, C. Mayer & B. Hubbard (2000) Water exchange between the subglacial Lake Vostok and the overlying ice sheet. *Nature,* 403**,** 643-646.
Siegert, M. J. & A. J. Payne (2004) Past rates of accumulation in central West Antarctica. *Geophysical Research Letters,* 31**,** L12403.
Siegert, M. J., A. J. Payne & I. Joughin (2003b) Spatial stability of Ice Stream D and its tributaries, West Antarctica, revealed by radio-echo sounding and interferometry. *Annals of Glaciology,* 37**,** 377-382.
Siegert, M. J., B. Welch, D. Morse, A. Vieli, D. D. Blankenship, I. Joughin, et al. (2004) Ice-flow direction change in interior West Antarctica. *Science,* 305**,** 1948-1951.
Sigl, M., M. Toohey, J. R. McConnell, J. Cole-Dai & M. Severi (2022) Volcanic stratospheric sulfur injections and aerosol optical depth during the Holocene (past 11,500 years) from a bipolar ice-core array. *Earth System Science Data,* 14**,** 3167-3196.
Sime, L. C., R. C. A. Hindmarsh & H. Corr (2011) Automated processing to derive dip angles of englacial radar reflectors in ice sheets. *Journal of Glaciology,* 57**,** 260-266.
Sime, L. C., N. B. Karlsson, J. D. Paden & S. P. Gogineni (2014) Isochronous information in a Greenland ice sheet radio echo sounding data set. *Geophysical Research Letters,* 41**,** 1593-1599.
Smith, B. E., N. E. Lord & C. R. Bentley (2002) Crevasse ages on the northern margin of Ice Stream C, West Antarctica. *Annals of Glaciology,* 34**,** 209-216.
Spaulding, N. E., J. A. Higgins, A. V. Kurbatov, M. L. Bender, S. A. Arcone, S. Campbell, et al. (2013) Climate archives from 90 to 250 ka in horizontal and vertical ice cores from the Allan Hills Blue Ice Area, Antarctica. *Quaternary Research,* 80**,** 562-574.
Steinhage, D., S. Kipfstuhl, U. Nixdorf & H. Miller (2013) Internal structure of the ice sheet between Kohnen station and Dome Fuji, Antarctica, revealed by airborne radio-echo sounding. *Annals of Glaciology,* 54**,** 163-167.
Steinhage, D., U. Nixdorf, U. Meyer & H. Miller (2001) Subglacial topography and internal structure of central and western Dronning Maud Land, Antarctica, determined from airborne radio-echo sounding. *Journal of Applied Geophysics,* 47**,** 183-189.
Stone, J.O., G. A. Balco, D. E. Sugden, M. W. Caffee, L. C. Sass III, S. G. Cowdery & C. Siddoway (2003) Holocene deglaciation of Marie Byrd Land, West Antarctica, Science, 299, 99-102.
Sutter, J., H. Fischer & O. Eisen (2021) Investigating the internal structure of the Antarctic Ice Sheet: The utility of isochrones for spatiotemporal ice-sheet model calibration. *The Cryosphere,* 15**,** 3839-3860.
Sutter, J., H. Fischer, K. Grosfeld, N. B. Karlsson, T. Kleiner, B. Van Liefferinge, et al. (2019) Modelling the Antarctic Ice Sheet across the mid-Pleistocene transition: Implications for Oldest Ice. *The Cryosphere,* 13**,** 2023-2041.
Svensson, A., M. Bigler, T. Blunier, H. B. Clausen, D. Dahl-Jensen, H. Fischer, et al. (2013) Direct linking of Greenland and Antarctic ice cores at the Toba eruption (74 ka BP). *Climate of the Past,* 9**,** 749-766.
Swithinbank, C. (1969) Airborne radio-echo sounding by the British Antarctic Survey. *The Geographical Journal,* 135**,** 551-553.
Tabacco, I., C. Bianchi, J. Baskaradas, L. Cafarella, S. Umberto, A. Zirizzotti, et al. (2008) Italian RES investigation in Antarctica: The new radar system. *Terra Antartica Reports,* 14**,** 213 - 216.

Tang, X., K. Luo, S. Dong, Z. Zhang & B. Sun (2022) Quantifying basal roughness and internal-layer continuity index of ice sheets by an integrated means with radar data and deep learning. *Remote Sensing,* 14, 4507.

Tarasov, L. & W. R. Peltier (2003) Greenland glacial history, borehole constraints, and Eemian extent. *Journal of Geophysical Research: Solid Earth,* 108, 2143.

Teisberg, T. O. & D. M. Schroeder (2023) Digital tools for analog data: Reconstructing the first ice-penetrating radar surveys of Antarctica and Greenland. In *International Geoscience and Remote Sensing Symposium (IGARRS) Proceedings*, 44-47.

Teisberg, T. O., D. M. Schroeder, A. L. Broome, F. Lurie & D. Woo (2022) Development of a UAV-borne pulsed ice-penetrating radar system. In *IGARSS 2022 - 2022 IEEE International Geoscience and Remote Sensing Symposium*, 7405-7408.

Thyssen, F. & K. Grosfeld (1988) Ekström Ice Shelf, Antarctica. *Annals of Glaciology,* 11, 180-183.

Tinto, K. J., L. Padman, C. S. Siddoway, S. R. Springer, H. A. Fricker, I. Das, et al. (2019) Ross Ice Shelf response to climate driven by the tectonic imprint on seafloor bathymetry. *Nature Geoscience,* 12, 441-449.

Traversa, G., D. Fugazza & M. Frezzotti (2023) Megadunes in Antarctica: Migration and characterization from remote and in situ observations. *The Cryosphere,* 17, 427-444.

Tsutaki, S., S. Fujita, K. Kawamura, A. Abe-Ouchi, K. Fukui, H. Motoyama, et al. (2022) High-resolution subglacial topography around Dome Fuji, Antarctica, based on ground-based radar surveys over 30 years. *The Cryosphere,* 16, 2967-2983.

Ulaby, F. & D. B. Lang. 2015. A Strategy for Active Remote Sensing Amid Increased Demand for Radio Spectrum. Washington DC: The National Academies Press.

Van Liefferinge, B. & F. Pattyn (2013) Using ice-flow models to evaluate potential sites of million year-old ice in Antarctica. *Climate of the Past,* 9, 2335-2345.

Van Liefferinge, B., D. Taylor, S. Tsutaki, S. Fujita, P. Gogineni, K. Kawamura, et al. (2021) Surface mass balance controlled by local surface slope in inland Antarctica: Implications for ice-sheet mass balance and Oldest Ice delineation in Dome Fuji. *Geophysical Research Letters,* 48, e2021GL094966.

Vaughan, D. G., H. F. J. Corr, C. S. M. Doake & E. D. Waddington (1999) Distortion of isochronous layers in ice revealed by ground-penetrating radar. *Nature,* 398, 323-326.

Višnjević, V., R. Drews, C. Schannwell, I. Koch, S. Franke, D. Jansen, et al. (2022) Predicting the steady-state isochronal stratigraphy of ice shelves using observations and modeling. *The Cryosphere,* 16, 4763-4777.

Waddington, E. D., T. A. Neumann, M. R. Koutnik, H.-P. Marshall & D. L. Morse (2007) Inference of accumulation-rate patterns from deep layers in glaciers and ice sheets. *Journal of Glaciology,* 53, 694-712.

WAIS Divide Project Members (2015) Precise interpolar phasing of abrupt climate change during the last ice age. *Nature,* 520, 661-665.

Wang, T. T., B. Sun, X. Y. Tang, X. P. Pang, X. B. Cui, J. X. Guo, et al. (2016) Spatio-temporal variability of past accumulation rates inferred from isochronous layers at Dome A, East Antarctica. *Annals of Glaciology,* 57, 87-93.

Wang, Z., A. Chung, D. Steinhage, F. Parrenin, J. Freitag & O. Eisen (2023) Mapping age and basal conditions of ice in the Dome Fuji region, Antarctica, by combining radar internal-layer stratigraphy and flow modeling. *The Cryosphere,* 17, 4297-4314.

Wearing, M. G. & J. Kingslake (2019) Holocene formation of Henry Ice Rise, West Antarctica, inferred from ice-penetrating radar. *Journal of Geophysical Research: Earth Surface,* 124, 2224-2240.

Weertman, J. (1976) Sliding-no sliding zone effect and age determination of ice cores. *Quaternary Research,* 6, 203-207.

Welch, B. C. & R. W. Jacobel (2003) Analysis of deep-penetrating radar surveys of West Antarctica, US-ITASE 2001. *Geophysical Research Letters,* 30, 1444.

Welch, B. C. & R. W. Jacobel (2005) Bedrock topography and wind erosion sites in East Antarctica: observations from the 2002 US-ITASE traverse. *Annals of Glaciology,* 41, 92-96.

Welch, B. C., R. W. Jacobel & S. A. Arcone (2009) First results from radar profiles collected along the US-ITASE traverse from Taylor Dome to South Pole (2006–2008). *Annals of Glaciology,* 50, 35-41.

Wilkinson, M. D., M. Dumontier, I. J. Aalbersberg, G. Appleton, M. Axton, A. Baak, et al. (2016) The FAIR guiding principles for scientific data management and stewardship. *Scientific Data,* 3, 160018.

Winski, D. A., T. J. Fudge, D. G. Ferris, E. C. Osterberg, J. M. Fegyveresi, J. Cole-Dai, et al. (2019) The SP19 chronology for the South Pole Ice Core – Part 1: volcanic matching and annual layer counting. *Climate of the Past,* 15, 1793-1808.

Winter, A., D. Steinhage, E. J. Arnold, D. D. Blankenship, M. G. P. Cavitte, H. F. J. Corr, et al. (2017) Comparison of measurements from different radio-echo sounding systems and synchronization with the ice core at Dome C, Antarctica. *The Cryosphere,* 11, 653-668.

Winter, A., D. Steinhage, T. T. Creyts, T. Kleiner & O. Eisen (2019a) Age stratigraphy in the East Antarctic Ice Sheet inferred from radio-echo sounding horizons. *Earth System Science Data,* 11, 1069-1081.

Winter, K., J. Woodward, S. A. Dunning, C. S. M. Turney, C. J. Fogwill, A. S. Hein, et al. (2016) Assessing the continuity of the blue-ice climate record at Patriot Hills, Horseshoe Valley, West Antarctica. *Geophysical Research Letters,* 43**,** 2019-2026.

Winter, K., J. Woodward, N. Ross, S. A. Dunning, R. G. Bingham, H. F. J. Corr, et al. (2015) Airborne-radar evidence for tributary flow switching in Institute Ice Stream, West Antarctica: Implications for ice-sheet configuration and dynamics. *Journal of Geophysical Research: Earth Surface,* 120**,** 1611-1625.

Winter, K., J. Woodward, N. Ross, S. A. Dunning, A. S. Hein, M. J. Westoby, et al. (2019b) Radar-detected englacial debris in the West Antarctic Ice Sheet. *Geophysical Research Letters,* 46**,** 10454-10462.

Wolovick, M. J. & T. T. Creyts (2016) Overturned folds in ice sheets: Insights from a kinematic model of traveling sticky patches and comparisons with observations. *Journal of Geophysical Research: Earth Surface,* 121**,** 1065-1083.

Wolovick, M. J., T. T. Creyts, W. R. Buck & R. E. Bell (2014) Traveling slippery patches produce thickness-scale folds in ice sheets. *Geophysical Research Letters,* 41**,** 8895-8901.

Wolovick, M. J., J. C. Moore & L. Zhao (2021a) Joint inversion for surface accumulation rate and geothermal heat flow from ice-penetrating radar observations at Dome A, East Antarctica. Part I: Model description, data constraints, and inversion results. *Journal of Geophysical Research: Earth Surface,* 126**,** e2020JF005937.

Wolovick, M. J., J. C. Moore & L. Zhao (2021b) Joint inversion for surface accumulation rate and geothermal heat flow from ice-penetrating radar observations at Dome A, East Antarctica. Part II: Ice-sheet state and geophysical analysis. *Journal of Geophysical Research: Earth Surface,* 126**,** e2020JF005936.

Woodward, J. & E. C. King (2009) Radar surveys of the Rutford Ice Stream onset zone, West Antarctica: Indications of flow (in)stability? *Annals of Glaciology,* 50**,** 57-62.

Wrona, T., M. J. Wolovick, F. Ferraccioli, H. Corr, T. Jordan & M. J. Siegert (2018) Position and variability of complex structures in the central East Antarctic Ice Sheet. *Geological Society Special Publications,* 461**,** 113-129.

Xiong, S., J.-P. Muller & R. C. Carretero (2018) A new method for automatically tracing englacial layers from MCoRDS data in NW Greenland. *Remote Sensing,* 10**,** 43.

Xu, B., S. Lang, X. Cui, L. Li, X. Liu, J. Guo, et al. (2022) Focused synthetic-aperture-radar processing of ice-sounding data collected over East Antarctic Ice Sheet via spatial-correlation-based algorithm using fast back projection. *IEEE Transactions on Geoscience and Remote Sensing,* 60**,** 5233009.

Yan, Y., E. J. Brook, A. V. Kurbatov, J. P. Severinghaus & J. A. Higgins (2021) Ice-core evidence for atmospheric oxygen decline since the Mid-Pleistocene Transition. *Science Advances,* 7**,** eabj9341.

Yari, M., O. Ibikunle, D. Varshney, T. Chowdhury, A. Sarkar, J. Paden, et al. (2021) Airborne snow-radar data simulation with deep learning and physics-driven methods. *IEEE Journal of Selected Topics in Applied Earth Observations and Remote Sensing,* 14**,** 12035-12047.

Yilmaz, Ö. 2001. *Seismic Data Analysis: Processing, Inversion, and Interpretation of Seismic Data*. Tulsa, OK: Society of Exploration Geophysicists.

Young, D. A., D. M. Schroeder, D. D. Blankenship, S. D. Kempf & E. Quartini (2016) The distribution of basal water between Antarctic subglacial lakes from radar sounding. *Philosophical Transactions of the Royal Society A: Mathematical, Physical and Engineering Sciences,* 374**,** 20140297.

Zeising, O., T. A. Gerber, O. Eisen, M. R. Ershadi, N. Stoll, I. Weikusat, et al. (2023) Improved estimation of the bulk ice-crystal-fabric asymmetry from polarimetric phase co-registration. *The Cryosphere,* 17**,** 1097-1105.

Zhao, L. Y., J. C. Moore, B. Sun, X. Y. Tang & X. R. Guo (2018) Where is the 1-million-year-old ice at Dome A? *The Cryosphere,* 12**,** 1651-1663.

Zirizotti, A., J. A. Baskaradas, C. Bianchi, U. Sciacca, I. E. Tabacco & E. Zuccheretti (2008) Glacio RADAR systems and results. Proceedings of 2008 IEEE National Radar Conference, doi: 10.1109/RADAR.2008.4720993.

## Appendix: Suggested standardised structure for the publication of traced IRHs across Antarctica

For publishing future radiostratigraphy datasets, we recommend scientists to follow the structure and naming convention specified in Table A1 for the first ten columns, after which additional columns may be added at the discretion of the scientists.

In the metadata, we recommend that authors also provide at least the following information:

(a) Name(s), version(s) and frequency of RES system(s) used.

(b) Value for speed of radar wave in ice used to convert IRH depths to metres below the ice surface.

(c) Value for any firn correction applied.

(d) The coordinate system(s) used following the World Geodetic System 1984 datum and appropriate projection (i.e., EPSG:3031 for Antarctica).

(e) If applicable, the type of radar product (e.g. waveform) on which the IRHs were traced.

(f) The uncertainties associated with either the IRH age or depth based on RES system resolution and IRH picking, amongst others. Ideally, if the metadata vary throughout the dataset, then such information should be attached to each data point as additional columns to those shown in Table A1.

(g) The source of age control (i.e., ice-core age scale, model).

Additional information may also be added to the metadata, such as the type of processing used to extract the IRHs (if different from the processing used to trace the bed); the distance in the along-track direction along the RES transect for each data point; a flag number indicating whether the ice thickness, surface and bed elevations come directly from the along-track radar or from an interpolated gridded product, if applicable; the spatial resolution (or spacing distance between each data point); the dating method (s) used to provide an age for each IRH; and the type of software and tools used to pick the IRHs. Missing values in the float data should be set to NaN and specified in the metadata. We also recommend the use of open-access and FAIR data formats for storing the data, such as CSV or tabular data file (or netcdf if CSV or tabular data file is not suitable) where metadata can be easily embedded together with the data. Finally, we recommend scientists to publish their data in open-access repositories alongside the paper publication, with a DOI that can be linked back to the original paper. Together, these suggested protocols will ensure the longevity of the data products for future applications and enable faster retrieval thereof, particularly with regards to the large data volumes expected from automatic IRH tracking algorithms in the future.

**Table A1.** Suggested standardised structure for the publication of IRH datasets associated with the AntArchitecture community effort following FAIR data standards.

(For EGUsphere formatting, this 12-column table is presented across two rows.)

Table rows 1-6:

| Line ID or transect name | Trace timestamp (GPS time) | Longitude (decimal degrees) | Latitude (decimal degrees) | X coordinate (EPSG:3031; metres) | Y coordinate (EPSG:3031; metres) |
|---|---|---|---|---|---|

Table rows 7-12

| IRH name | IRH (two-way travel-time through ice only) | IRH depth below ice surface (metres) | Ice thickness (metres) | Surface elevation (WGS84 ellipsoid; metres) | Bed elevation (WGS84 ellipsoid; metres) |
|---|---|---|---|---|---|